

Title	Electrochemical Reactions on Polymer Electrolyte Membrane/Electrode Composites(Dissertation_全文)
Author(s)	Inaba, Minoru
Citation	Kyoto University (京都大学)
Issue Date	1995-01-23
URL	http://dx.doi.org/10.11501/3099110
Right	
Type	Thesis or Dissertation
Textversion	author

新 制
工
982

京大附図

**ELECTROCHEMICAL REACTIONS
ON POLYMER ELECTROLYTE
MEMBRANE/ELECTRODE COMPOSITES**

MINORU INABA

1994

Electrochemical Reactions on Polymer Electrolyte Membrane/Electrode Composites

Minoru Inaba

Kyoto University
Kyoto, Japan

1994

Preface

The present thesis is a result of the research work for electrochemical reactions on polymer electrolyte membrane/electrode composites. The studies collected in this thesis have been carried out under the supervision of Professors Zen-ichiro Takehara and Zempachi Ogumi at Department of Industrial Chemistry, Faculty of Engineering, Kyoto University (1993- Division of Energy and Hydrocarbon Chemistry, Graduate School of Engineering, Kyoto University).

The research work in this thesis is largely indebted to the continuous help of many researchers. I wish to express my sincere gratitude to Professors Zen-ichiro Takehara and Zempachi Ogumi for their continuous guidance and suggestion throughout this work. I wish to thank Professor Seiichi Nishimoto for his helpful comments and discussion. I also grateful to Drs. Takeshi Yao, Yoshiro Tomida, Hidetaka Hayashi, Kiyoshi Kanamura, Yoshiharu Uchimoto, Kenji Kikuchi and Mr. Katsumi Katakura for many fruitful discussions.

Finally, I wish to thank my wife for sacrificing many precious hours which rightfully belonged to her.

Minoru Inaba

Contents

Introduction	1
Background of the work	
Outline of the work	
Part I Effects of Hydrophilic/Hydrophobic Interactions on the Reduction of Aromatic Nitro Compounds	23
Chapter 1. Reduction of Nitrobenzene on Modified Pt-Nafion	25
1.1. Introduction	
1.2. Experimental	
1.3. Results	
1.4. Discussion	
1.5. Conclusion	
Chapter 2. Effects of Solvents on the Electroreduction of Nitrobenzene on Cu,Pt-Nafion	43
2.1. Introduction	
2.2. Experimental	
2.3. Results and Discussion	
2.4. Conclusion	
Chapter 3. Influence of the Multi-phase Structure of Nafion on Electroreduction of Substituted Aromatic Nitro Compounds on Cu,Pt-Nafion	63
3.1. Introduction	
3.2. Experimental	
3.3. Results	
3.4. Discussion	
3.5. Conclusion	

Chapter 4.	Reduction of Nitrobenzene on Solid Polymer Electrolyte Composite Electrodes Using a Hydrocarbon Sulfonate Ion-Exchange Membrane	89
	4.1. Introduction	
	4.2. Experimental	
	4.3. Results and Discussion	
Chapter 5.	Reduction of Nitrobenzene Using a Flow-Through Pt-Nafion Cell	97
	5.1. Introduction	
	5.2. Experimental	
	5.3. Results and Discussion	
	5.4. Conclusions	
Part II	Utilization of Phase-Transfer Mediators Incorporated into Nafion	117
Chapter 6.	Indirect Electrochemical Debromination Using Viologen as Microscopic Phase-Transfer Mediators	119
	6.1. Introduction	
	6.2. Experimental	
	6.3. Results and Discussion	
	6.4. Conclusions	
Chapter 7.	Structure of Perfluorinated Ionomer Membranes Incorporating Organic Cations	155
	7.1. Introduction	
	7.2. Experimental	
	7.3. Results and Discussion	
Chapter 8.	Raman Spectroscopic Analysis of Electrochemical Behavior of Propylviologen in Nafion	165
	8.1. Introduction	
	8.2. Experimental	
	8.3. Results	
	8.4. Discussion	
	8.5. Conclusion	

Chapter 9. Bromination of the Methyl Group of Toluene on a Pt-Nafion Composite Electrode	189
9.1. Introduction	
9.2. Experimental	
9.3. Results and Discussion	
Publication List	201

Introduction

Background of the work

Problems in electrochemical organic synthesis

The energy applied to systems in electrochemical organic synthesis can be controlled precisely by electrode potential and current, and this brings many advantages to electrochemical organic synthesis.¹⁻³⁾ The field of electroorganic chemistry has been existent since 1801.⁴⁾ From that time on, a great deal of published information about synthetic and mechanistic aspects of electrochemical organic synthesis has accumulated. Nevertheless, only a limited number of reactions have been commercialized owing to intrinsic disadvantages of electroorganic chemistry:

- (i) Organic electrochemical reactions are usually slow, i.e., high current densities cannot be used, when compared with typical inorganic electrochemical reactions or conventional homogeneous reactions. The slowness is attributed to a low surface-to-volume ratio of most preparative electrochemical cells as well as a slow electron-transfer rate between organic reactant and electrode.
- (ii) The requirement that highly polar solvent should be capable of ioniz-

ing a suitable supporting electrolyte to obtain a high ionic conductivity is restrictive. Furthermore, the addition of the supporting electrolyte often leads to unwanted side reactions, and makes the product separation processes energy consuming.

In order to improve the former characteristic, the enhancement of the surface-to-volume ratio of the cells using pseudo three-dimensional electrodes,⁵⁻⁹⁾ highly active electrode catalysts¹⁰⁾ and electron mediators¹¹⁻¹³⁾ have been studied. In order to overwhelm the latter disadvantage, emulsion electrolysis¹⁴⁻¹⁷⁾ using immiscible two-phase systems, and the solid polymer electrolyte (SPE) method¹⁸⁻³⁴⁾ that utilizes ion-exchange membranes as electrolyte have been developed.

SPE electrolytic method

The use of ion-exchange membranes as electrolytes has been originally developed for fuel cells (polymer electrolyte fuel cells, PEFCs).^{35,36)} The first PEFCs were demonstrated in the early stages of the United States space program (Gemini) in the 1960s.^{35,36)} In PEFCs the reactions at the anode and cathode generally involve only gaseous species, hydrogen and oxygen, respectively, as shown in Fig. 1a and the overall cell reaction is



Electrical energy is obtained through a load inserted between the cathode and anode. On the other hand, supplying electrical power to PEFCs conversely produces hydrogen and oxygen from water:



This system is called as "SPE electrolytic method", and has attracted much attention for use in water electrolyzers,³⁷⁾ brine electrolyzers,³⁸⁾ and electrolyzers for organic synthesis.¹⁸⁻³⁴⁾

Figure 1b shows the principle of SPE method for the oxidation of

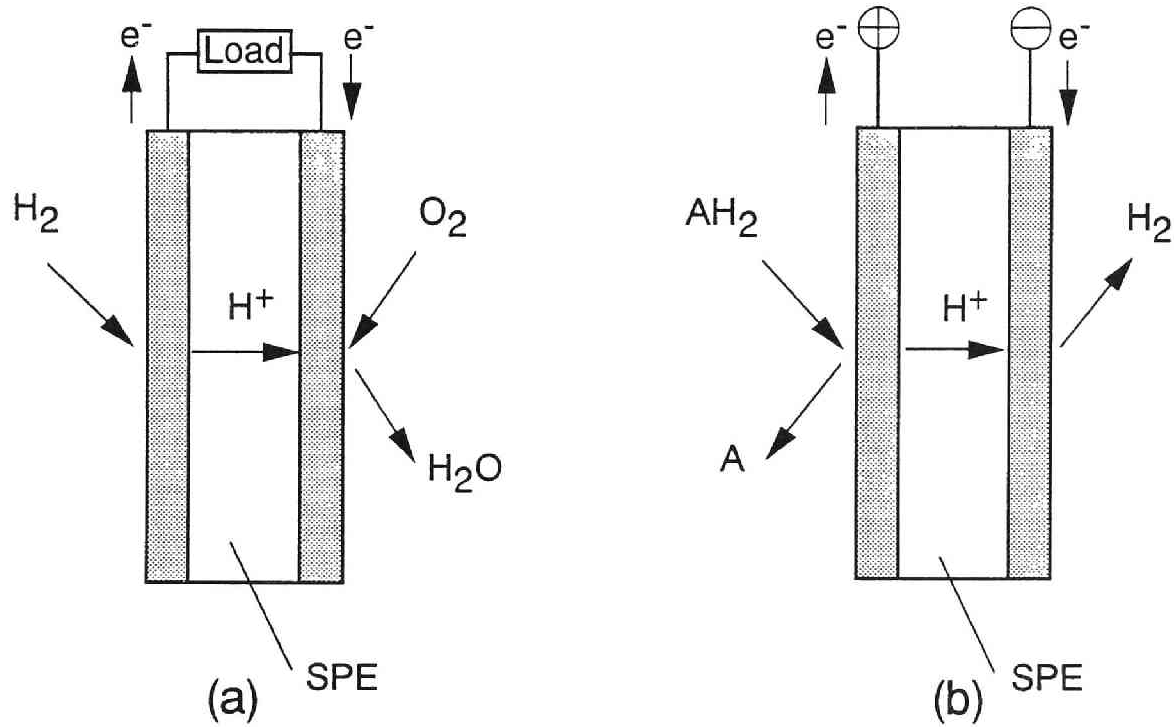
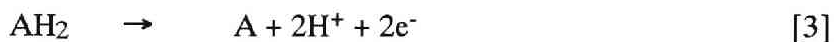
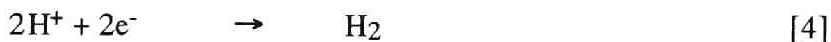


Fig. 1. Principles of (a) PEFC and (b) electrochemical dehydrogenation of AH_2 to A by SPE method. SPE: solid polymer electrolyte.

AH₂ to A on a Pt-SPE composite electrode consisting of a cation-exchange membrane and porous platinum. One porous platinum layer deposited on the cation-exchange membrane is used as anode, and the other as cathode. An organic solution containing AH₂ and water are filled in the anode and cathode compartments of the electrolytic cell, respectively, and a DC voltage is applied between the electrodes. On the anode the following reaction proceeds:



While the A molecule produced by reaction [3] stays in the anode compartment, the proton moves through the cation-exchange membrane to the cathode, where it is reduced to produce hydrogen gas:



The counter-ion of the cation-exchange membrane i.e., proton, sustains ionic conductivity between the anode and cathode. The anolyte and catholyte, hence, do not need to have ionic conductivity; that is, no supporting electrolyte is required. This extends solvent selection and eliminates difficulties in subsequent product purification processes. The SPE method is therefore promising for use in commercial electroorganic synthesis.

Application of SPE method to electroorganic synthesis

The application of the SPE method to electrochemical synthesis has been so far reported for the hydrogenation of olefinic compounds (Pt-, Au-, Au-modified Pt-, and Pt-modified Au-Nafion),¹⁹⁾ the Kolbe-type reactions of acetic acid and monomethyl adipate (Pt-Nafion),²⁰⁾ the reduction of nitrobenzene sulfonic acid and nitrobenzene (Pt-Nafion),²¹⁾ the reduction of benzaldehyde to benzylalcohol (Pt-Nafion and Pb-modified Pt-Nafion),³⁰⁻³²⁾ etc. The utilization of simple redox couples as mediators may elongate the life of the electrodes and enhance reaction selectivity. The oxidation of cyclohexanol to cyclohexanone on Pt-Nafion using an I⁻/I(+) mediatory system²³⁾ and the

methoxylation of furan using a Br^-/Br_2 mediatory system²²⁾ have been so far reported.

SPE composite electrodes incorporating cationic mediators

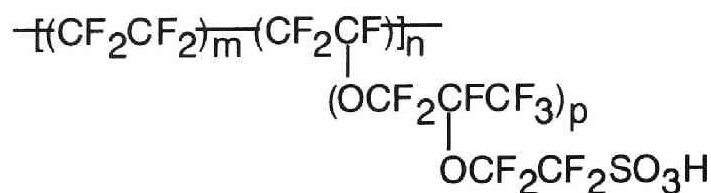
Electrodes coated with Nafion, which are prepared by casting of dissolved Nafion in alcohol on solid electrodes, also have received much attention owing to their properties that various electrochemically and optically active cations can be incorporated into the Nafion film.³⁹⁻⁴⁴⁾ In SPE composite electrodes, the electrode materials are covered with Nafion polymer electrolyte; hence, SPE composite electrodes may be regarded as a kind of polymer-coated electrodes. In addition, the polymer layer of the SPE composite electrode is bounded more tightly to the electrode material, more well-defined, and more stable than those of the polymer coated electrode.

Cationic mediators can be incorporated electrostatically into the Nafion membrane of the SPE composite electrode. This incorporation may lead to a greater selectivity compared with conventional methods and eliminate the separation process of the mediator. The use of mediatory system has been reported for the oxidation of cinnamyl alcohol to cinnamaldehyde^{26,27)} ($\text{Mn}^{2+}/\text{MnO}_2$ and $\text{Pb}^{2+}/\text{PbO}_2$), the oxidation of geraniol²⁹⁾ ($\text{Mn}^{2+}/\text{MnO}_2$), etc.

Perfluorinated ion-exchange membranes^{35,36)}

The early membranes tested in PEFCs include the hydrocarbon-type polymers such as cross-linked polystyrene-divinylbenzene sulfonic acids and sulfonated phenolformaldehyde. However, it was observed that the life of PEFCs was limited by oxidative degradation of the polymer. Hydrocarbon-type polymers are unstable because of C-H bond cleavage, particularly at the α -H sites where the functional groups are attached. The research developed in the early 1960s led to the development of Nafion (registered trademark of E. I. DuPont de Nemours) membranes, which are perfluorosulfonic acid membranes that are electrochemically stable in PEFCs at temperatures up to about

100°C. This polymer consists of the following ionomer units:



$$m = 6 - 10$$

$$p \geq 1$$

Nafion has two features in common: (i) the polymer chains consist mainly of a PTFE backbone, which statistically forms segments of several units in length, and (ii) the perfluorinated vinyl polyether, which joins these segments to form a flexible pendant branched from the main perfluoro chain and carries a terminal acidic group to provide the cation-exchange property. Nafion membranes with sulfonic acid groups meet all the required characteristics of ion-exchange membranes for use in fuel cells. Nafion was first used in fuel cells in 1966, and it is still the most widely tested ion-exchange membranes in PEFCs.

The Nafion membranes, which are fully fluorinated polymers, exhibit exceptionally high chemical and thermal stability; that is, they are stable against chemical attack in strong oxidizing and reducing agents at temperatures up to 125°C. A high degree of dissociation and a high concentration of mobile H⁺ ions give a conductivity of greater than 0.05 S cm⁻¹ at 25°C. The range of equivalent weights, which is defined as the weight of polymer that neutralizes one equivalent of base, and is inversely proportional to the ion-exchange capacity, for Nafion is 950-1800. The perfluorinated sulfonic acid group provides a highly acidic environment (comparable to a 10 wt.% H₂SO₄ solution) in a hydrated membrane.

For SPE composite electrodes for use in electroorganic synthesis, Nafion membranes have been mainly used because they are chemically and thermally stable, and have high ionic conductivity.

A new series of perfluorosulfonic acid membranes that has recently

become available from Dow Chemical Company provides an attractive alternative to Nafion in PEFCs.^{45,46)} This new polymer has a PTFE-like backbone similar to that of Nafion, but the pendant side chain containing the sulfonic acid group is shorter. This polymer possesses ion-exchange properties similar to those of Nafion, and it is also available with higher acid strength and lower equivalent weight (600-950), which leads to a higher ionic conductivity than that of Nafion. PEFCs using the Dow membranes are capable of achieving a maximum power density as high as 2.7 W cm^{-2} (5.38 A cm^{-2} and 0.5 V) with H_2 and O_2 at 0.68 MPa .⁴⁵⁾

Perfluorinated ion-exchange membranes that have carboxylate groups as ion-exchange sites have also been produced for chlor-alkali cells and other applications. These are the Flemion[®] membranes⁴⁹⁾ (Asahi Glass Co.,Ltd.), Nepsepta[®]-F membranes⁵⁰⁾ (Tokuyama Soda Co.,Ltd.), and the perfluorinated membranes produced by the Asahi Chemical Industry Co.⁵¹⁾

Microstructure of Nafion

As observed in other non-crosslinked ion-exchange membranes such as ethylene-methacrylic acid copolymer, the ion-exchange sites in Nafion membranes aggregate and form clusters. Ionic clustering in Nafion membranes has been indicated by a variety of physical studies including dielectric relaxation, small angle X-ray scattering (SAXS),⁵⁰⁾ neutron scattering,⁵¹⁾ electron microscopy,⁵²⁾ NMR,⁵³⁾ IR,⁵⁴⁾ and several transport studies.⁵⁵⁻⁵⁷⁾ Gierke *et al.*^{58,59)} developed a cluster-network model shown in Fig. 2 to describe Na^+ ion-transport through Nafion in chlor-alkali cells. This structure can be described as an reversed micelle in which the ion-exchange sites, counter-ions and absorbed water are microscopically separated into a spherical domain from the perfluoro backbone domain. Tables 1 and 2 show the cluster diameters obtained for Nafion membranes of different EWs and counter-ions assuming cubic close packing of clusters.⁵⁸⁾ As EW increases, the cluster diameter decreases (Table 1). This trend may be understood by recognizing that the crystallinity and polymer stiffness increase with increasing EW. As the cation weight increases, the cluster diameter decreases (Table 2). Clearly, the

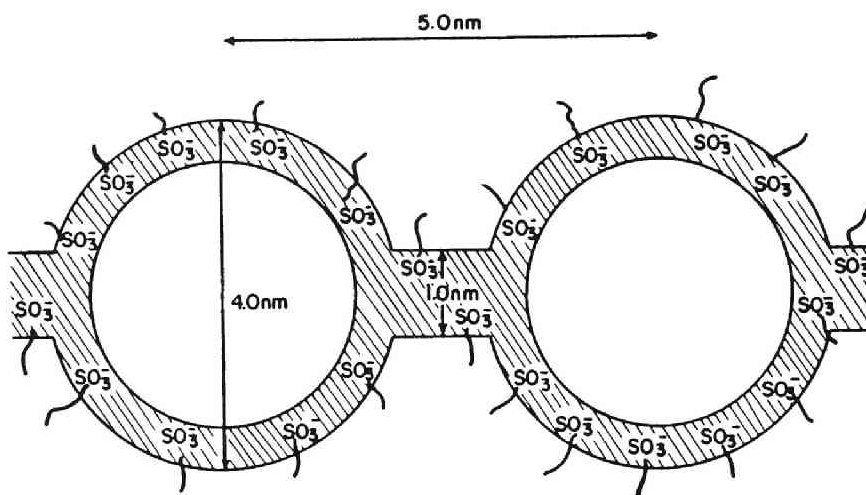


Fig. 2. Cluster-network model for Nafion perfluorinated membranes.⁵⁸⁾
 The shaded area around the interface and inside a channel are the double layer regions from which the hydroxyl ions are excluded electrostatically.

Table 1. Cluster morphology for Nafion membranes^{a)} with various EW in Na⁺-form.⁵⁸⁾

EW	Polymer density $\rho / \text{g cm}^{-3}$	% mass gain 100 Δm	% volume gain 100 ΔV	H ₂ O/Cluster	Fixed Charge/ Cluster	Bragg spacing d / nm	Cluster diameter d _c / nm
944	2.088	42.0	87.3	2102	95	5.12	5.09
971	2.093	37.5	78.2	1944	96	5.09	4.97
1100	2.103	23.8	49.8	1200	84	4.78	4.31
1200	2.113	17.8	37.5	863	73	4.55	3.88
1600	2.135	8.1	17.2	370	52	4.22	3.03
1800	2.144	6.3	13.3	266	43	4.07	2.74

^{a)} Samples were conditioned by boiling 1 h in 0.2% NaOH.

Table. 2. Cluster morphology for 1200 EW Nafion membranes^{a)} in different cation forms.⁵⁸⁾

Cation form	Polymer density $\rho / \text{g cm}^{-3}$	% mass gain 100 Δm	% volume gain 100 ΔV	H ₂ O/Cluster	Fixed Charge/ Cluster	Bragg spacing d / nm	Cluster diameter d _c / nm
H ⁺	2.075	33.6	69.7	1690	76	4.98	4.74
Li ⁺	2.078	29.7	61.7	1430	72	4.82	4.49
Na ⁺	2.113	21.0	44.3	1120	80	4.78	4.21
K ⁺	2.141	8.7	18.7	520	89	4.61	3.45
Rb ⁺	2.221	8.1	17.9	560	103	4.78	3.56
Cs ⁺	2.304	5.9	13.6	470	120	4.90	3.50

a) Samples were conditioned by boiling 1 h in H₂O.

hydrophilicity of the exchange site is lower with the heavier cations, which is consistent with the fact that the heavier cations are more strongly interacted with the exchange sites.

Yeager and Steck⁶⁰⁾ later studied Na⁺ and Cs⁺ transport through swollen Nafion. While the diffusion coefficient of Na⁺ was greatly affected by a change in the water content of Nafion, that of Cs⁺ remained unchanged. These results allowed them to propose a three phase model that an interfacial region exists between the two domains of Gierke's model, and to conclude that, while Na⁺ permeates through the ionic cluster domain, Cs⁺ permeates through the interfacial region which is not affected by the change in water content. Ogumi *et al.*⁶¹⁾ studied the permeation of hydrogen and oxygen through Nafion membranes with different counter-ions. They observed that the solubility values of H₂ and O₂ in the Nafion membranes (about 10 mM) were independent of the water content of the membranes and were close to those in perfluorocarbon media rather than to that in water. They also observed that the diffusion coefficients of H₂ and O₂ in the Nafion membranes were independent of their water contents. From these observations, they concluded that the interfacial region is the main path of hydrogen and oxygen molecules permeating through Nafion, and consists of the amorphous part of the backbone and the flexible side chains of Nafion, as shown in Fig. 3. Various properties such as solvent uptake,^{62,63)} ion-exchange selectivity,⁶⁴⁾ permeation of organic molecules,^{65,66)} etc., have been explained in terms of the multi-phase structure of Nafion.

Outline of the work

In the SPE composite electrodes, the electrode materials are covered with Nafion polymer electrolyte as mentioned above. Since the active sites of the SPE composite electrodes are located in the complex environment of the Nafion membrane as shown in Fig. 4, some hydrophilic/hydrophobic interactions between organic reactants and Nafion are expected. Such interactions

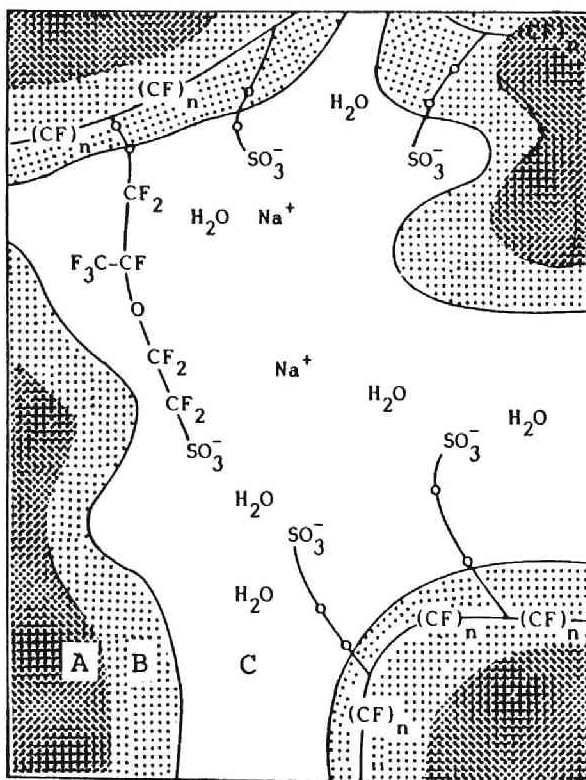


Fig. 3. Three-phase model for Nafion.⁶¹⁾ Region A: rigid hydrophobic backbone. Region B: flexible perfluorocarbon where gases permeate. Region C: ionic cluster region containing water similar to bulk water.

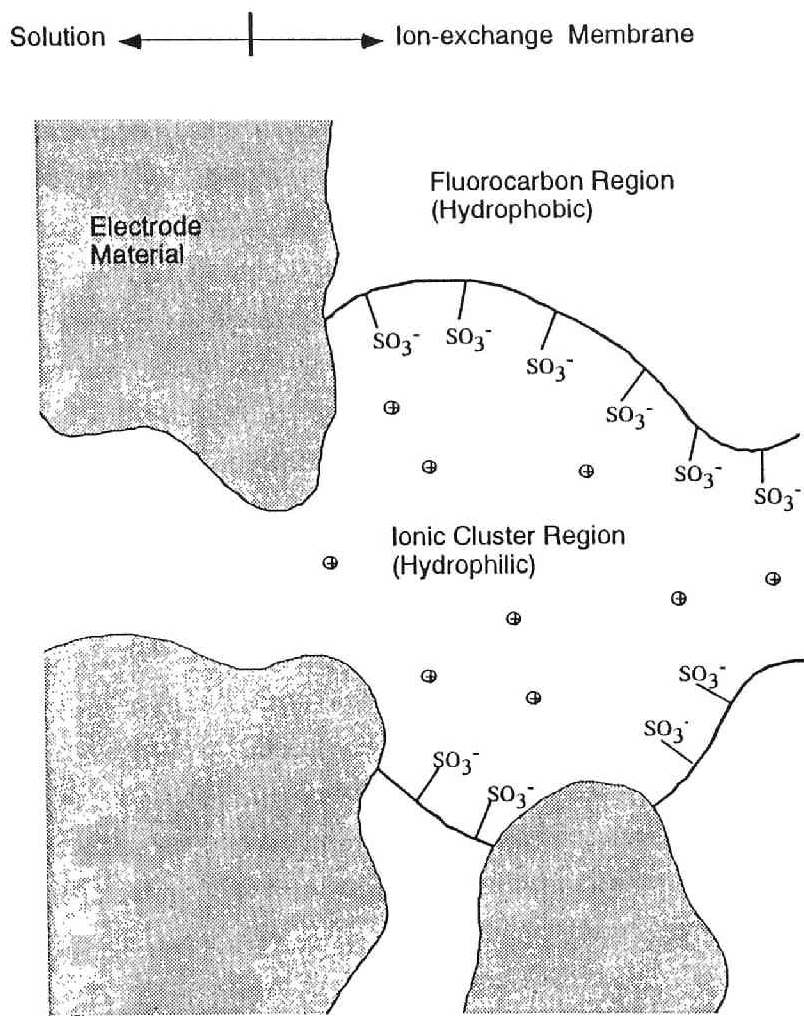


Fig. 4. Schematic model of the active sites of SPE composite electrode using Nafion as the SPE materials.

may affect reaction mechanism and enhance specific selectivity during electrolysis. The aim of the present work is to clarify the effects of the hydrophilic/hydrophobic interactions between organic reactants and Nafion and to develop a novel SPE method utilizing the multi-phase structure of Nafion.

Part I devoted to the studies on the effects of the hydrophilic/hydrophobic interactions between organic reactants and Nafion using the reduction of nitrobenzene on copper-modified Pt-Nafion as a model reaction. The location of the reaction sites of the SPE composite electrodes, and the effects of the Nafion polymer on the product distribution and the reactant selectivity are discussed in terms of the multi-phase structure of Nafion.

In chapter 1, SPE composite electrodes prepared by deposition of platinum on Nafion, Pt-Nafions, were modified by electrochemical deposition of nickel (Ni,Pt-Nafion) and copper (Cu,Pt-Nafion). The modified electrodes were applied to the reduction of nitrobenzene. The modification was effective for aniline formation, and suppressed side reactions such as hydrogen evolution. On Cu,Pt-Nafion the Bamberger rearrangement was inhibited and no *p*-aminophenol was obtained. The inhibition was caused by Nafion which covered the active sites of Cu,Pt-Nafion. It was suggested that SPE composite electrodes behaved in the same manner as polymer coated electrodes. The active sites for charge transfer reaction was concluded to be at the interior surface of the metal layer bound to Nafion.

In chapter 2, the effects of solvents on the electroreduction of nitrobenzene on Cu,Pt-Nafion were studied. The presence of a sufficient amount of a co-solvent in the catholyte or in the anolyte facilitated the reduction of nitrobenzene to aniline. Without a sufficient amount of a co-solvent, the mass transport of nitrobenzene to the active sites was suppressed, and hydrogen evolution became significant. The solubility parameter value, δ_{mix} , of the catholyte was found to be an important index for predicting the effectiveness of mass transport of nitrobenzene to the active sites of the SPE composite electrode. When an aqueous solution was used as the anolyte, catholytes with $\delta_{mix} > 11 \text{ cal}^{1/2} \text{ cm}^{-3/2}$ were effective for aniline production by the electroreduction of nitrobenzene on Cu,Pt-Nafion.

In chapter 3, the influence of Nafion and its multi-phase structure on reactant selectivity in the electroreduction of aromatic nitro compounds on Cu,Pt-Nafion was investigated. An equimolar solution of *p*-nitrotoluene and *p*-nitrophenol, and an equimolar solution of *o*- and *p*-nitrotoluene were subjected to electroreduction on Cu,Pt-Nafion. The reactant selectivity, that is, the relative ease with which the reactants are reduced to the corresponding amino compounds, was compared with that on a conventional Cu electrode. *Para*-nitrotoluene was preferentially electroreduced in both of the equimolar solutions tested. Enhanced selectivity was observed with Cu,Pt-Nafion relative to the Cu electrode. The enhanced selectivity with Cu,Pt-Nafion was explained in terms of hydrophilic/hydrophobic interactions between the reactants and Nafion, which has a multi-phase structure consisting of the polytetrafluoroethylene backbone, ionic clusters, and an interfacial region (a hydrophobic amorphous region).

In chapter 4, an SPE composite electrode using a hydrocarbon sulfonate ion-exchange membrane, Selemion[®] CMV, was prepared (Cu-Selemion). Nitrobenzene was electroreduced on Cu-Selemion. At current densities greater than 32 mA cm^{-2} , the current efficiency for aniline production decreased significantly because of hydrogen evolution. In addition, a small amount of dimerized product was formed as a by-product. The reaction selectivity and the mass transport rate were improved by Nafion coating on Selemion. With Nafion-modified Cu-Selemion, aniline was obtained selectively and the current efficiencies for aniline production were as high as 90 % at current densities up to 70 mA cm^{-2} .

In chapter 5, a flow-through cell using Cu,Pt-Nafion with low Pt-loading (0.9 mg cm^{-2}) was fabricated, and was served for the reduction of nitrobenzene. The current efficiency of aniline production was ca. 80% at current densities up to 32 mA cm^{-2} . A small amount of a dimerized compound, which was not produced with the batch cell, was formed as a by-product. The current efficiency for aniline production decreased significantly at current densities greater than 32 mA cm^{-2} . Even in the low current density region (up to 32 mA cm^{-2}) the current efficiency decreased with increasing charge passed

beyond ca. 2000 C. This decrease in current efficiency was caused by hydrogen evolution and the permeation of aniline to the anolyte. The oxidation of iodide ion was examined as the anodic reaction in place of oxygen evolution. The cell voltage was lower than 1.0 V, and was stable for a long period. However, the decrease in current efficiency with charge passed was more significant than that using oxygen evolution as the anode reaction.

Part II is devoted to the development of a novel SPE method that takes advantage of the multi-phase structure of Nafion. A phase-transfer mediator, viologen, was incorporated into the Nafion membrane, and the phase-transfer reaction between the hydrophilic ionic cluster domain and the hydrophobic interfacial region was applied to electroorganic synthesis. The structure of the Nafion incorporating viologen and the residence sites of viologen were analyzed by small angle X-ray scattering and Raman spectroscopy, respectively. Part II includes another phase-transfer system using a Br_2/Br^- redox couple.

In chapter 6, various *N, N'*-dialkyl-4,4'-bipyridinium salts (viologens) were incorporated in Cu,Pt-Nafion as phase transfer mediators. Electrochemical debromination of *meso*-1,2-dibromo-1,2-diphenylethane was carried out on the SPE composite electrode. The results were compared with those obtained in an emulsion system consisting of water and dichloromethane. Of the viologen compounds tested, propyl viologen was the most effective mediator for the SPE composite electrode, while octyl viologen dibromide was the most effective mediator in the emulsion system. The active species for the debromination in the emulsion system was shown to be the doubly reduced neutral form of viologen that was generated by the disproportionation of cation radicals. The disproportionation constant, K_d , of octyl viologen cation radical in a two-phase system consisting of water and dichloromethane was estimated to be 809. The reaction mechanism on the SPE composite electrode was discussed, and it was proposed that the active species was generated by disproportionation at the microscopically heterogeneous interface between the hydrophilic and hydrophobic domains of the

Nafion.

In chapter 7, the structure of Nafion membranes incorporating large organic cations, tetraethylammonium (TEA^+) and 1,1'-dialkyl-4,4'-bipyridinium cations (C_nV^{2+} , $n = 3$ and 8), was studied using small-angle X-ray scattering (SAXS). For TEA^+ - and C_3V^{2+} -form membranes, the SAXS maxima show the presence of the ionic clusters as large as those for Na^+ -form (ca. 4 nm in diameter). For C_8V^{2+} -form membranes, the inter-cluster distance expanded to a value larger than that of the original H^+ -form after the ion-exchange reaction for 5 days. However, the water content and cluster size decreased significantly after the ion-exchange reaction for 50 days or boiling treatment.

In chapter 8, the electrochemical and Raman spectroscopic behavior of propylviologen incorporated into the Nafion film coated on a silver electrode was studied. The results were compared with those on Ag in solutions containing Triton X-100, cetyltrimethylammonium bromide (CTAB) and sodium dodecyl sulfate (SDS) micelles. Propylviologen incorporated into Nafion showed unusual electrochemical and Raman spectroscopic behavior. The half-wave potential for the second step was shifted to a negative potential with respect to that in an aqueous solution, and only a small amount of the doubly reduced form was detected by Raman spectroscopy. Similar behavior was observed in the anionic SDS micellar solution. On the basis of the observed similarity, the residence sites of propylviologen in Nafion were discussed.

In chapter 9, the anodic bromination of toluene was studied on a Pt-Nafion composite electrode using neat toluene as the anolyte without adding a supporting electrolyte. While brominated products were sparingly produced in the dark, benzyl bromide was obtained selectively with a high current efficiency of 70.5% under irradiation with fluorescent light. The current efficiency was greatly affected by the HBr concentration in the catholyte, and was the highest at 5 M. The reaction mechanism for bromination and the mass transport of the reactant in the SPE composite electrode were discussed.

References

1. M. M. Baizer and H. Lund (eds.), "Organic Electrochemistry", 2nd Edn., Marcel Dekker, New York (1983).
2. M. R. Rifi and F. H. Covitz, "Introduction to Organic Electrochemistry", Marcel Dekker, New York (1974).
3. S. Torii, "Yuki Denkai Gosei", Kodansha, Tokyo (1981).
4. D.-T. Chin and C. Y. Cheng, in "Technique of Electroorganic Synthesis", ed by N. L. Weinberg and B. V. Tilak, John Wiley & Sons, New York (1982) Chap. 1.
5. S. Yoshizawa, Z. Takehara, Z. Ogumi, M. Matsubara, and T. Tsuji, *J. Appl. Electrochem.*, **6**, 403 (1976).
6. F. Beck, *J. Appl. Electrochem.*, **2**, 59 (1972).
7. R. E. Shinoda, *Electrochem. Acta*, **20**, 457 (1975).
8. D. N. Bennion and J. Newman, *J. Appl. Electrochem.*, **2**, 113 (1970).
9. M. Fleishmann and J. Oldfield, *J. Electroanal. Chem.*, **29**, 211 (1971).
10. B. V. Tilak, S. Serangapani, and N. L. Weinberg, in "Technique of Electroorganic Synthesis", ed by N. L. Weinberg and B. V. Tilak, John Wiley & Sons, New York (1982) Chap. 4.
11. T.-C. Chou, J.-S. Do, and C.-H. Chen, in "Modern Methodology in Organic Synthesis", ed by T. Shono, Kodansha, Tokyo (1992) pp. 283-301.
12. K. Kramer, P. M. Robertson, and N. Ibl, *J. Appl. Electrochem.*, **10**, 29 (1980).
13. H. Wendt and H. Shineider, *J. Appl. Electrochem.*, **16**, 134 (1986).
14. H. Feess and H. Wendt, in "Technique of Electroorganic Synthesis", ed by N. L. Weinberg and B. V. Tilak, John Wiley & Sons, New York (1982) Chap. 2.
15. J. P. Milington, *Chem. Ind. (Lond.)*, **1975**, 780 (1975).
16. P. Yer and T. Kuwana, *J. Electrochem. Soc.*, **123**, 1334 (1976).
17. R. Dworak and H. Wendt, *Ber. Bunsen-Ges. Phys. Chemie*, **82**,

- 728 (1977).
18. Z. Ogumi, K. Nishio, and S. Yoshizawa, *Denki Kagaku*, **49**, 212 (1981).
 19. Z. Ogumi, K. Nishio, and S. Yoshizawa, *Electrochim. Acta*, **26**, 1779 (1982).
 20. Z. Ogumi, H. Yamashita, K. Nishio, Z. Takehara, and S. Yoshizawa, *Electrochim. Acta*, **28**, 1687 (1983).
 21. Z. Ogumi, H. Yamashita, K. Nishio, Z. Takehara, and S. Yoshizawa, *Denki Kagaku*, **52**, 180 (1984).
 22. Z. Ogumi, S. Ohashi, and Z. Takehara, *Nippon Kagaku Kaishi*, **1984**, 1788 (1984).
 23. Z. Ogumi, S. Ohashi, and Z. Takehara, *Electrochim. Acta*, **30**, 121 (1985).
 24. Z. Ogumi, T. Mizoe, N. Yoshida, and Z. Takehara, *Bull. Chem. Soc., Jpn.*, **60**, 4233 (1987).
 25. Z. Ogumi, T. Mizoe, and Z. Takehara, *Bull. Chem. Soc., Jpn.*, **61**, 4183 (1988).
 26. Z. Ogumi, T. Mizoe, C. Zhen, and Z. Takehara, *Bull. Chem. Soc., Jpn.*, **63**, 3365 (1990).
 27. Z. Chen, T. Mizoe, Z. Ogumi, and Z. Takehara, *Bull. Chem. Soc., Jpn.*, **64**, 537 (1991).
 28. Z. Chen, Z. Ogumi, and Z. Takehara, *Bull. Chem. Soc., Jpn.*, **64**, 1261 (1991).
 29. Z. Ogumi, K. Inatomi, J. T. Hinatsu, and Z. Takehara, *Electrochim. Acta*, **37**, 1295 (1992).
 30. Y.-L. Chen, T.-C. Chou, *Electrochim. Acta*, **38**, 2171 (1993).
 31. Y.-L. Chen, T.-C. Chou, *J. Electroanal. Chem.*, **360**, 247 (1993).
 32. Y.-L. Chen, T.-C. Chou, *J. Appl. Electrochem.*, **24**, 434 (1994).
 33. Z. Ogumi and Z. Takehara, *Denki Kagaku*, **52**, 70 (1984).
 34. Z. Takehara and Z. Ogumi, *J. Synthtic Org. Chem., Jpn.*, **43**, 575 (1985).
 35. A. J. Applby and F. R. Foulkes, "Fuel Cell Handbook", Van Nostrand

- Reinhold, New York (1989) pp. 284-296.
36. K. Konoshita, "Electrochemical Oxygen Technology", John Wiley & Sons, New York (1992) pp. 168-176.
 37. P. W. T. Lu and S. Srinivasan, *J. Appl. Electrochem.*, **9**, 269 (1979).
 38. A. P. Laconti, *Japan Tokkyo Kokai*, 54-112398 (1979).
 39. H. S. White, J. Leddy and A. J. Bard, *J. Am. Chem. Soc.*, **104**, 4811 (1982).
 40. D. A. Buttry and F. C. Anson, *J. Electroanal. Chem.*, **130**, 333 (1981).
 41. N. E. Prieto and C. R. Martin, *J. Electrochem. Soc.*, **131**, 751 (1984).
 42. M. N. Szentirmay and C. R. Martin, *Anal. Chem.*, **56**, 1898 (1984).
 43. C. R. Martin and K. A. Dollard, *J. Electroanal. Chem.*, **159**, 127 (1983).
 44. I. Rubinstein, *J. Electroanal. Chem.*, **188**, 227 (1985).
 45. K. Prater, *J. Power Sources*, **29**, 239 (1990).
 46. G. A. Eisman, *J. Power Sources*, **29**, 389 (1990).
 47. H. Ukihashi and M. Yamabe, in "Perfluorinated Ionomer Membranes", ed by A. Eisenberg and H. L. Yeager, ACS Symposium Series No. 180, Washington DC (1982) Chap. 17.
 48. T. Sata and Y. Onoue, in "Perfluorinated Ionomer Membranes", ed by A. Eisenberg and H. L. Yeager, ACS Symposium Series No. 180, Washington DC (1982) Chap. 16.
 49. M. Seko, S. Ogawa, and K. Kimoto, in "Perfluorinated Ionomer Membranes", ed by A. Eisenberg and H. L. Yeager, ACS Symposium Series No. 180, Washington DC (1982) Chap. 15.
 50. S. C. Yeo and A. Eisenberg, *J. Appl. Polym. Sci.*, **21**, 875 (1977).
 51. E. J. Roche, M. Pineri, R. Duplessix, and A. M. Levelut, *J. Polym. Sci. Polym. Phys. Ed.*, **19**, 1 (1981).
 52. J. Ceynowa, *Polymer*, **19**, 73 (1978).
 53. R. A. Komoroski, K. A. Mauritz, *J. Amer. Chem. Soc.*, **100**, 7487

- (1978).
54. M. Falk, in "Perfluorinated Ionomer Membranes", ed by A. Eisenberg and H. L. Yeager, ACS Symposium Series No. 180, Washington DC (1982) Chap. 8.
 55. F. G. Will, *J. Electrochem. Soc.*, **126**, 36 (1979).
 56. M. Lopez, B. Kipling, and H. L. Yeager, *Anal. Chem.*, **49**, 629 (1979).
 57. C. R. Martin and K. A. Dollard, *J. Electroanal. Chem.*, **159**, 127 (1983).
 58. T. D. Gierke and W. Y. Hsu, in "Perfluorinated Ionomer Membranes", ed by A. Eisenberg and H. L. Yeager, ACS Symposium Series No. 180, Washington DC (1982) Chap. 13.
 59. T. D. Gierke, G. E. Mann and F. C. Wilson, *J. Polym. Sci., Polym. Phys.*, **19**, 1687 (1981).
 60. H. L. Yeager and A. Steck, *J. Electrochem. Soc.*, **128**, 1880 (1981).
 61. Z. Ogumi, T. Kuroe and Z. Takehara, *J. Electrochem. Soc.*, **132**, 2601 (1985).
 62. R. S. Yeo, *Polymer*, **21**, 432 (1980).
 63. M. N. Szentirmay and C. R. Martin, *Anal. Chem.*, **56**, 1898 (1984).
 64. Z. Ogumi, K. Toyama, Z. Takehara, K. Katakura and S. Inuta, *J. Membrane Sci.*, **65**, 205 (1992).
 65. K. Katakura, M. Inaba, K. Toyama, Z. Ogumi and Z. Takehara, *J. Electrochem. Soc.*, **140**, 1827 (1994).

Part I

Effects of Hydrophilic/Hydrophobic Interactions on the Reduction of Aromatic Nitro Compounds

Chapter 1

Reduction of Nitrobenzene on Modified Pt-Nafion

1.1. Introduction

Electrochemical organic synthesis has many merits and has so far been investigated by many workers. However, only a few processes have been commercialized because of inherent weaknesses in electrochemical methods. One of the greatest problems is that the addition of supporting electrolyte is required. This requirement often leads to difficulties in product isolation and facilitates side reactions. To overcome these problems, Ogumi *et al.*¹⁻⁴⁾ have proposed the application of solid polymer electrolyte (SPE) electrolyzers to electro-organic synthesis. The SPE electrolyzers have been applied to electrolysis of water,⁵⁾ brine,⁶⁾ etc. The advantage of the SPE electrolyzers that no supporting electrolyte is required simplifies product separation and purification and diminishes side reactions.

The electroreduction of nitrobenzene has been a subject of considerable interest because it is one of valuable and promising reactions for industrial

aniline synthesis. The mechanism of the electrochemical reduction of nitrobenzene is complicated, and the distribution of the products is affected by many factors such as electrode material, electrolyte composition, electrode potential, temperature, etc., as shown in Scheme 1.1. In acidic media, the main products are aniline (6-electron process), and *p*-aminophenol and *p*-anisidine (4-electron process followed by Bamberger rearrangement) as shown in Scheme 1.2.^{7,8)} Ogumi *et al.*⁴⁾ studied on the reduction of nitrobenzene on Pt-Nafion, which was prepared by deposition of platinum on Nafion. Although aniline and *p*-aminophenol were obtained on Pt-Nafion, the current efficiencies were low. Platinum is a desirable material for deposition on Nafion as the electrode material because of its chemical stability and easy deposition by electroless plating methods;¹⁾ however, it is not suitable for the reduction of nitrobenzene because of its very low hydrogen overvoltage.

In this chapter, Pt-Nafion is modified by depositing nickel and copper onto the platinum layer bound to Nafion, so that hydrogen overvoltage of Pt-Nafion is enhanced. The modified Pt-Nafion composite electrodes are then utilized for the reduction of nitrobenzene and the effect of the modification on the product distribution is examined. The location of the active sites of the modified electrodes and the influence of Nafion on the reaction selectivity in the reduction of nitrobenzene are discussed.

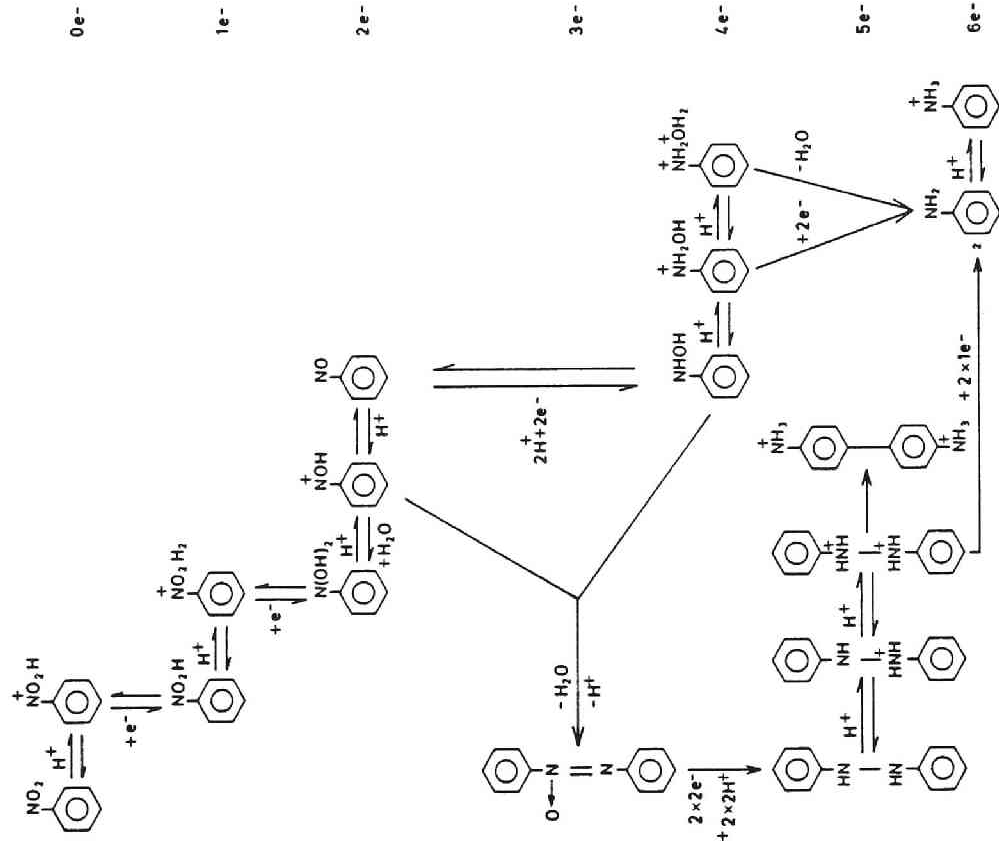
1.2. Experimental

1.2.1. Pt-Nafion

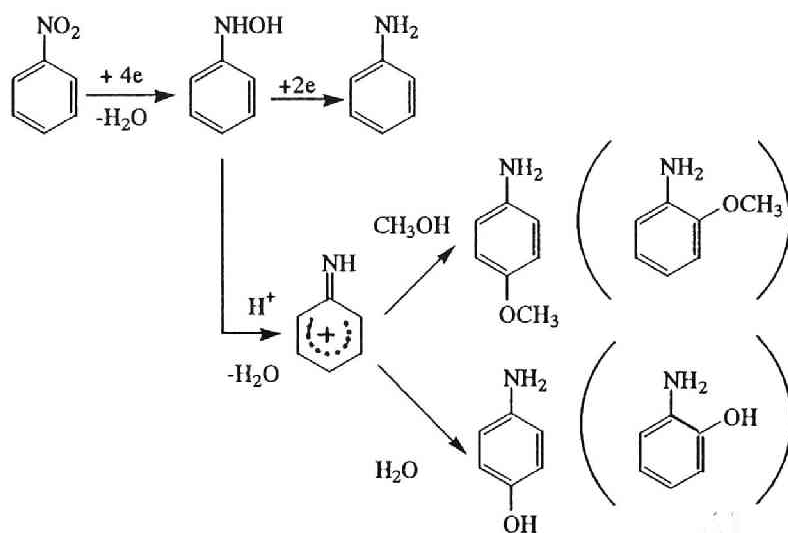
Nafion[®] 415 (product of du Pont Co.) was used as the SPE material. Pt-Nafion was prepared by an electroless plating method reported by Ogumi *et al.*¹⁾ using hydrazine as a reductant.

1.2.2. Modification of Pt-Nafion with Ni and Cu

Method A. Pt-Nafion was immersed in 0.5 M CuSO₄ or 0.5 M NiSO₄ for 12 h, and the counter-ion of Nafion was changed from H⁺ to Cu²⁺ or



Scheme 1.1. Electrochemical reduction of nitrobenzene.



Scheme 1.2. Reaction mechanism for the reduction of nitrobenzene in acidic media.

Ni^{2+} , respectively. After washed with distilled water, the treated Pt-Nafion was mounted in an electrolytic cell shown in Fig. 1.1. Distilled water was filled in the cathode and anode compartments. Counter ion, Cu^{2+} or Ni^{2+} , was cathodically reduced by passing a charge of 3.2 C cm^{-2} at 1.6 mA cm^{-2} . Copper or nickel was deposited on the interior surface of platinum layer of Pt-Nafion.

Method B. After Pt-Nafion was immersed in 0.04 M CuSO_4 for 3-4 h, it was mounted in the electrolytic cell. 0.02 M CuSO_4 and air were filled in the anode and cathode compartments, respectively. The counter-ion, Cu^{2+} , was galvanostatically reduced by passing a charge of 4.2 C cm^{-2} at 5.0 mA cm^{-2} .

Method C. Copper was deposited according to method B except that nitrogen instead of air was passed through the cathode compartment.

Method D. After Pt-Nafion was immersed in 0.04 M CuSO_4 for 3-4 h, it was placed at the bottom of a beaker type cell shown in Fig. 1.2 that was filled with 0.02 M CuSO_4 . Copper was deposited on Pt-Nafion by passing a charge of 4.2 C cm^{-2} at 5.0 mA cm^{-2} .

1.2.3. Electrolysis

The electrolytic cell consisted of two compartments as shown in Fig. 1.1. The SPE composite functioned as a separator dividing the anode and cathode compartments. The effective geometric surface area of the composite electrode was 3.1 cm^2 . The volume of each compartment was 12 cm^3 . Two sheets of expanded Ti mesh covered with platinum gauze were pressed onto both sides of the composite and functioned as current feeders. A methanol solution containing 30% by volume (vol.%) and pure water were used as the catholyte and anolyte, respectively. Electrolysis was carried out galvanostatically using a power supply (Kikusui Electronic Co., Model PAC 55-2).

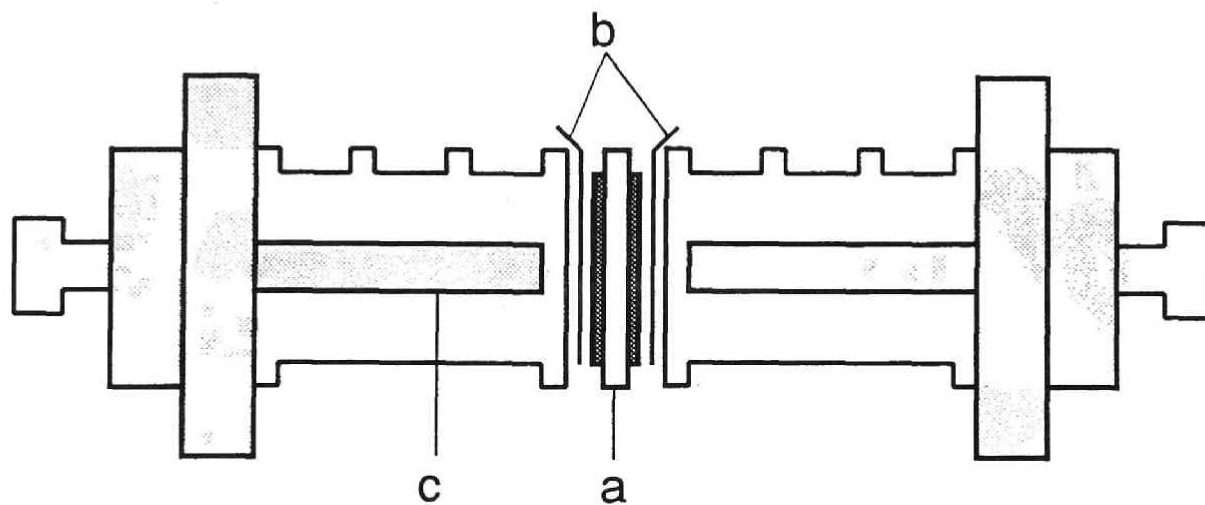


Fig. 1.1. Schematic diagram of the electrolytic cell. (a) SPE composite electrode; (b) Ti mesh covered with Pt gauze; (c) PTFE rod to press Ti mesh onto SPE.

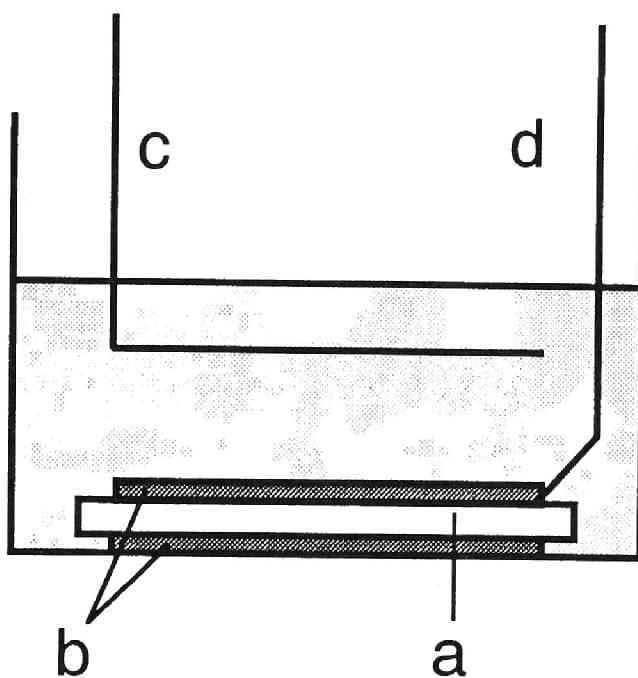


Fig. 1.2. A cell for plating copper on Pt-Nafion by Method D. (a) Pt-Nafion; (b) Platinum bound to Nafion; (c) Pt wire counter electrode, (d) Lead for cathode.

1.2.4. Amounts of deposited copper

Cu,Pt-Nafions prepared by methods A, B and C were immersed in a mixed solution of 20 cm³ of 1 M HCl and 1 cm³ 30% hydrogen peroxide, and the copper layer deposited on the Cu,Pt-Nafion was dissolved. The amount of dissolved copper ion was measured spectroscopically.

1.2.5. Chemicals

Nitrobenzene, methanol, NiSO₄•H₂O, and CuSO₄•5H₂O were of reagent grade (Wako Pure Chemical), and were used without further purification.

1.2.6. Analysis

Product mixtures were analyzed with an HPLC fitted with a Hitachi Gel 3010 column. The isolated products were identified by IR spectroscopy. Acetophenone was used as the internal standard for quantitative analysis.

1.3. Results

1.3.1. Copper deposition

The amounts of copper deposited by methods A, B and C were 0.7, 1.2, and 1.4 mg cm⁻², respectively. By method A, the copper ion that resided in Nafion as the counter-ion was deposited. The amount of deposited copper (0.7 mg cm⁻²) was consistent with the value calculated from the exchange capacity of Nafion 415. Despite the same charge passed for the copper deposition, the amount of copper deposited by method B was less than that by method C. By method B, the reduction of oxygen in the air filled in the cathode compartment competed with the copper deposition.⁹⁾ This is the reason for the observed difference in the amounts of copper deposited by methods B and C. It is reasonable to consider that in the three methods, A, B and C, copper was deposited on the interior surface of the platinum layer of Pt-

Nafion, where the membrane and the platinum layer overlapped. This was supported by the observation that only the interior surface of the platinum layer of Pt-Nafion changed in color from gray (Pt) to brown (Cu) during copper deposition while the exterior surface remained gray. In the case of method D, on the other hand, the color of the exterior surface of the platinum layer changed from gray to brown. This clearly shows that copper was deposited mainly on the exterior surface of platinum layer of Pt-Nafion by method D.

1.3.2. Ni,Pt-Nafion

Constant current electrolysis was carried out using Ni,Pt-Nafion prepared by method A. Figure 1.3 shows the current efficiencies for aniline and *p*-aminophenol production after 2000 C were passed. It was previously reported by Ogumi *et al.* that the current efficiencies for aniline and *p*-aminophenol production on Pt-Nafion were ca. 30% and ca. 15%, respectively.⁴⁾ The current efficiency for aniline production was enhanced markedly by the deposition of nickel on Pt-Nafion. This indicates that nickel deposition on Pt-Nafion resulted in an enhanced hydrogen overvoltage. On the other hand, the current efficiency for *p*-aminophenol production was lowered. Consequently, the deposition of nickel on Pt-Nafion enhanced a selectivity for aniline production. Solanki¹⁰⁾ reported that electrochemical reduction of nitrobenzene on a nickel cathode in an ethanol solution containing sulfuric acid gave aniline at a current efficiency of 52%. The acidity in Nafion used as the SPE material was estimated from its exchange capacity and water up-take to be as strong as 1-3 M sulfuric acid. Under the present electrolytic conditions, water, which permeates from the anode compartment through Nafion, and methanol in the catholyte undergo mixing in the vicinity of the reaction sites. Therefore the conditions at the reaction sites in Ni,Pt-Nafion should be similar to those in the case of Solanki. This similarity can explain the comparable current efficiencies for aniline production.

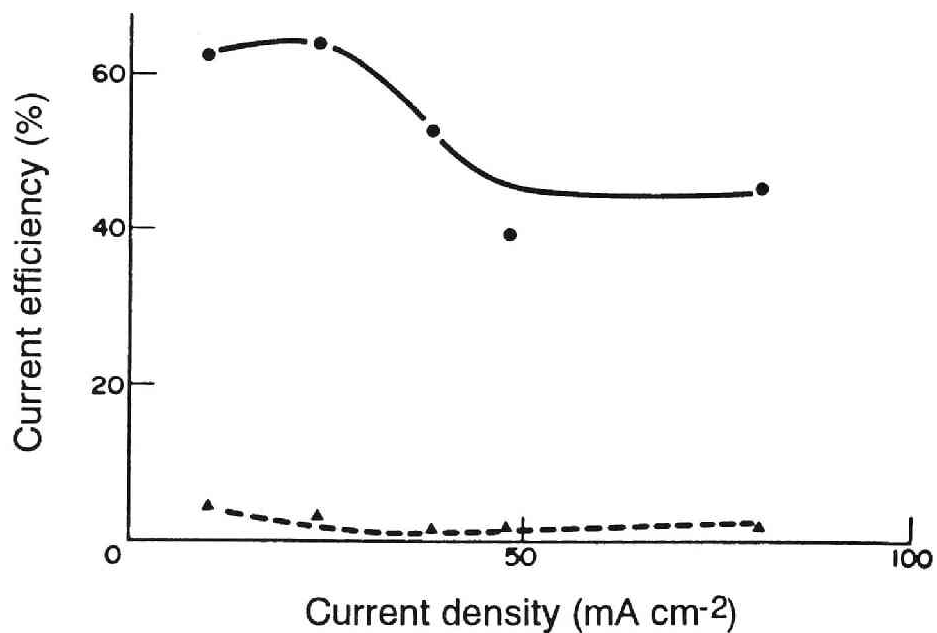


Fig. 1.3. Dependencies of current efficiencies for aniline and *p*-aminophenol formation on current density on Ni,Pt-Nafion in nitrobenzene 30% in methanol. ●; aniline, ▲; *p*-aminophenol.

1.3.3. *Cu,Pt-Nafion*

Cu,Pt-Nafion was expected to have a higher hydrogen overvoltage than Ni,Pt-Nafion, and was applied to the reduction of nitrobenzene under similar conditions. Figure 1.4 shows the dependencies of the current efficiency for aniline production and the terminal voltage on the current density. Curves A, B and C in Fig. 1.4 correspond to the results using the Cu,Pt-Nafion composite electrodes prepared by methods A, B and C, respectively. Although Pt-Nafion and Ni,Pt-Nafion gave *p*-aminophenol, no *p*-aminophenol was produced on Cu,Pt-Nafion. Only hydrogen was formed as a side reaction on the latter composite electrode. Cu,Pt-Nafion prepared by method C gave a current efficiency as high as 98%. While an increase in the amount of deposited copper up to 1.4 mg cm^{-2} led to a higher current efficiency for aniline formation, the amount of copper deposition beyond 1.4 mg cm^{-2} did not enhance the current efficiency further. The terminal voltage was as low as 4 V at 130 mA cm^{-2} , and remained unchanged for more than several hours. The terminal voltage was not affected by a change in the amount of deposited copper. The linear current density dependence of the terminal voltage suggests that the ohmic drop through the membrane is responsible for the major part of the terminal voltage. Figure 1.5 shows the dependencies of the current efficiency and terminal voltage on current density using the composite electrode prepared by method D. Despite the same amount of copper as that by method C, the current efficiency was at most 70%, and hydrogen evolution was observed during electrolysis.

1.4. Discussion

Electrolytic deposition of copper on Pt-Nafion should preferentially cover the electrochemically active platinum surface. An effective surface roughness factor of 6 was reported for Pt-Nafion in Kolbe-type reactions.³⁾ SEM micrographs of the surface of platinum deposited by the electroless plating method showed a very rough surface similar to platinum black. This large

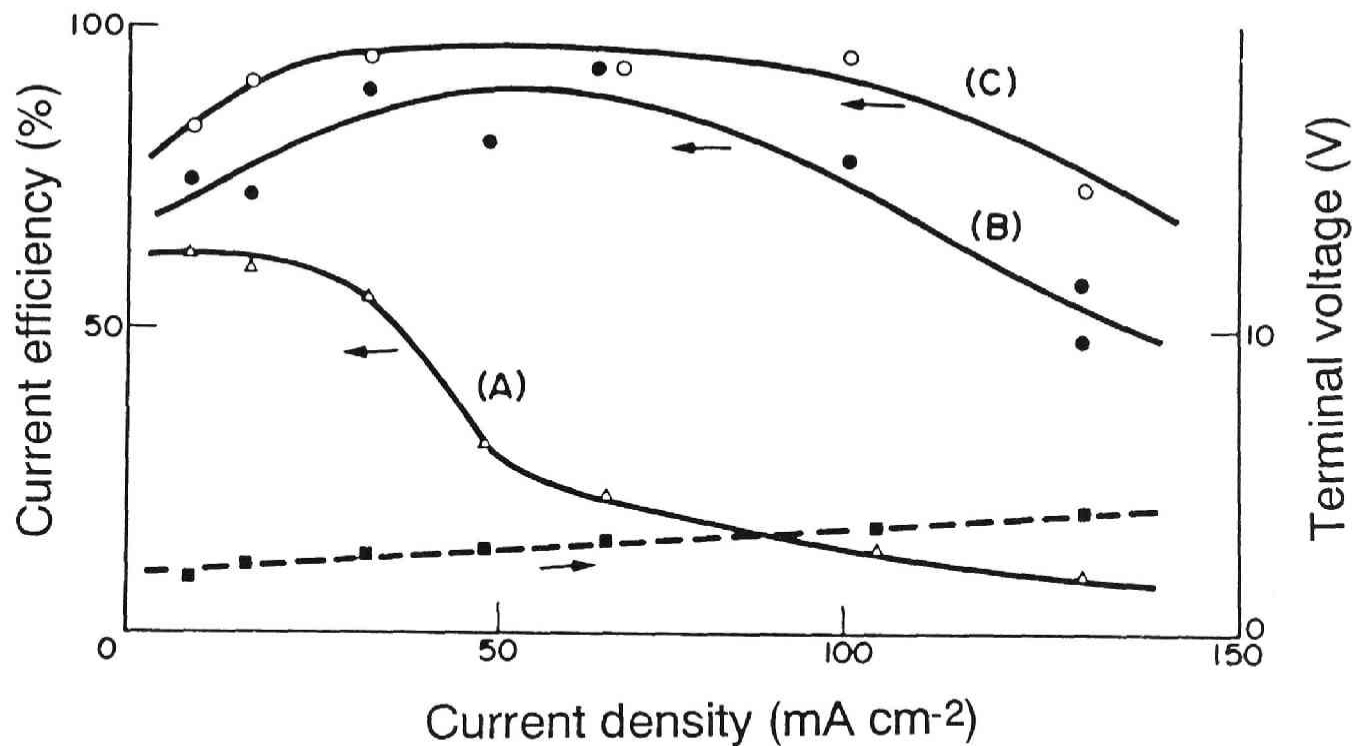


Fig. 1.4. Dependencies of current efficiency for aniline formation and terminal voltage on current density on Cu,Pt-Nafion prepared by Methods A (Δ), B (\bullet), and C (\circ) in nitrobenzene 30% in methanol. \blacksquare ; Terminal voltage.

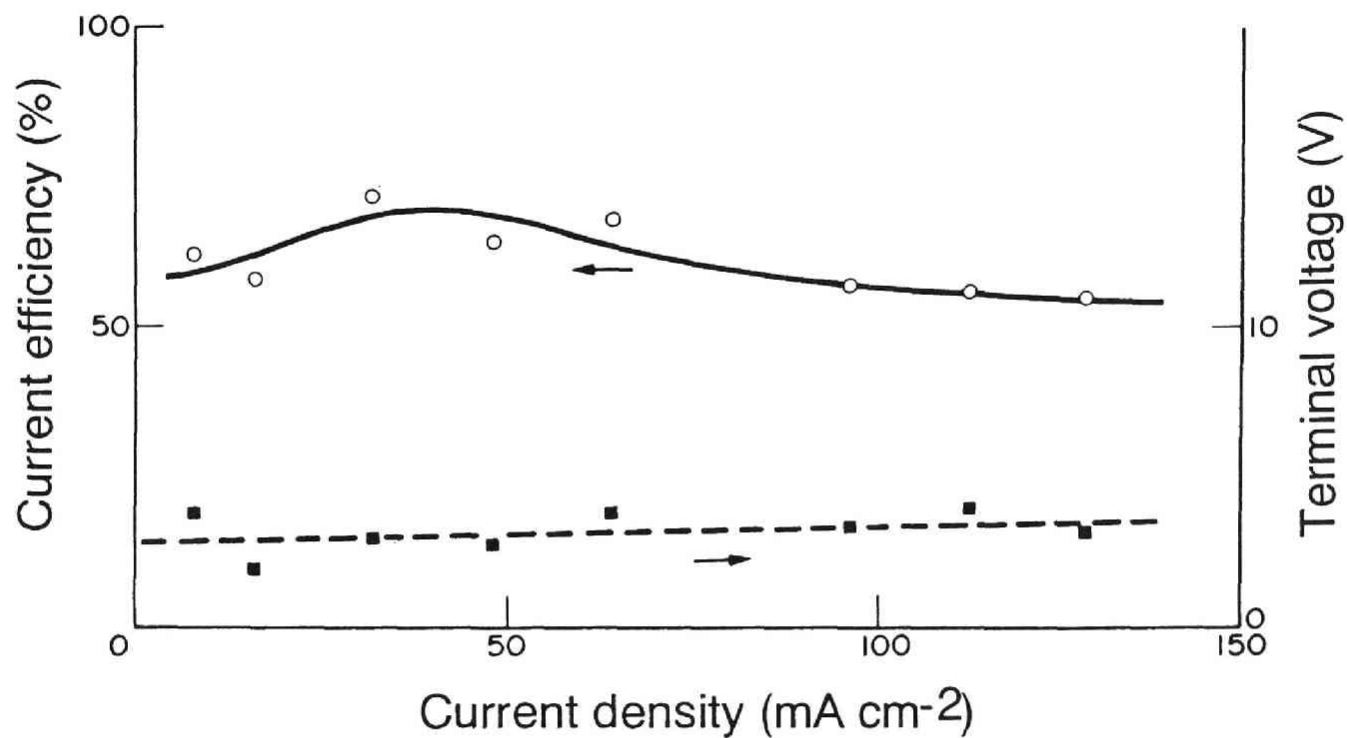


Fig. 1.5. Dependencies of current efficiency for aniline production and terminal voltage on Cu,Pt-Nafion prepared by Method D in nitrobenzene 30% in methanol.

surface area required a copper deposition of 1.4 mg cm^{-2} in order to cover the whole active platinum surface bound to Nafion effectively. When copper deposition was less than 1.4 mg cm^{-2} , the remaining bare platinum surface was used for hydrogen evolution. The current efficiency for aniline production was consequently low as shown by curves A and B in Fig. 1.4. Although copper might be oxidized by oxygen in air, the oxidized copper was reduced during the next electrochemical reduction process and effectively re-deposited on the platinum surface. Although bare platinum might have remained after deposition of 1.4 mg cm^{-2} , it was not active for the reduction of nitrobenzene at low current densities. At higher current densities, the penetration depth of current into the electrode layer embedded on Nafion becomes deeper, and the platinum surface that remains uncovered with copper begins to function as the active sites for hydrogen evolution. The current efficiency for aniline production thus decreased at current densities greater than 100 mA cm^{-2} .

In the SPE method, mass transport is complicated. In the reduction of nitrobenzene, the reactant and product must move to and from the active sites on the electrode deposited on Nafion through a thin porous electrode layer, respectively. It is important to know about the location of the active sites for a charge transfer reaction on SPE composite electrodes in order to improve performance. Two typical cases are schematically shown in Fig. 1.6. In case (a), the active sites are located at the interior surface of the deposited metal layer (in contact with Nafion). In case (b), the active sites are located at the exterior surface. In the former case, nitrobenzene must move through the porous metal layer, and the reaction would be affected by the polymer (Nafion) surrounding the reaction sites. In the latter case, charge has to be carried by ionic species through the catholyte penetrating into the porous metal layer. Since the catholyte did not contain any ionic species, ionic conduction was difficult. On the Cu,Pt-Nafion composite electrodes prepared by methods A, B and C, the interior surface of platinum layer should be covered by copper [case (a) in Fig. 1.6]. On the other hand, in the case of Cu,Pt-Nafion prepared by method D, most of the deposited copper should cover the exterior

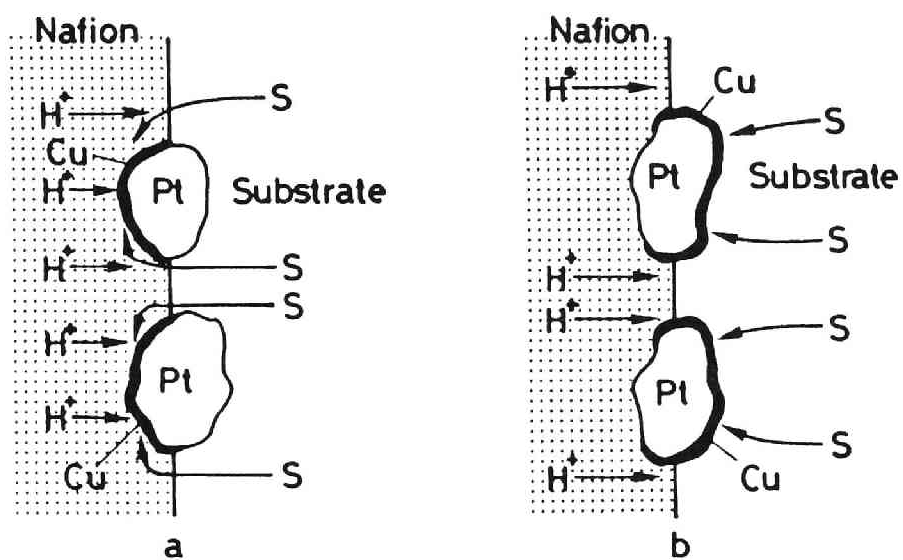


Fig. 1.6. Schematic figures of the active site on Pt-Nafion. The active sites are located at the inner (a) and out (b) side of deposited platinum.

surface of the platinum layer [case (b) in Fig. 1.6]. On the latter electrode, the enhancement of the current efficiency was less pronounced than on the former electrodes (see Fig. 1.5 and curve C in Fig. 1.4). These results suggest that copper coating on the exterior surface of the platinum layer was not effective as a modifier of Pt-Nafion. It is therefore concluded that the active sites are located on the interior surface of the platinum layer deposited on Nafion. Nitrobenzene is known to receive electrons directly from cathode. The electron transfer is a key step;^{7,8)} hence, the charge transfer reaction takes place on the interior surface of the deposited metal on SPE composite electrodes. This conclusion does not contradict a result reported by Ogumi *et al.*²⁾ that the electrochemical hydrogenation took place on the exterior surface of the deposited Pt-layer of Pt-Nafion. In the hydrogenation, the reaction proceeds through an initial charge transfer to protons followed by a catalytic chemical reaction. This following chemical reaction takes place on the exterior surface of Pt-Nafion. In their paper the active sites for the charge transfer reaction were not discussed. In electrochemical hydrogenation, the charge transfer reaction would take place on the interior surface as concluded in this chapter. The atomic hydrogen, which is produced by the charge transfer reaction, can move fairly rapidly through the platinum layer¹¹⁾, and could easily reach the exterior surface of the platinum layer, where it participates in the hydrogenation.

It should be noted that aniline was selectively formed on Cu,Pt-Nafion. Marquez and Pletcher¹²⁾ reported that *p*-aminophenol was a major product in the reduction of nitrobenzene in 3 M H₂SO₄ in acetone/water (50:50 by volume) at a copper cathode. As discussed above, the reaction sites on Cu,Pt-Nafion are located at the interior surface of deposited metal which is in contact with the Nafion. The acidity of Nafion is calculated to be as strong as 1-3 M H₂SO₄; the present reaction conditions are similar to those of Marquez and Pletcher.¹²⁾ In contrast to their results, no *p*-aminophenol was obtained in the present conditions. The Bamberger rearrangement of the intermediate, which is catalyzed by acid, gives *p*-aminophenol.^{7,8)} This rearrangement was inhibited in the present conditions regardless of the similar

acidity at the reaction site. This inhibition is attributable to the influence of Nafion that covers the active surface of Cu,Pt-Nafion. Details of the effect are not yet clear, but some hydrophobic interactions between Nafion and the intermediates are inferred. The influence of Nafion on reaction selectivity will be discussed in subsequent chapters.

1.5. Conclusion

Electrolytic plating of copper or nickel on Pt-Nafion modified the electrochemical properties of Pt-Nafion. This technique expands the application area of Pt-Nafion. The modification was very effective in the reduction of nitrobenzene, and the current efficiency for aniline formation was enhanced beyond 95% on Cu,Pt-Nafion. On the copper-modified composite electrode, aniline was predominantly produced despite strongly acidic conditions at the reaction sites. The reaction selectivity that favored aniline formation was attributable to the influence of Nafion. The charge transfer reaction of nitrobenzene was concluded to take place at the interior surface of the metal layer deposited on Nafion.

References

1. Z. Ogumi, K. Nishio, and S. Yoshizawa, *Denki Kagaku*, **49**, 2124 (1981).
2. Z. Ogumi, K. Nishio, and S. Yoshizawa, *Electrochim. Acta*, **26**, 1179 (1981).
3. Z. Ogumi, H. Yamashita, K. Nishio, Z. Takehara, and S. Yoshizawa. *Electrochim. Acta*, **28**, 1687 (1983).
4. Z. Ogumi, H. Yamashita, K. Nishio, and Z. Takehara, *Denki Kagaku*, **52**, 180 (1984).
5. P. W. Lu and S. Srinivasan, *J. Appl. Electrochem.*, **9**, 269 (1979).
6. General Electric Co., *Japan Patent Koukai*, Shou 53-102278 (1978).

7. M. M. Baizer (ed.), *Organic Electrochemistry*, Marcel Dekker, New York (1973).
8. M. R. Rifi and F. H. Covitz, *Introduction to Organic Electrochemistry*, Marcel Dekker, New York (1974).
9. Z. Ogumi, N. Yoshida, Z. Takehara, and S. Yoshizawa, *Denki Kagaku*, **52**, 503 (1984).
10. D. N. Solanki, *Trans. Electrochem. Soc.*, **88**, 98 (1945).
11. S. Yoshizawa and K. Yamakawa, *Boushoku Gijyutsu*, **24**, 365, 511 (1975).
12. J. Marquez and D. Pletcher, *J. Appl. Electrochem.*, **10**, 576 (1980).

Chapter 2

Effects of Solvents on the Electroreduction of Nitrobenzene on Cu,Pt-Nafion

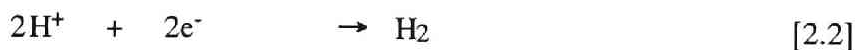
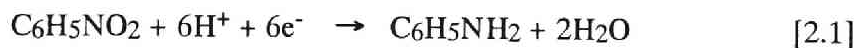
2.1. Introduction

The application of solid polymer electrolyte (SPE) electrolyzers to organic syntheses has been reported by Ogumi *et al.*¹⁻³⁾ The SPE method eliminates the need for a supporting electrolyte, the addition of which often leads to difficulties in subsequent product purification processes and to unwanted side reactions.

In chapter 1, the reduction of nitrobenzene using Cu-modified Pt-Nafion was studied.⁴⁾ The charge transfer reaction was found to proceed at the interface between the Nafion and the platinum layer of SPE composite electrodes. Deposition of copper on the platinum surface in contact with the Nafion suppressed hydrogen evolution, and nitrobenzene was reduced preferentially to aniline with current efficiencies greater than 95%. These results imply that some interactions between nitrobenzene and Nafion may be at work.

Chen *et al.*⁵⁾ have previously reported on the effects of solvents on the oxidation of cinnamyl alcohol to cinnamaldehyde using Pt-Nafion incorporating a manganese redox couple. When an aqueous solution was used as the catholyte, solvents in the anolyte such as tetrahydrofuran (THF) or dimethyl ether, which have high solubility in water, were adequate for the electrooxidation of cinnamyl alcohol to cinnamaldehyde. On the other hand, when carbon tetrachloride, which has low solubility in water, was used as a solvent in the anolyte, oxygen evolution became dominant. The structure of Nafion is generally accepted to be microscopically separated into two phases: hydrophilic ionic clusters and hydrophobic polytetrafluoroethylene-like backbones.^{6,7)} The active sites of the SPE composite electrode are located in the ionic clusters in the Nafion, and the manganese redox couple is also found in this region. Since cinnamyl alcohol is sparingly soluble in water, it is difficult for cinnamyl alcohol to penetrate into the ionic clusters, and therefore to reach the reactive sites on the anode, without the help of a co-solvent. Therefore, it was concluded that a solvent that is highly soluble in water is necessary to facilitate the mass transport of cinnamyl alcohol.

In this chapter, the effects of solvents on the electroreduction of nitrobenzene was studied using Cu-modified Pt-Nafion. It is known that various reaction products are obtained by the electroreduction of nitrobenzene.^{8,9)} On Cu-modified Pt-Nafion in chapter 1, however, aniline was obtained as the sole organic product, and other complicated reactions did not occur.⁴⁾ Hence, the following two reactions are expected to proceed competitively on the electrode.



Both nitrobenzene and proton receive electrons directly from the electrode. Since the nitrobenzene in Eq. [2.1] is sparingly soluble in water, it cannot

penetrate by itself into the ionic clusters where the active sites of the SPE composite electrode are located. A sufficient amount of a co-solvent is necessary in order for nitrobenzene to penetrate into the ionic clusters and receive electrons from the electrode. Proton can be reduced at the active sites of the electrode, since they can move through the ionic clusters. When the mass transport of nitrobenzene is insufficient, hydrogen evolution becomes dominant on the electrode. Such mass transport of nitrobenzene from the electrolyte to the active sites of the SPE composite electrode is discussed in detail in this chapter.

2.1. Experimental

2.1.1. Pt-Nafion

A perfluorosulfonate cation-exchange membrane, Nafion[®] 415 (E. I. du Pont de Nemours and Co.) was used as the SPE material. After treating the Nafion 415 membrane in boiling water, platinum was deposited on one side of the membrane by an electroless plating method reported by Ogumi *et al.* that uses NaBH₄ as a reductant.¹⁰⁾

2.2.2. Modification of Pt-Nafion with copper (Cu,Pt-Nafion)

Pt-Nafion was immersed in 0.5 M CuSO₄ for about 12 h in order to change the counter-ion in the Nafion membrane to Cu²⁺. After washing the Cu²⁺-loaded Pt-Nafion well with distilled water, it was mounted in the electrolytic cell shown in Fig. 2.1. The anode compartment was filled with 0.1M CuSO₄ and argon gas was passed through the cathode compartment. A platinum wire was used as the counter electrode. Copper ion was cathodically reduced on the interior surface of the platinum of the Pt-Nafion by passing a charge of 4.2 C cm⁻² at a constant current of 5 mA cm⁻². The total amount of Cu deposited on the Pt and incorporated into the Nafion was measured spectroscopically to be about 1.4 mg cm⁻².⁴⁾ The resulting Cu-modified Pt-Nafion is referred to herein as "Cu,Pt-Nafion".

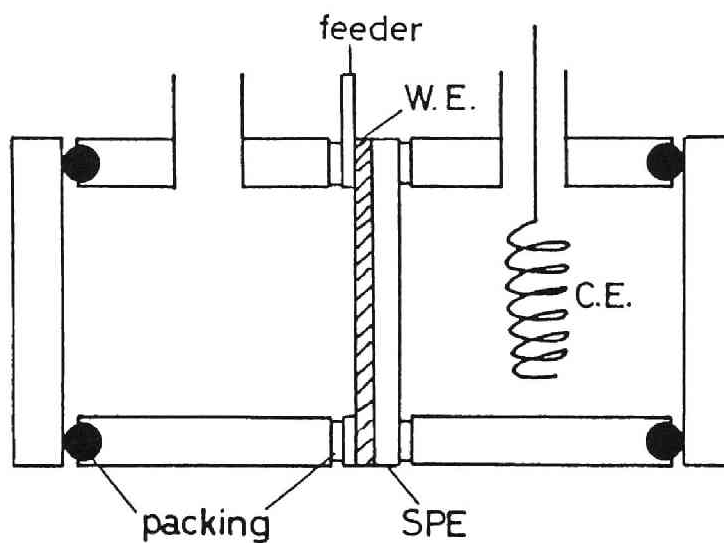


Fig. 2.1. Schematic diagram of electrolytic cell. WE = porous platinum cathode deposited on Nafion-415 solid polymer electrolyte; SPE = Nafion 415; CE = platinum wire anode; feeder = gold ring current feeder.

2.2.3. *Electrolytic cell*

The electrolytic cell, shown in Fig. 2.1, was composed of two compartments which were separated by the SPE composite electrode. The effective geometric surface area of the SPE composite electrode was 3.1 cm². A platinum wire was used as the counter electrode. The volume of each compartment was 6 cm³. The current feeder for the SPE composite electrode consisted of a gold ring, which was pressed onto the outer surface of the deposited Pt. During runs, the cathode compartment (left-hand side) was filled with nitrobenzene/alcohol solution, and the anode compartment (right-hand side) was filled with aqueous 0.025 M H₂SO₄ (unless otherwise noted).

Electrolysis was carried out at a constant current of 32 mA cm⁻², using a potentiostat/galvanostat (Hokuto Denko, HA301). The total charge passed during each run was 800 C.

2.2.4. *Product analysis*

Product mixtures were analyzed by HPLC, using a Hitachi 638-30 liquid chromatograph fitted with a Zorbax ODS column (du Pont Co.). After electrolysis, the catholyte was analyzed without pre-treatment.

2.2.5. *Chemicals*

All chemicals were of reagent grade, and were used without further purification.

2.3. **Results and Discussion**

2.3.1. *Effect of nitrobenzene concentration in catholyte*

Nitrobenzene was reduced galvanostatically with several different concentrations of nitrobenzene in the catholyte, which consisted of nitrobenzene and methanol, using an aqueous sulfuric acid solution as the anolyte. The variation of the current efficiency for aniline production is shown in Fig. 2.2. Nitrobenzene was reduced to aniline at current efficiencies of about 80% at nitrobenzene concentrations less than about 70 vol.%. No products except ani-

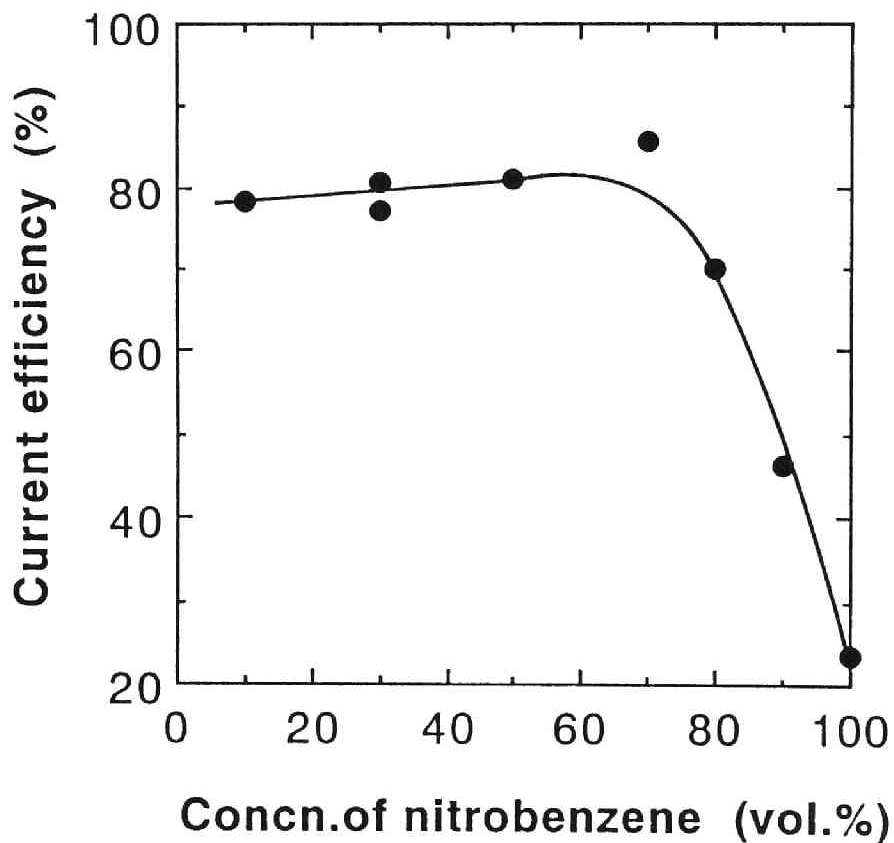


Fig. 2.2. Variation of current efficiency for aniline production with nitrobenzene concentration in the catholyte of methanol solution. The anolyte was aqueous 0.025 M H₂SO₄. $I = 32 \text{ mA cm}^{-2}$.

line were detected by HPLC. These results are in good agreement with those in chapter 1.⁴⁾ The current efficiency losses are attributed to hydrogen evolution and to aniline accumulation inside the SPE composite.

The aniline production current efficiency suddenly decreased at nitrobenzene concentrations above 80 vol.% (Fig. 2.2). No other products were detected by HPLC at these concentrations, and hydrogen evolution was observed as a side reaction.

When an aqueous solution is used as the anolyte, nitrobenzene cannot penetrate into the hydrophilic ionic clusters in the Nafion membrane because of its low solubility in water. The active sites for charge-transfer reactions in SPE composite electrodes are located in the ionic clusters at the metal/Nafion interface. Consequently, without a sufficient amount of a co-solvent (methanol in these experiments), the mass transport of nitrobenzene to the active sites of the SPE composite electrode is suppressed, and hydrogen evolution becomes significant. At high concentrations of methanol, the methanol helps the nitrobenzene to penetrate into the ionic cluster region, where the nitrobenzene can receive electrons from the electrode.

Aniline was the sole organic product obtained over the entire concentration range. It is well known that in acidic solutions *p*-aminophenol^{8,11)} and *p*-anisidine¹²⁾ also produced, *via* Bamberger rearrangement of phenylhydroxylamine intermediate, in addition to aniline.⁸⁾ The acidity of the type of Nafion used as the SPE material (H⁺-form) has been estimated to be comparable with that of 1-3 M sulfuric acid,¹³⁾ based on its exchange capacity and water uptake. Hence, the reduction of nitrobenzene was carried out in a highly acidic environment. However, production of *p*-aminophenol and *p*-anisidine was suppressed. Although the reasons for the selective aniline production observed with the SPE method are not yet completely clear, it is inferred that the selectivity involves interactions between nitrobenzene and Nafion, the interactions being related to the complex structure of Nafion.^{6,7,13,18)}

2.3.2. *Effect of methanol concentration in anolyte*

The mass transport of nitrobenzene to the active sites of SPE composite electrodes may also be facilitated by methanol permeating through the Nafion membrane from an anolyte containing methanol to the active sites. The effect of methanol concentration in the anolyte was examined using pure nitrobenzene as the catholyte. An as-prepared SPE composite is swollen only with water, and does not contain methanol. Therefore, it was necessary to equilibrate the SPE composites with the anolyte prior to the electrolysis. The SPE composite was immersed in a solution of the same composition as the anolyte before each electrolysis. The effect of immersion time is shown in Fig. 2.3. The anolyte was a solution of 0.1 M H₂SO₄ in 1:1 (by volume) methanol/water. The current efficiency for aniline production increased with immersion time up to 5 h. Beyond 5 h, the current efficiency remained constant at about 50%. Consequently, the SPE composite was considered to be equilibrated with a 1:1 methanol/water solution after immersion of 5 h. However, at other concentrations, especially at methanol concentrations higher than 50 vol.%, a longer time may be required for the SPE composite to be equilibrated. Therefore, a longer immersion time of 10 h was used in the subsequent experiments.

The dependence of the current efficiency for aniline production on the concentration of methanol in the anolyte is shown in Fig. 2.4. Aniline was the only product detected by HPLC, and hydrogen evolution occurred as a side reaction. The current efficiency was low at methanol concentrations below 50%, but increased with increasing methanol concentration. Hence, the mass transport of nitrobenzene to the active sites of the SPE composite electrode was facilitated by methanol supplied from the anolyte. However, the current efficiencies were lower than those obtained in the previous section, showing that methanol is more effective as a co-solvent in the catholyte than in the anolyte.

When the anolyte contains methanol, some of the aniline produced on the cathode may permeate through the Nafion membrane into the anolyte. However, as shown in Fig. 2.4, the current efficiency for aniline permeation

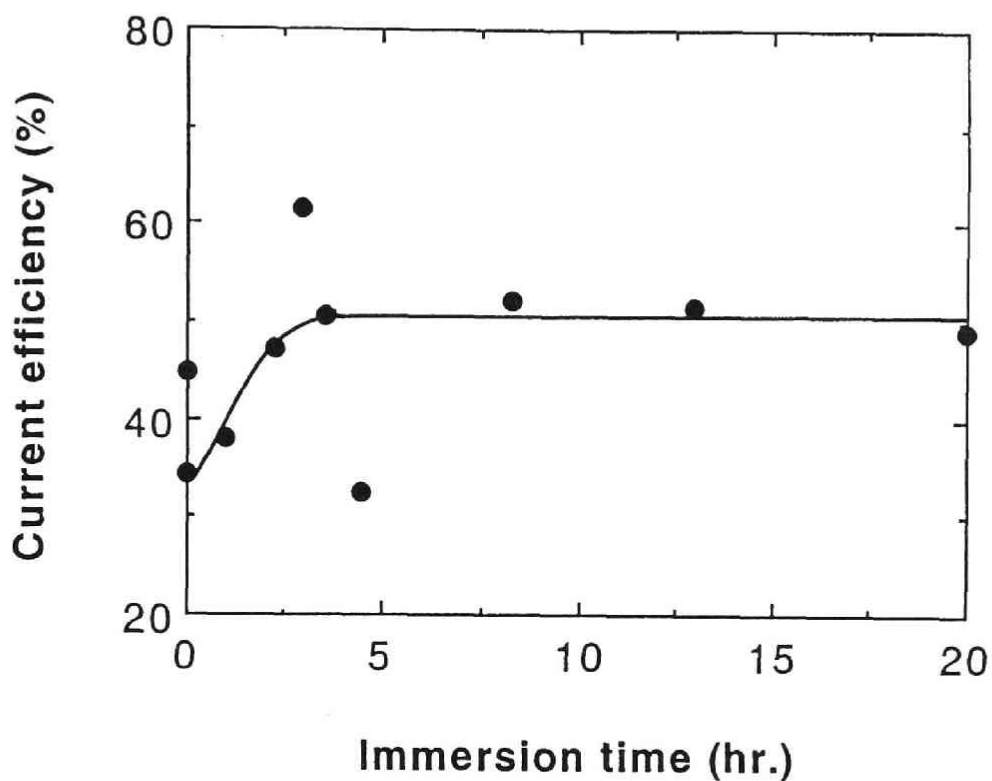


Fig. 2.3. Variation of current efficiency for aniline production with pre-immersion time of Cu,Pt-Nafion in methanol/water (1:1) solution. The catholyte and anolyte were pure nitrobenzene and a methanol/water (1:1) solution containing 0.1 M H₂SO₄, respectively. $I = 32 \text{ mA cm}^{-2}$.

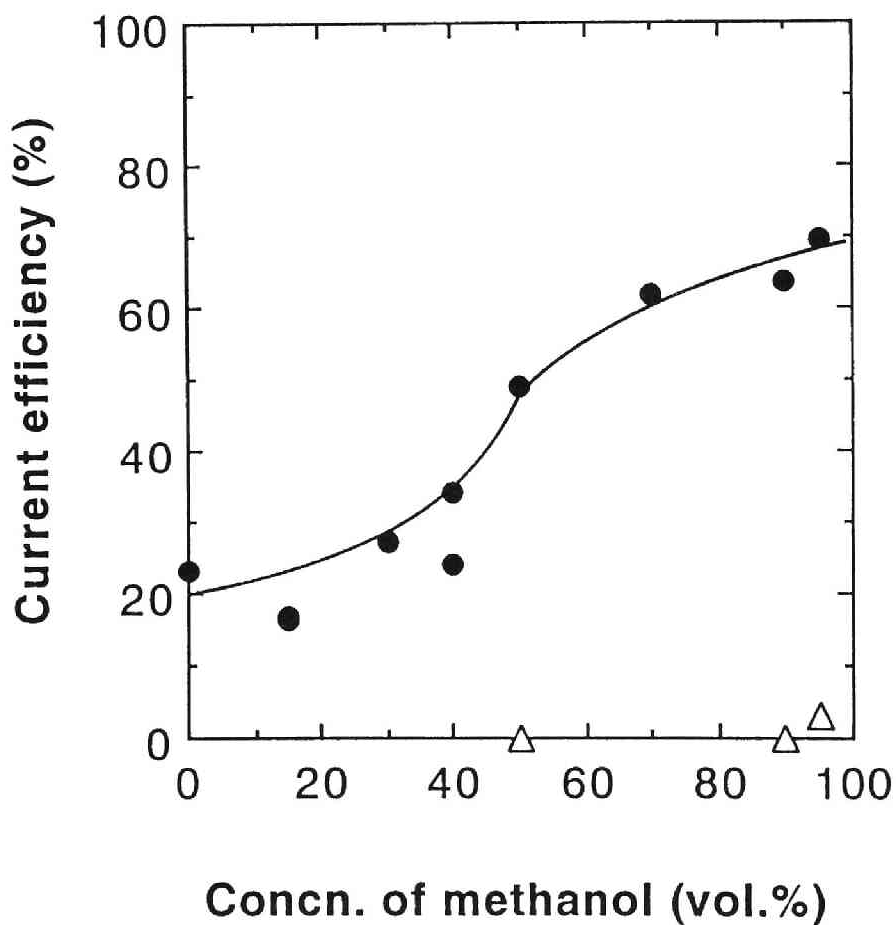


Fig. 2.4. Variation of current efficiency for aniline production (●) with methanol concentration in the anolyte; △ : aniline recovered from anolyte. The catholyte was pure nitrobenzene. The anolyte contained 0.1 M H₂SO₄. $I = 32 \text{ mA cm}^{-2}$.

to the analyte was lower than 1% at a methanol concentration of 90 vol.%, and 3.2% at 95 vol.%.

2.3.3. Effect of different solvents in catholyte

The mass transport of nitrobenzene to the active sites of the SPE composite electrode is expected to depend on the solubility of the solvents in water. *Normal*-alkyl alcohols with different chain lengths were examined as solvents, and the effect of the chain length was elucidated. The variation of current efficiency for aniline production with the chain length (N) of the alcohols is shown in Fig. 2.5. The concentration of nitrobenzene was 30 vol.%, and the analyte was aqueous 0.025 M H₂SO₄. While nitrobenzene was reduced to aniline at a current efficiency greater than 70% when N ≤ 4, the current efficiency decreased significantly at N ≥ 5. The solubilities of *n*-alkyl alcohols in water are listed in Table 2.1.¹⁴⁾ *Normal*-alkyl alcohols with N ≤ 3 are freely miscible with water. These alcohols improve the mass transport of nitrobenzene to the active sites of the SPE composite electrode. The solubilities of *n*-alkyl alcohols with N ≥ 5 in water are low. This low miscibility leads to retardation of the mass transport of nitrobenzene, and accordingly, hydrogen evolution becomes significant. It should be noted that the current efficiency at N = 4 was as high as those at N ≤ 3, even though the solubility of 1-butanol in water is only 7.9 wt.%. This fact indicates that even a relatively small amount of co-solvent in the ionic clusters can facilitate the mass transport of nitrobenzene.

2.3.4. Correlation of results with solubility parameters

The solubility parameter, δ , which has been proposed by Hildebrand,¹⁵⁻¹⁷⁾ is often used on discussing mutual solubility. It is defined as

$$\delta^2 = c = \Delta U_{\text{vap}} / V_0 = (\partial U / \partial V)_T \quad [2.3]$$

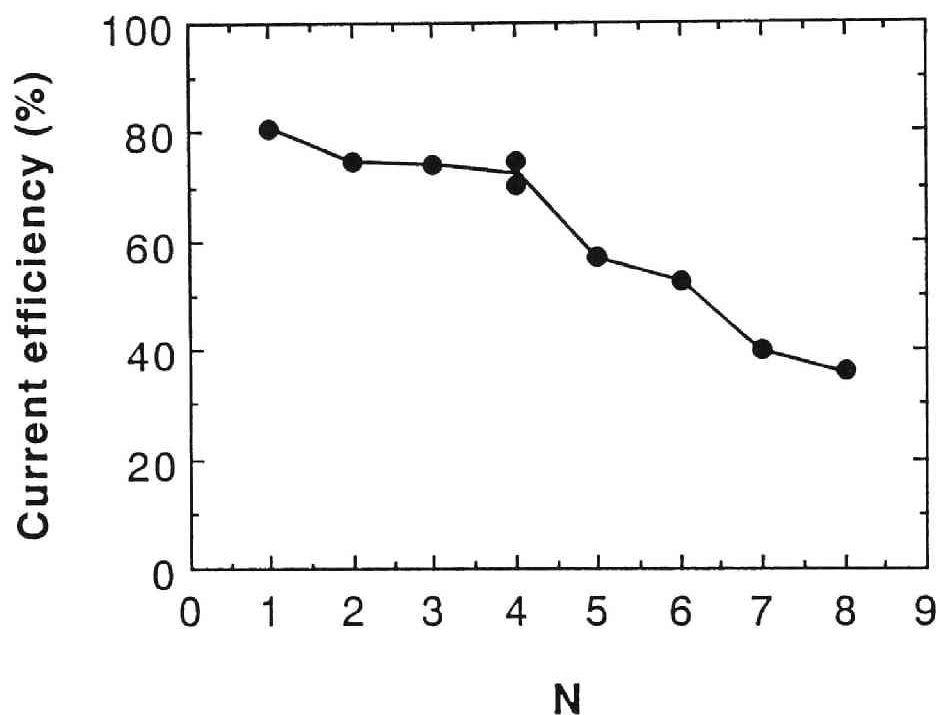


Fig. 2.5. Variation of current efficiency for aniline production with chain length (N) of *n*-alkyl alcohol solvent in the catholyte. The catholyte contained 30 vol.% nitrobenzene. The anolyte was aqueous 0.025 M H₂SO₄. $I = 32 \text{ mA cm}^{-2}$.

Table 2.1. Solubilities of *n*-alkyl alcohols in water.¹⁴⁾

Alcohols	Solubility in water (g/100ml water)
Methanol	∞
Ethanol	∞
1-Propanol	∞
1-Butanol	7.9
1-Pentanol	2.4
1-Hexanol	0.6
1-Heptanol	0.2
1-Octanol	0.05

where c is the cohesive energy density, ΔU_{vap} is the vaporization energy, V_0 is the molar volume, and $(\partial U / \partial V)_T$ is the internal pressure. The basic assumption in the solubility parameter concept is that there is a correlation between the cohesive energy density (potential energy per unit volume) and mutual solubility. It is well known that a good solvent for a certain solute such as a polymer has a "solubility parameter" value close to that of the solute. The values of the solubility parameter of a mixed solvent can be calculated using the following expression:¹⁵⁾

$$\delta_{\text{mix}} = \sum \phi_i \delta_i \quad [2.4]$$

where ϕ_i is the volume fraction of each of the components of the mixed solvent, and δ_i is the solubility parameter of the corresponding pure solvent. The current efficiencies in Figs. 2.2 and 2.5 are plotted against δ_{mix} of the catholyte¹⁵⁾ in Fig. 2.6. The results from the different experiments fall on the same curve. This fact indicates that the solubility parameter value of the catholyte, that is, the solubility of the catholyte in the Nafion membrane, primarily determines the efficiency for nitrobenzene reduction on Cu,Pt-Nafion.

Nafion is known to have two solubility parameter values.^{16,17)} Figure 2.7 shows the solvent uptake in Nafion (EW = 1200) plotted against solubility parameter value reported by Yeo.¹⁶⁾ Using the structural model proposed by Gierke *et al.*,⁶⁾ Yeo concluded that solvents with δ in the range of envelope I strongly interact with the hydrophobic backbone, and that solvents with δ in the range of envelope II interact with the ionic clusters. Yeager and Steck¹⁸⁾ and Ogumi *et al.*¹³⁾ have proposed the existence of an hydrophobic amorphous region which consists of the flexible amorphous part of the PTFE backbone and the side chains of Nafion. It is reasonable to consider that the solvents with δ in the range of envelope I interact with this amorphous region.

Water, with a solubility parameter of $23.4 \text{ cal}^{1/2} \text{ cm}^{-3/2}$,¹⁵⁾ interacts with the ionic clusters. Nitrobenzene, with δ of $10 \text{ cal}^{1/2} \text{ cm}^{-3/2}$,¹⁵⁾ interacts

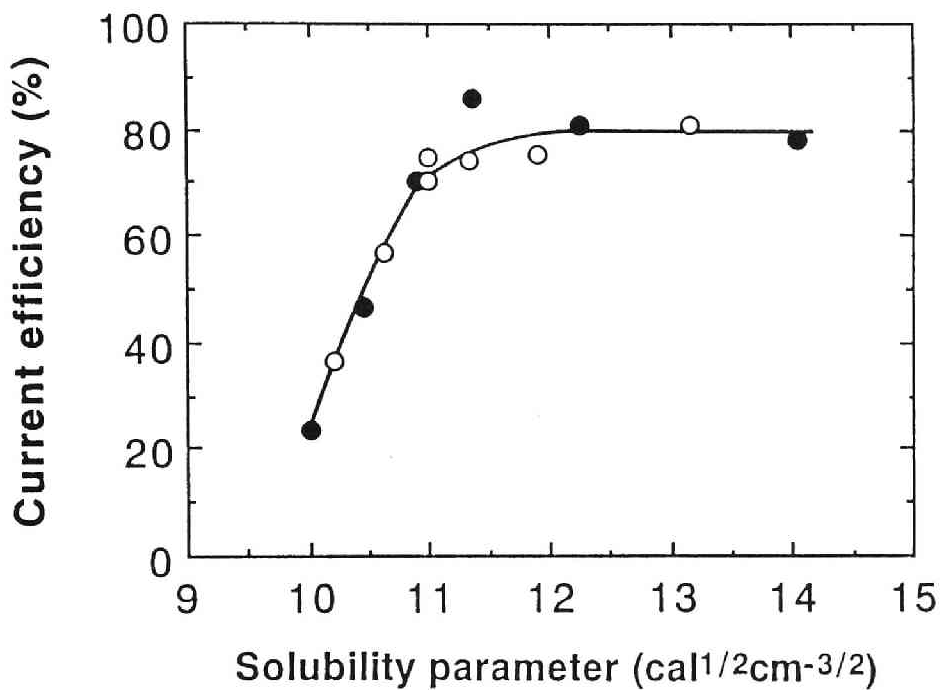


Fig. 2.6. Variation of current efficiency for aniline production with solubility parameter values δ_{mix} of the catholyte; ● : nitrobenzene/methanol; ○ : nitrobenzene/*n*-alkyl alcohol. The analyte was aqueous 0.025 M H₂SO₄. $I = 32 \text{ mA cm}^{-2}$.

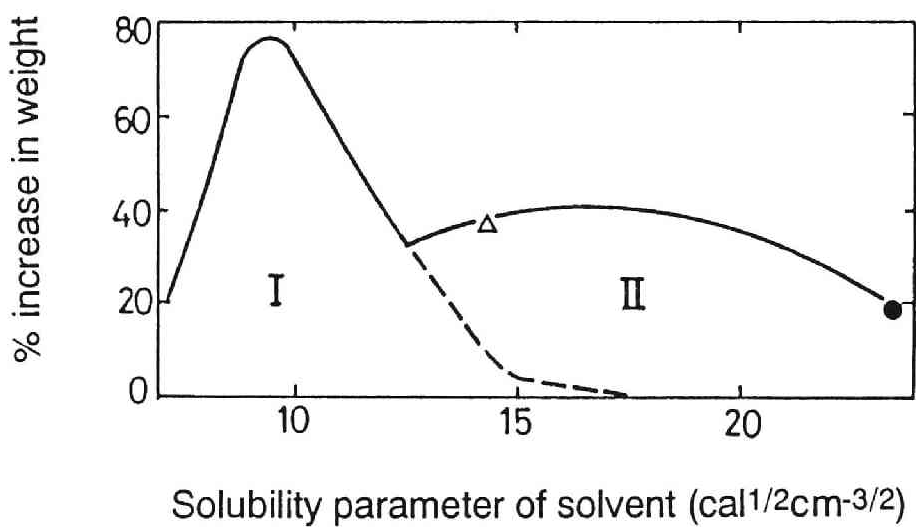


Fig. 2.7. Solvent uptake vs. solubility parameters of solvents;¹⁶⁾
 ● : water; ▲ : methanol.

with the hydrophobic amorphous region. Thus, without a co-solvent, nitrobenzene cannot penetrate into the ionic clusters where the active sites of the SPE composite electrode exist. As shown in Fig. 2.7, solvents with δ in the range from about 12.5 to 18 cal^{1/2} cm^{-3/2} can interact with both the hydrophobic amorphous region and the ionic clusters. Consequently, the mass transport of nitrobenzene is expected to be facilitated when catholytes with δ_{mix} in the range from 12.5 to 18 cal^{1/2} cm^{-3/2} are used. On the other hand, solvents with δ below 12.5 cal^{1/2} cm^{-3/2} can only interact with the hydrophobic amorphous region, and cannot penetrate into the ionic clusters. Consequently, aniline production is expected to be suppressed when a catholyte with δ_{mix} below 12.5 cal^{1/2} cm^{-3/2} is used. This expectation is supported by the results of Fig. 2.6, which shows that nitrobenzene was effectively electroreduced using catholytes with δ_{mix} of 11-14 cal^{1/2} cm^{-3/2}, whereas the current efficiencies decreased suddenly at $\delta_{\text{mix}} < 11$ cal^{1/2} cm^{-3/2}. It should be noted that the data in Fig. 2.7 were obtained using Nafion of EW = 1200, and cannot be directly compared with the results in Fig. 2.6, because Nafion of EW = 1100 was used in this chapter. Although the onset of the decrease in the current efficiency was observed at a slightly lower solubility parameter value than that predicted by Yeo's data, the trend obtained in this study is in good agreement with those deduced from Yeo's data. This fact suggests that some hydrophilic/hydrophobic interactions between reactants and Nafion may occur during electrolysis on SPE composite electrodes.

2.4. Conclusion

The effects of solvents on the electroreduction of nitrobenzene on Cu,Pt-Nafion were discussed. The presence of a sufficient amount of a co-solvent in the catholyte or in the anolyte facilitated the reduction of nitrobenzene to aniline. Without a sufficient amount of a co-solvent, hydrogen evolution was significant. These results reveal that the mass transport of nitrobenzene into the ionic clusters, where the active sites of the SPE composite electrode are located, is enhanced with the help of co-solvents. The solubility pa-

parameter value was found to be an important index for the efficiency of the mass transport. When an aqueous solution ($\delta = 23.4 \text{ cal}^{1/2} \text{ cm}^{-3/2}$) was used as the anolyte, catholytes with $\delta_{\text{mix}} > 11 \text{ cal}^{1/2} \text{ cm}^{-3/2}$ were effective for aniline production by the electroreduction of nitrobenzene on Cu,Pt-Nafion.

References

1. Z. Ogumi, H. Yamashita, K. Nishio, Z. Takehara and S. Yoshizawa, *Electrochim. Acta*, **28**, 1687 (1983).
2. Z. Ogumi, S. Ohashi and Z. Takehara, *Nippon Kagaku Kaishi*, 1788 (1984).
3. Z. Ogumi, T. Mizoe, N. Yoshida and Z. Takehara, *Bull. Chem. Soc. Jpn.*, **60**, 4233 (1987).
4. Z. Ogumi, M. Inaba, S. Ohashi, M. Uchida and Z. Takehara, *Electrochim. Acta*, **33**, 365 (1988).
5. Z. Chen, T. Mizoe, Z. Ogumi and Z. Takehara, *Bull Chem. Soc. Jpn.*, **64**, 537 (1991).
6. T. D. Gierke and W. Y. Hsu, in "Perfluorinated Ionomer Membranes", ed by A. Eisenberg and H. L. Yeager, ACS Symposium Series No. 180, American Chemical Society, Washington DC (1982) Chap. 13.
7. T. D. Gierke, G. E. Mann and F. C. Wilson, *J. Polym. Sci., Polym. Phys. Ed.*, **19**, 1687 (1991).
8. M. Baizer and H. Lund, "Organic Electrochemistry", 2nd Ed., Marcel Dekker, New York (1983) Chap. 8.
9. M. R. Rifi and F. H. Covitz, "Introduction to Organic Electrochemistry", Marcel Dekker, New York (1974) Chap. 4.
10. Z. Ogumi, K. Nishio and S. Yoshizawa, *Denki Kagaku*, **49**, 2124 (1981).
11. J. Marquez and D. Pletcher, *J. Appl. Electrochem.*, **10**, 567 (1980).
12. I. Nishiguchi and T. Hirashima, *Kagaku to Kogyo*, **56**, 298 (1982).
13. Z. Ogumi, T. Kuroe and Z. Takehara, *J. Electrochem. Soc.*, **132**, 260 (1985).

14. T. W. G. Solomons, "Organic Chemistry", 4th Edn., John Wiley & Sons, New York (1988) p 353.
15. A. F. M. Barton, *Chem. Rev.*, **75**,731 (1975).
16. R. S. Yeo, *Polymer*, **21**, 432 (1980).
17. R. S. Yeo, in "Perfluorinated Ionomer Membranes", ed by A. Eisenberg and H. L. Yeager, ACS Symposium Series No.180, American Chemical Society, Washington DC (1982) Chap 5.
18. H. L. Yeager and A. Steck, *J. Electrochem. Soc.*, **128**, 1880 (1981).

Chapter 3

Influence of the Multi-Phase Structure of Nafion on Electroreduction of Substituted Aromatic Nitro Compounds on Cu,Pt-Nafion

3.1 Introduction

The application of solid polymer electrolyte (SPE) electrolyzers to organic syntheses has been reported by Ogumi *et al.*¹⁻³⁾ In the SPE method, interactions between the reactant molecules and the solid polymer electrolyte can lead to greater selectivity compared with conventional methods. The SPE method is therefore a promising method for electro-organic syntheses.

Gierke *et al.*^{4,5)} presented a model that Nafion, which is used as an SPE material, is microscopically separated into two phases: a hydrophilic ionic cluster domain and a hydrophobic polytetrafluoroethylene backbone domain. Yeager and Steck⁶⁾ proposed a three phase model where an "interfacial" region exists between the two domains of Gierke's model. Ogumi *et al.*⁷⁾ considered that the interfacial region is the main path of hydrogen and oxygen molecules permeating through Nafion, and consists of the amorphous part of the backbone and the flexible side chains of Nafion. Electrodes coated with Nafion have been a subject of considerable recent interest.⁸⁻¹⁴⁾ Many workers have

reported that the unusual properties of large organic ions incorporated into Nafion resulted from the multi-phase structure of the Nafion.¹⁰⁻¹⁴) Nafion has strong affinity for hydrophobic organic cations because of the interaction of such cations with the hydrophobic region in Nafion.^{10,11}) Buttry and Anson¹²) explained unusual results regarding the diffusion coefficients of $\text{Ru}(\text{bpy})_3^{3+}/\text{Ru}(\text{bpy})_3^{2+}$ and $\text{Co}(\text{bpy})_3^{3+}/\text{Co}(\text{bpy})_3^{2+}/\text{Co}(\text{bpy})_3^+$ (bpy = bipyridine) in Nafion films in terms of the partition of ions between different domains in the Nafion. Rubinstein^{13,14}) observed a considerable shift of the electrochemical half-wave potential of the incorporated ferricinium/ferrocene (Fc^+/Fc^0) couple with respect to the same couple in solution, and two well-defined oxidation waves were obtained for Fc^0 in Nafion. He interpreted the observations in terms of the different moieties of Fc^+ and Fc^0 residing in the different domains of Nafion. The structure of SPE composite electrodes, which are covered with Nafion polymer electrolyte, is similar to that of polymer-coated electrodes. Since the active sites of SPE composite electrodes exist in the complex environment of the Nafion membrane, some hydrophilic/hydrophobic interactions between reactants and Nafion can be expected. Such interactions may enhance specific selectivity during electrolysis. In chapter 1, the effect of Nafion was found to lead to the selective production of aniline in the electroreduction of nitrobenzene on Cu-modified Pt-Nafion (Cu,Pt-Nafion),¹⁵) that is, the Bamberger rearrangement of phenylhydroxylamine intermediate to *p*-aminophenol¹⁶) or to *p*-anisidine¹⁷) was inhibited, despite the strong acidic conditions inside the Nafion. Although the reasons for the selective aniline production on Cu,Pt-Nafion are not yet exactly known, it is suspected that much of the observed selectivity can be attributed to interactions between nitrobenzene and Nafion.

In this chapter, the interactions between reactants and Nafion in the electroreduction on SPE composite electrodes of aromatic nitro compounds having a hydrophilic or a hydrophobic substituent is studied. An equimolar solution of *p*-nitrotoluene, which has a hydrophobic substituent, and *p*-nitrophenol, which has a hydrophilic substituent, is subjected to electroreduction on Cu,Pt-Nafion, and the effect of hydrophilic/hydrophobic properties of the

substituents on the reactant selectivity, that is, the difference in the ease of reducibility of the two reactants to the corresponding amino compounds, is examined. The reactant selectivity in an equimolar solution of *o*-nitrotoluene and *p*-nitrotoluene, which have a common hydrophobic substituent (methyl group) at different positions, is also examined. The corresponding selectivities on a conventional copper plate electrode are determined for comparison. The interactions between the reactants and the Nafion are discussed based on the observed reactant selectivities.

3.2. Experimental

3.2.2. *Cu,Pt-Nafion*

Cu-modified Pt-Nafion composite electrodes (Cu,Pt-Nafion) were prepared as described in chapter 2.¹⁸⁾ A perfluorosulfonate cation-exchange membrane, Nafion[®] 415 (E. I. du Pont de Nemours and Co.), was used as the SPE material. A porous platinum layer was first deposited on one side of the membrane by an electroless plating method.¹⁹⁾ The Pt-layer was then modified with copper by an electroplating method^{15,18)} to enhance its hydrogen overvoltage.

3.2.2. *Copper plate electrode*

A copper plate electrode (30mm × 30mm) was polished with no. 800 emery paper, then washed with methanol and dried in air prior to electrolysis.

3.2.3. *Electrolytic cell for Cu,Pt-Nafion*

The electrolytic cell for Cu,Pt-Nafion is shown in Fig. 3.1a. The cell was composed of two compartments, which were separated by the SPE composite electrode. The volume of each compartment was 6 cm³. The apparent geometric surface area of the SPE composite electrode was 3.1 cm². A platinum wire counter electrode was inserted into the anode compartment. The current feeder for the SPE composite electrode consisted of a gold ring, which was pressed onto the outer surface of the deposited Pt layer. During runs, the

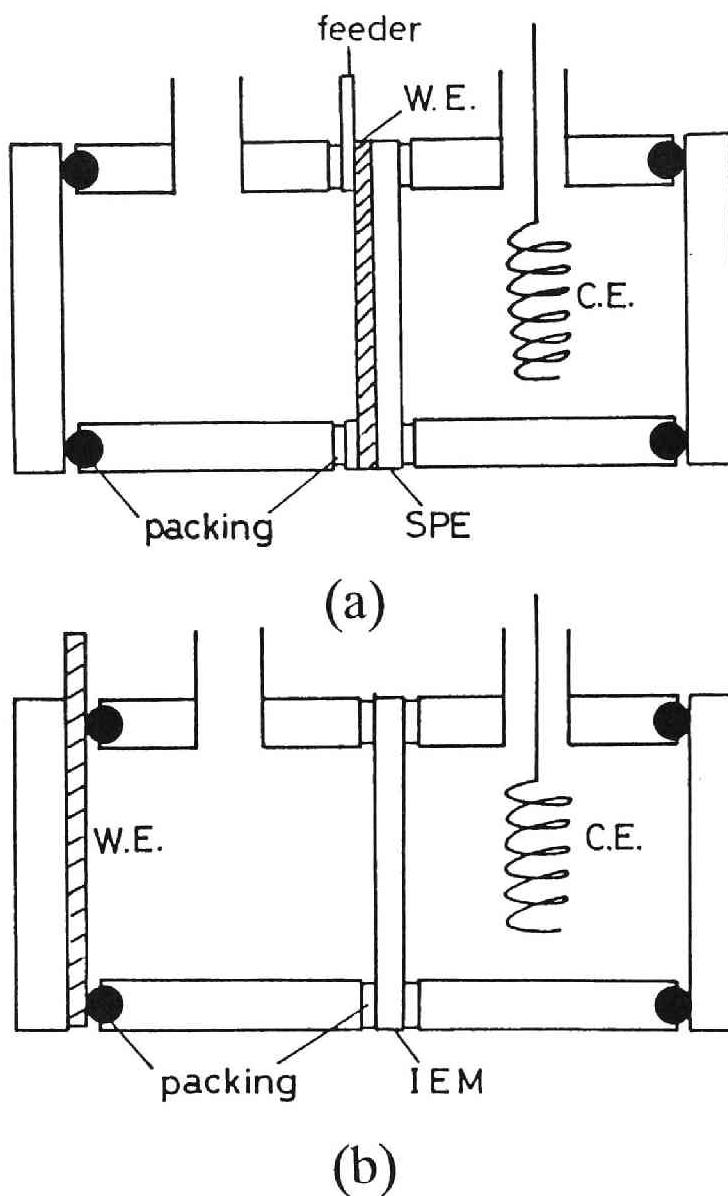


Fig. 3.1. Schematic diagrams of electrolytic cells (a) for Cu,Pt-Nafion, and (b) for a Cu-plate electrode. WE = porous platinum cathode deposited on Nafion 415 in (a), Cu plate electrode in (b); SPE = Nafion 415; CE = platinum wire anode; feeder = gold ring current feeder; IEM = Nafion 415.

cathode compartment (left-hand side in Fig. 3.1a) was filled with a methanol or 1-butanol solution containing either 1.0 M *p*-nitrotoluene and 1.0 M *p*-nitrophenol, or 1.0 M *p*-nitrotoluene and 1.0 M *o*-nitrotoluene. The anode compartment (right-hand side in Fig. 3.1a) was filled with aqueous 1.0 M H₂SO₄.

3.2.4. *Electrolytic cell for copper plate electrode*

The electrolytic cell for the copper plate electrode is shown in Fig. 3.1b. The cell was composed of two compartments of the same size as those in the SPE electrolyzer. The copper electrode was placed at the end of the cathode compartment (left-hand side in Fig. 3.1b), and an O-ring was used to give a geometric electrode surface area of 3.1 cm². Nafion 415 was used as the separator. The catholyte and the anolyte were of the same compositions as those for Cu,Pt-Nafion except that 1.0 M H₂SO₄ was added to the catholyte in order to obtain ionic conductivity and to make the catholyte acidic.

3.2.5. *Electrolysis*

Electrolysis was carried out galvanostatically, using a constant current power supply (Kikusui Electronics Co., PAB-32-0.5) and a coulomb meter (Hokuto Denko, HF201). The total charge passed during each run was 900 C.

3.2.6. *Product analysis*

Electrolysis products were analyzed by HPLC, using a Hitachi 638-30 liquid chromatograph fitted with a Zorbax ODS column (du Pont Co.). After electrolysis, the catholyte was analyzed without pre-treatment.

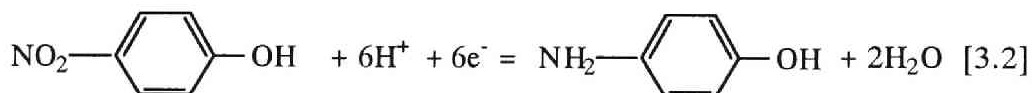
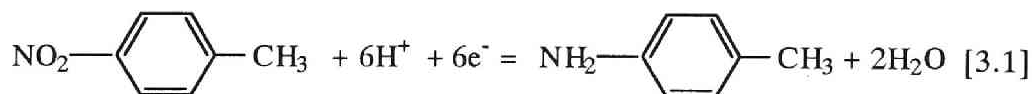
3.2.7. *Chemicals*

All chemicals were of reagent grade, and were used without further purification.

3.3. Results

3.3.1. Effect of hydrophilicity/hydrophobicity of substituents on reactant selectivity

An equimolar mixture of *p*-nitrotoluene and *p*-nitrophenol dissolved in methanol was subjected to electroreduction on Cu,Pt-Nafion, and the reactant selectivity, i.e., the relative ease with which the two reactants were electroreduced on Cu,Pt-Nafion and on the copper plate electrode, was determined. Figure 3.2 shows the variation of the current efficiencies for *p*-toluidine and *p*-aminophenol production with current density on Cu,Pt-Nafion, using a methanol solution containing 1.0 M *p*-nitrotoluene and 1.0 M *p*-nitrophenol as the catholyte. No other organic products were detected by HPLC. The Bamberger rearrangement to the *ortho* position *via* a 4-electron reduction product did not occur because of steric hindrance,^{16,17)} and the reactions therefore proceeded as follows:



The current efficiency for *p*-toluidine production decreased with increasing current density, while that of *p*-aminophenol production increased. The total current efficiency for the two products decreased slightly with increasing current density, probably because hydrogen evolution occurred as a side reaction at high current densities.

Figure 3.3 shows the current efficiencies for *p*-toluidine and *p*-aminophenol production on the conventional copper plate cathode at various current densities and the same reactant concentrations as in the above experiment (except for the addition of 1.0 M H₂SO₄ in the catholyte). The reaction product in the reduction of aromatic nitro compounds is known to vary with the acidity of the solution.¹⁶⁻¹⁸⁾ The acidity of the Nafion membrane used as

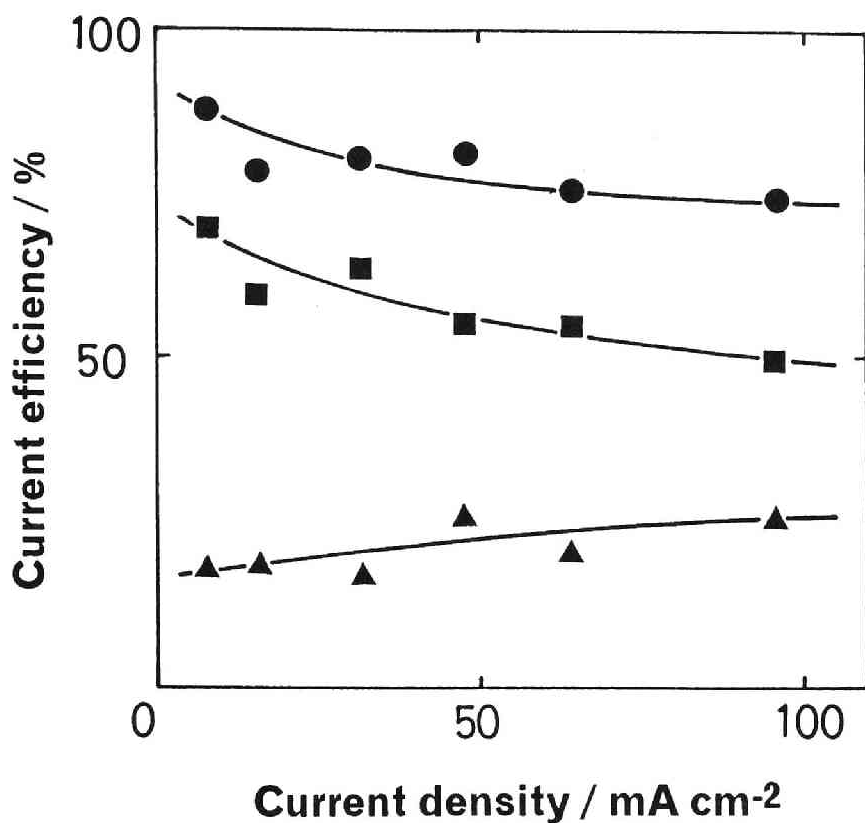


Fig. 3.2. Variation of the current efficiencies for (■) *p*-toluidine, (▲) *p*-aminophenol and (●) total amino compound production with current density in methanol solution containing 1.0 M *p*-nitrotoluene and 1.0 M *p*-nitrophenol on Cu,Pt-Nafion.

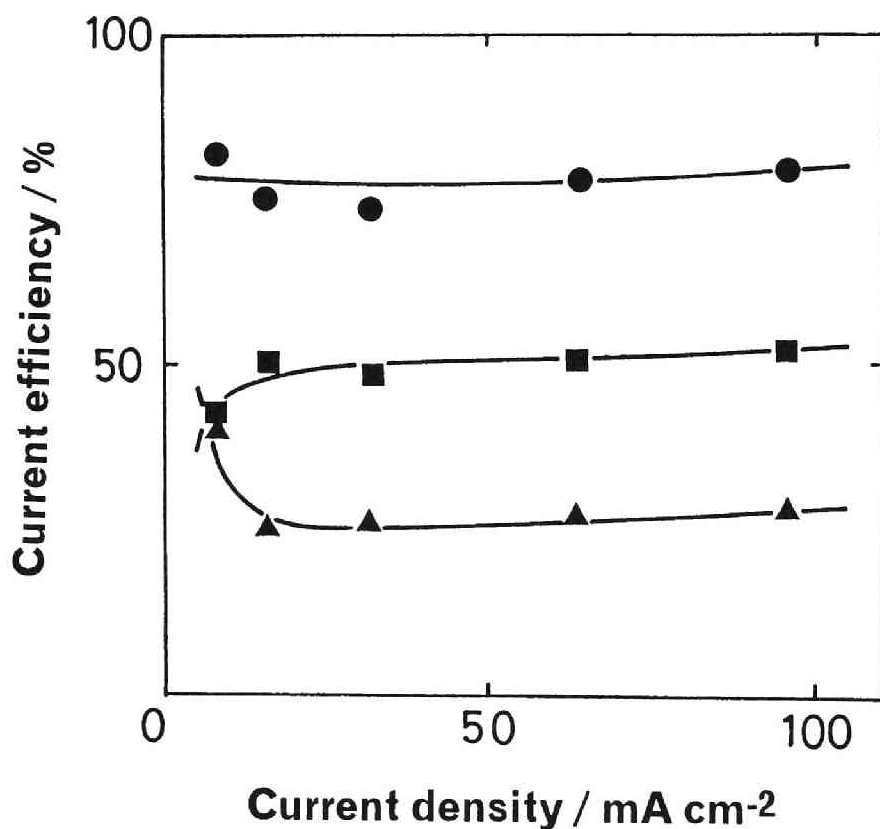


Fig. 3.3. Variation of the current efficiencies for (■) *p*-toluidine, (▲) *p*-aminophenol and (●) total amino compound production with current density in methanol solution containing 1.0 M *p*-nitrotoluene and 1.0 M *p*-nitrophenol on a Cu-plate electrode.

the SPE material (H^+ -form) has been estimated to be comparable with that of 1-3 M sulfuric acid,¹⁵⁾ based on its exchange capacity and water uptake. Hence, 1.0 M H_2SO_4 was added to the catholyte in the solid copper case to adjust the acidity similar to that in the vicinity of the reaction sites of the SPE composite electrode, as well as to give ionic conductivity in the catholyte. The current efficiencies for *p*-toluidine and *p*-aminophenol production were constant at current densities higher than about 15 mA cm^{-2} . Abrupt changes in the current efficiencies were observed at 8 mA cm^{-2} ; the current efficiency for *p*-toluidine production decreased, while that for *p*-aminophenol production increased. No other organic products were detected by HPLC.

The effect of solvent on the selectivity was also examined. The variation of the current efficiencies for *p*-toluidine and *p*-aminophenol production with current density on Cu,Pt-Nafion are shown in Fig. 3. 4 for the same concentrations as in Fig. 3.2; however, 1-butanol was used as the solvent instead of methanol. The total current efficiency decreased remarkably at current densities greater than 15 mA cm^{-2} . Hydrogen evolution was observed at the high current densities.

The selectivity for *p*-toluidine production, that is, the ratio of the current efficiency for *p*-toluidine production to that for total amino-compound production, was calculated from the data in Figs. 3.2, 3.3 and 3.4. The respective variations of the selectivity with current density are shown in Fig. 3.5. The selectivity for *p*-toluidine production on Cu,Pt-Nafion from both methanol and 1-butanol solutions at current densities less than 50 mA cm^{-2} was higher than those on the Cu-plate electrode. The selectivity on Cu,Pt-Nafion in methanol solution decreased with increasing current density, approaching the values for the Cu-plate electrode at high current densities, while the selectivity on Cu,Pt-Nafion in 1-butanol solution remained high even at high current densities [although the total current efficiency for the reduction of the two nitro compounds decreased with increasing current density (see Fig. 3.4)]. The selectivity for *p*-toluidine production with the Cu-plate electrode was almost constant (except for the abrupt change at 8 mA cm^{-2}).

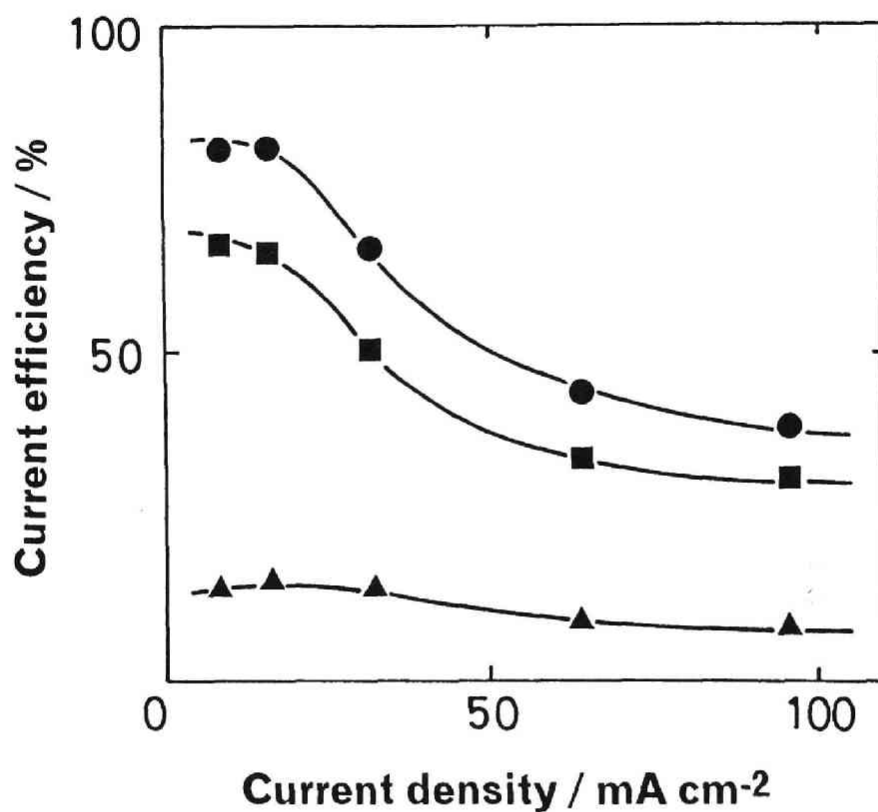


Fig. 3.4. Variation of the current efficiencies for (■) *p*-toluidine, (▲) *p*-aminophenol and (●) total amino compound production with current density in butanol solution containing 1.0 M *p*-nitrotoluene and 1.0 M *p*-nitrophenol on Cu,Pt-Nafion.

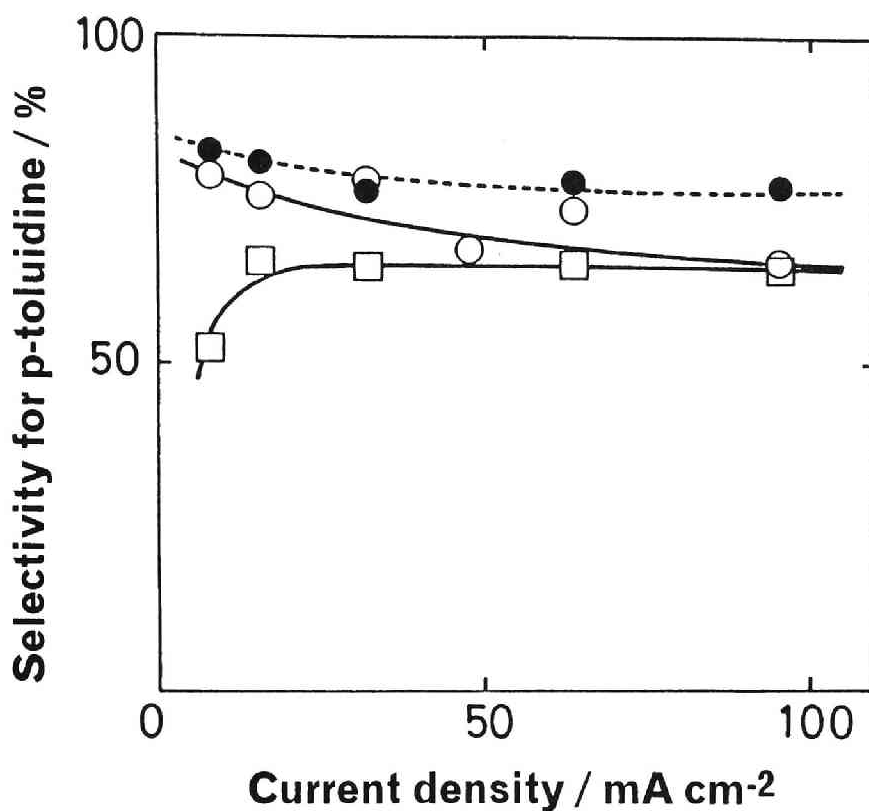
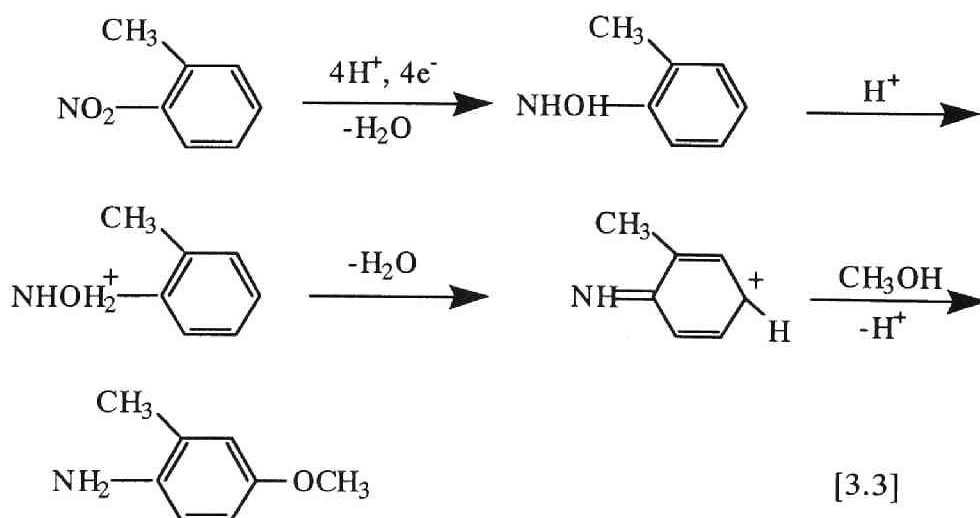


Fig. 3.5. Variations of the selectivity for *p*-toluidine production in solutions containing 1.0 M *p*-nitrotoluene and 1.0 M *p*-nitrophenol with current density. ○ : on Cu,Pt-Nafion in methanol solution; ● : on Cu,Pt-Nafion in butanol solution; □ : on a Cu plate electrode in methanol solution.

3.3.2. Effect of position of hydrophobic substituent on reactant selectivity

The effect of the position of the methyl group in nitrotoluene on the reactant selectivity was also examined. A catholyte consisting of a mixture of 1.0 M *p*-nitrotoluene and 1.0 M *o*-nitrotoluene dissolved in methanol was subjected to electroreduction using Cu,Pt-Nafion and the copper plate electrode, and the reactant selectivity between the two nitrotoluene isomers for reduction to the corresponding toluidine isomers was determined for each case. Figure 3.6 shows the current efficiencies for *p*-toluidine and *o*-toluidine production on Cu,Pt-Nafion at various current densities. No other organic products were detected by HPLC. The current efficiency for *p*-toluidine production decreased with increasing current density, while that of *o*-toluidine production increased. The total current efficiency for the two products decreased slightly with increasing current density because of increasing hydrogen evolution, which occurred as a side reaction.

Figure 3.7 shows the current efficiencies for *p*-toluidine, *o*-toluidine and 4-methoxy-2-methylaniline production on the conventional copper plate cathode for the same reactant concentrations as in the above experiments (except for the addition of 1.0 M H₂SO₄ in the catholyte). In this series of experiments, 4-methoxy-2-methylaniline was produced by Bamberger rearrangement via a 4-electron reduction process for *o*-nitrotoluene as follows:



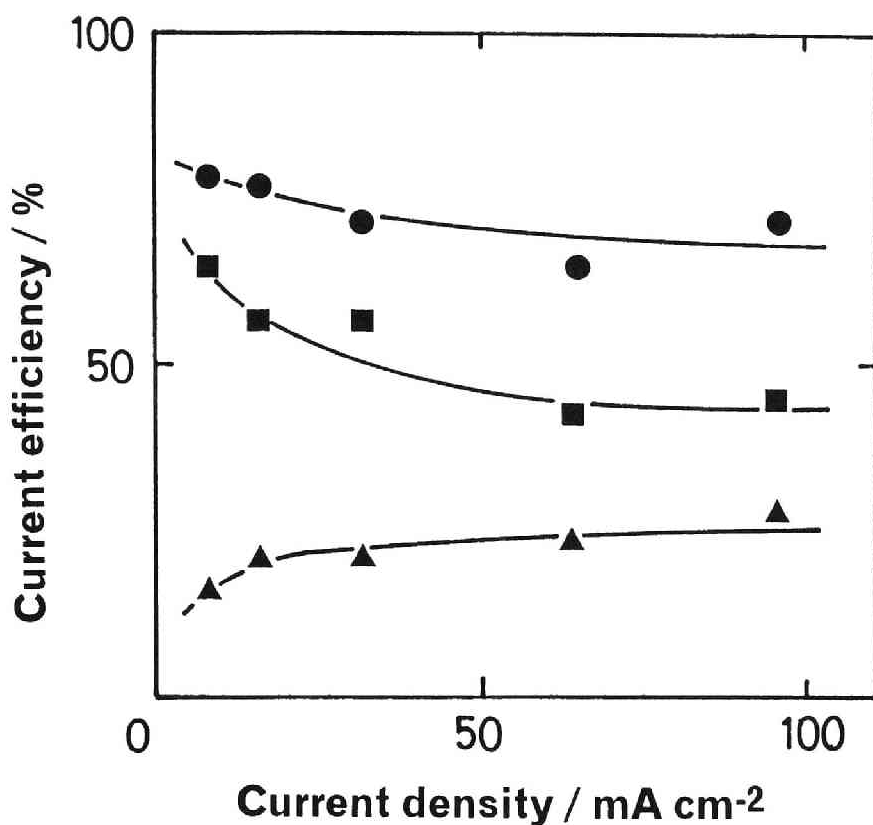


Fig. 3.6. Variation of the current efficiencies for (■) *p*-toluidine, (▲) *o*-toluidine and (●) total amino compound production with current density in methanol solution containing 1.0 M *p*-nitrotoluene and 1.0 M *o*-nitrotoluene on Cu,Pt-Nafion.

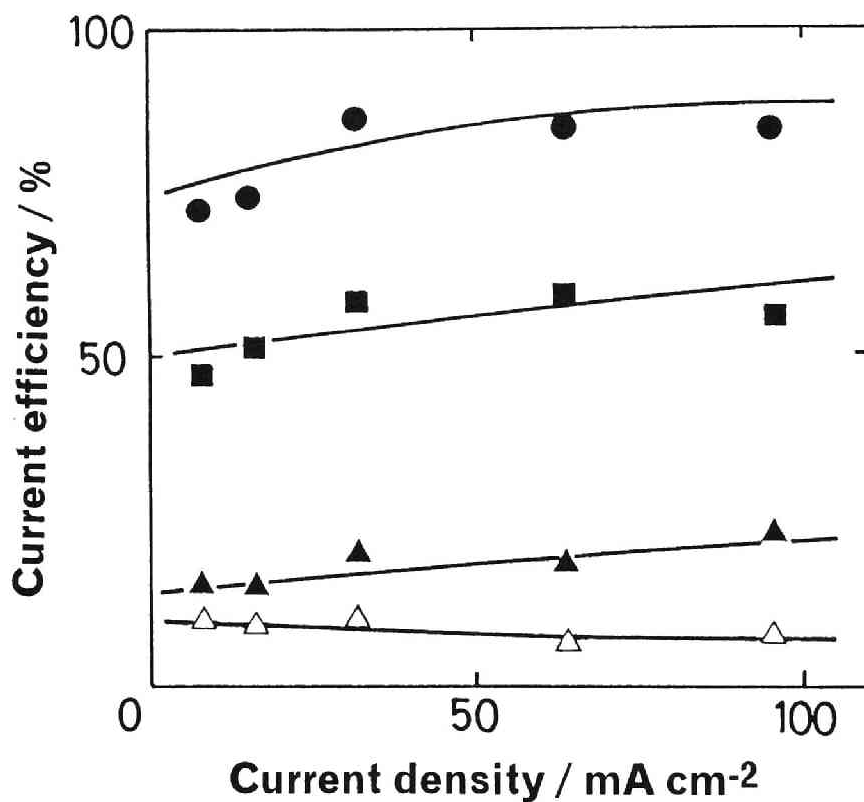


Fig. 3.7. Variation of the current efficiencies for (■) *p*-toluidine, (▲) *o*-toluidine, (△) 4-methoxy-2-methylaniline and (●) total amino compound production with current density in methanol solution containing 1.0 M *p*-nitrotoluene and 1.0 M *o*-nitrotoluene on a Cu-plate electrode.

No other organic products were detected by HPLC. It is noted that the product of the Bamberger rearrangement, 4-methoxy-2-methylaniline, was not obtained with Cu,Pt-Nafion, which is in accordance with the results in the electroreduction of nitrobenzene on Cu,Pt-Nafion in chapters 1 and 2.^{15,18)}

The selectivities for *p*-toluidine production were calculated from the data in Figs. 3.6 and 3.7, and the results are shown in Fig. 3.8. The selectivity on Cu,Pt-Nafion was higher than that on the Cu-plate electrode at low current densities, but decreased with increasing current density, approaching the (approximately constant) values for the Cu-plate electrode at current densities greater than about 50 mA cm⁻².

3.4. Discussion

The selectivity for a reactant having a hydrophobic substituent at the *para*-position was higher for the SPE composite electrode than for the Cu-plate electrode. Possible reasons for the higher selectivity observed with Cu,Pt-Nafion are: (i) differences in the reduction potentials of the reactants, (ii) factors related to mass transport of the reactants, and (iii) interactions between the reactants and the Nafion during electrolysis.

3.4.1. Effects of reduction potentials of reactants

Reported values of the polarographic half-wave potentials of the three reactants used in this study in acetic acid²⁰⁾ are as follows: *p*-nitrophenol, -0.670 V; *p*-nitrotoluene, -0.665 V; *o*-nitrophenol, -0.715 V vs a saturated chloranil electrode. Thus, according to the reduction potentials, the electroreduction of *p*-nitrotoluene should occur most preferentially. While the reduction potentials may be shifted on the SPE composite electrode due to hydrophobic interactions like those reported by Rubinstein for Fc⁺/Fc⁰ couples,¹⁴⁾ measurement of junction-free potentials for SPE composite electrodes is very difficult, and was not attempted here. Therefore, only the values of reduction potential in solution are considered in the following discussion. Differences in reduction potential with the SPE and Cu-plate electrodes were minimized by using

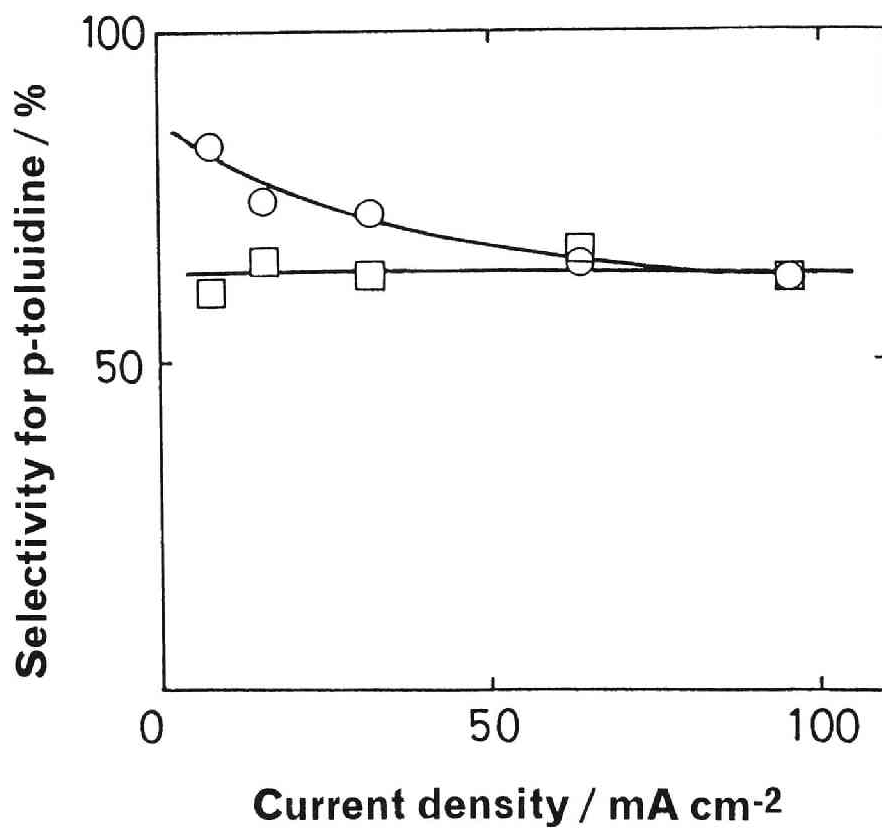


Fig. 3.8. Variations of the selectivity for *p*-toluidine production in solutions containing 1.0 M *p*-nitrotoluene and 1.0 M *o*-nitrotoluene with current density. ○ : on Cu,Pt-Nafion in methanol solution; □ : on a Cu plate electrode in methanol solution.

solutions containing the same concentrations of reactants in both cells. The polarization curves for the electrode reactions probably are very similar to one another because the reactions are very similar, i.e., the reduction of nitrobenzene compounds. In fact, given the closeness of the half-wave potentials, the polarization curves should run almost parallel to one another. This means that if the reactant selectivity was determined mainly by differences in reduction potential, then the selectivity should be independent of the current density (i.e., the electrode potential), since the fraction of the total current supplied by each reaction would be constant. This is the case for the reactant selectivity with the Cu-plate electrode in Figs. 3.5 and 3.8 (except for the selectivity at a low current density in Fig. 3.5, probably because of the effects of the specific absorption of the reactants). However, as seen in Figs. 3.5 and 3.8, the observed selectivity varied significantly with the current density, and therefore differences in reduction potential were not the main factor responsible for the enhanced selectivity with Cu,Pt-Nafion.

3.4.2. Effects of mass transport of reactants

The active sites of SPE composite electrodes are known to be located in the ionic clusters of the Nafion membrane.^{15,21} Mass transport from the catholyte to the active sites in the ionic clusters is necessary for the reactants to receive electrons from the electrode. Two paths for such mass transport are possible. In the first path, the reactants directly enter the ionic clusters after diffusing through the porous metal deposited on the Nafion, and are then subjected to electroreduction. This path is referred to herein as path 1. In the second path, the reactants first enter the flexible hydrophobic interfacial region of the Nafion membrane (which consists of the amorphous part of the backbone and the flexible side chains), and then diffuse toward the active sites in the ionic clusters. This path is referred to as path 2. Diffusion via path 2 predominates when lipophilic organic solutions are used as the catholyte.

There are three "steps" which can be involved in the mass transport of reactants via paths 1 and 2, namely, mass transport in the porous metal (path 1 and 2), in the ionic clusters (path 1 and 2), and in the interfacial region (path

2). The reactants can be considered to have comparable diffusion rates in each of the respective steps, because they have similar molecular sizes. However, the solubilities of the respective reactants may differ from one another in the three steps. If one of the reactants had a very low solubility in one of the three steps, the mass transport of the reactant would be limited by that step, and the selectivity for the reactant would be diminished. Considering each step in turn, in the porous metal, the reactants should have solubilities similar to those in the catholyte. Therefore, the solubilities of the reactants in the porous metal should not affect the reactant selectivity. As for the solubilities of the reactants in the ionic clusters, when methanol solution is used as the catholyte, the ionic clusters are considered to be composed both of methanol from the catholyte and of water that permeated through the Nafion membrane from the anolyte. The solubilities of *p*-nitrotoluene and *p*-nitrophenol in water and in a 9:1 water/methanol (by volume) solution were determined at 25°C, and are listed in Table 3.1. The solubilities of *p*-nitrophenol in water and in 9:1 water/methanol solution are much larger than those of *p*-nitrotoluene, which would lead one to expect preferential selectivity for *p*-nitrophenol. However, as seen in Fig. 3.5, preferential selectivity for *p*-nitrotoluene is observed instead, and therefore differences in the solubilities of the reactants in the ionic clusters are not responsible for the observed selectivity enhancement. In the case of the interfacial region, *p*-nitrotoluene can be considered to be more soluble than *p*-nitrophenol, because *p*-nitrotoluene is more hydrophobic and interacts more strongly with the hydrophobic interfacial region. While this is consistent with the observed preferential selectivity for *p*-nitrotoluene reduction over *p*-nitrophenol reduction, in general, mass transport limitations should become greater at higher current densities. Therefore, if factors related to mass transport (*i.e.*, solubility differences in the hydrophobic interfacial region of Nafion) were responsible for the selectivity, we expect that the selectivity for *p*-toluidine would increase at high current densities. Since this was not observed (see Fig. 3.5), therefore, the mass transport of the reactants was not the main factor responsible for the selectivity enhancement observed with Cu,Pt-Nafion.

Table 3.1. Solubilities of *p*-nitrotoluene and *p*-nitrophenol in water and in 9:1 (by volume) water/methanol solution at 25°C.

	water * (g)	water/methanol (9/1)* (g)
<i>p</i> -nitrophenol	1.5	1.5
<i>p</i> -nitrotoluene	0.039	0.062

* solubility in 100g-sat. solution.

3.4.3. Effect of interactions between the reactants and Nafion

From the above discussion, interactions between the reactants and Nafion may play an important role in the enhanced reactant selectivity observed with Cu,Pt-Nafion. The interfacial region (flexible hydrophobic region) and the ionic clusters in the Nafion membrane form an interface that is analogous to an oil-water interface. A molecule that has a hydrophilic functional group and a hydrophobic functional group is oriented at an oil-water interface according to hydrophilic/hydrophobic interactions. Similar hydrophilic/hydrophobic interactions probably occur with reactions on the SPE composite electrode, in which the active sites of the electrode are located in the ionic clusters, at the interface of the ionic clusters and the flexible hydrophobic region of the Nafion. *Para*-nitrotoluene has a hydrophobic methyl group, and *p*-nitrophenol has a hydrophilic hydroxyl group. The order of the affinities for water of the substituents is in the order of hydroxyl group > nitro group > methyl group, and therefore the nitro group of *p*-nitrotoluene and the hydroxyl group of *p*-nitrophenol are considered to be oriented toward the ionic clusters (and the active electrode sites), as shown schematically in Fig. 3.9. Therefore, the nitro group of *p*-nitrotoluene is favorably oriented for electroreduction, while that of *p*-nitrophenol is not. This difference leads to the observed enhancement of the preferential production of *p*-toluidine over *p*-aminophenol (Figs. 3.2-3.5). Such interactions may occur with both path 1 and 2.

Similarly, in the case of *o*-nitrotoluene, the nitro group tends to be oriented away from the ionic clusters (and therefore away from the active electrode sites), because the hydrophobic methyl group is in the vicinity of the nitro group. This orientation hinders the production of *o*-toluidine, and leads to the observed enhanced selectivity for *p*-toluidine over *o*-toluidine (see Figs. 3.6-3.8).

The selectivity for *p*-toluidine production decreased with increasing current density in methanol, while it remained constant in 1-butanol (see Fig. 3.5). Methanol has a solubility parameter value of $14.5 \text{ cal}^{1/2} \text{ cm}^{-3/2}$, and interacts with both the hydrophilic ionic clusters and the hydrophobic interfacial region in Nafion membranes.²²⁾ 1-butanol has a solubility parameter value of

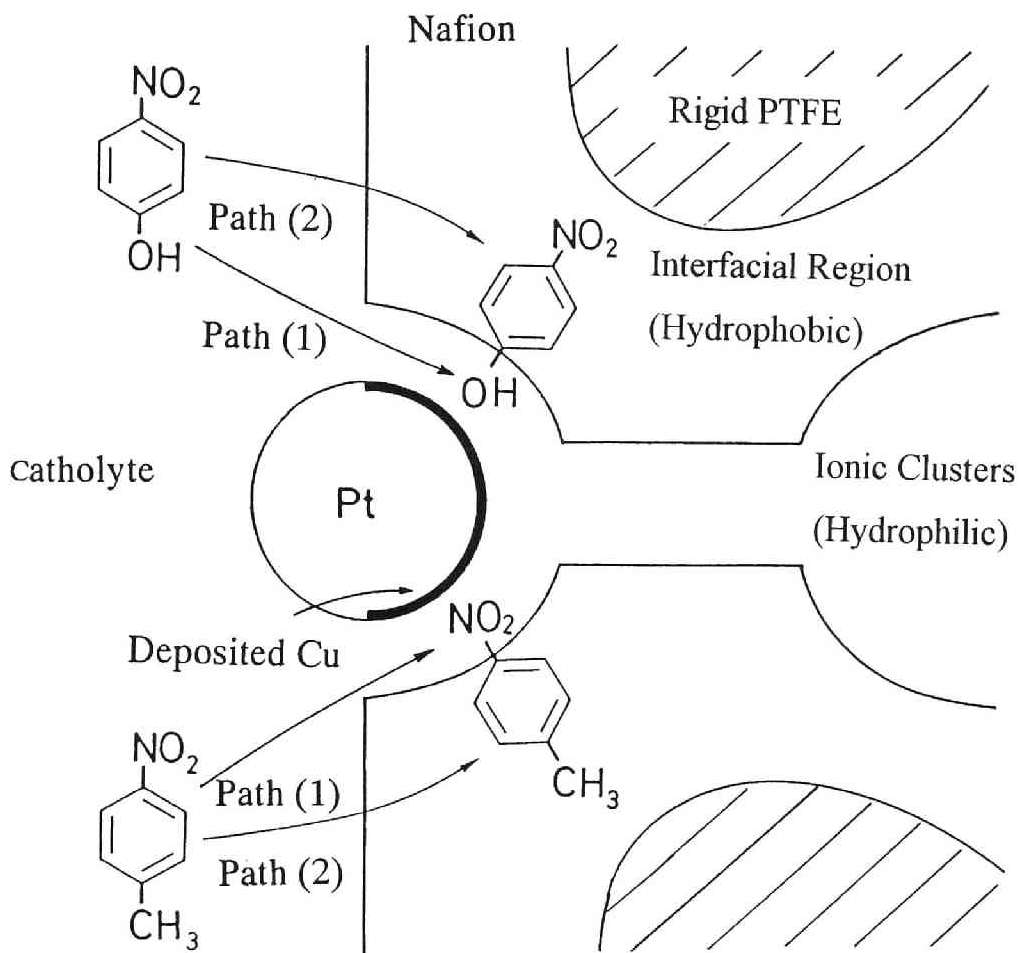


Fig. 3.9. Simplified model of the hydrophilic/hydrophobic interactions between aromatic nitro compounds and Nafion in SPE composite electrodes.

11.4 cal^{1/2} cm^{-3/2}, and interacts only with the hydrophobic interfacial region.²²⁾ Since methanol interacts with both regions, it tends to make the hydrophilic-hydrophobic interface indistinct, and weakens the interactions. Reactants oriented by the interactions are equilibrated with free reactants in the membrane. At high current densities, the oriented reactants cannot supply a sufficient flux by themselves, and the fraction of the reactants which are not oriented by hydrophilic/hydrophobic interactions increases. Therefore, as observed in Fig. 3.5, the reactant selectivity decreased with increasing current density in methanol solution. On the other hand, when 1-butanol, which interacts only with the interfacial region in Nafion, is used as the solvent, the interface between the ionic cluster region and the interfacial region remains distinct. Since the concentration of 1-butanol in the ionic clusters is low, the mass transport through path 1 (Fig. 3.9) is limited when 1-butanol is used as the solvent.¹⁸⁾ This leads to hydrogen evolution as a side reaction, especially at high current densities. Thus, while the current efficiencies decrease with increasing current density (see Fig. 3.4), the reactant selectivity does not decrease at high current densities (see Fig. 3.5) because all of the reactants are under the influence of the interactions at the hydrophilic-hydrophobic interface.

The water content is known to give a significant influence on the structure of Nafion.²³⁾ Bernardi and Verbrugge^{24,25)} reported a mathematical model of a polymer electrolyte fuel cell (PEFC). In their results, the spatial variation of water velocity in the SPE composite electrode of a fuel cell is affected greatly by the change in current density, in particular, in the vicinity of the active electrode layer. However, current densities in this study (lower than 100 mA cm⁻²) were not as high as those in fuel cells. Therefore, it is considered that water content in the membrane is not significantly affected by the change in current density in this study.

3.5. Conclusion

An equimolar solution of *p*-nitrotoluene, which has a hydrophobic substituent, and *p*-nitrophenol, which has a hydrophilic substituent, was electroreduced on Cu,Pt-Nafion. The reactant selectivity for the reduction of the two reactants to the corresponding amino products was determined, and compared with that on a conventional copper plate electrode. The reactant selectivity for an equimolar solution of *o*- and *p*-nitrotoluene, in which the hydrophobic substituent is located at different positions, was also determined. *Para*-nitrotoluene was electroreduced preferentially from both equimolar solutions, and this selectivity for *p*-nitrotoluene was enhanced for Cu,Pt-Nafion electrodes relative to the Cu-plate electrode. Thus, the electroreduction of the reactant having a hydrophobic substituent at the *para* position relative to the nitro group was enhanced with the SPE composite electrodes.

Of the factors which affect the reactant selectivity, hydrophilic/hydrophobic interactions between the reactants and Nafion are primarily responsible for the enhanced reactant selectivity observed with Cu,Pt-Nafion. The interactions are attributed to the multi-phase structure of Nafion. The interfacial region of Nafion interacts with the more hydrophobic substituent of the reactants. The ionic clusters region of Nafion interacts with the more hydrophilic part of the reactants. In *p*-nitrotoluene, which has a hydrophobic methyl group at the *para* position, the nitro group is oriented toward the ionic clusters of Nafion, where the active sites of the electrode are located. Therefore, the nitro group of *p*-nitrotoluene is preferentially positioned for the electroreduction in Cu,Pt-Nafion electrodes.

References

1. Z. Ogumi, H. Yamashita, K. Nishio, Z. Takehara and S. Yoshizawa, *Denki Kagaku*, **52**, 180 (1984).
2. Z. Ogumi, S. Ohashi and Z. Takehara, *Nippon Kagaku Kaishi*, 1788 (1984).

3. Z. Ogumi, T. Mizoe, N. Yoshida and Z. Takehara, *Bull. Chem. Soc. Jpn.*, **60**, 4233 (1987).
4. T. D. Gierke and W.Y. Hsu, in "Perfluorinated Ionomer Membranes", ed by A. Eisenberg and H. L. Yeager, ACS Symposium Series No.180, American Chemical Society, Washington DC (1982) Chap. 13.
5. T. D. Gierke, G. E. Mann and F. C. Wilson, *J. Polym. Sci., Polym. Phys. Ed.*, **19**, 1687 (1991).
6. H. L. Yeager and A. Steck, *J. Electrochem. Soc.*, **128**, 1880 (1981).
7. Z. Ogumi, T. Kuroe and Z. Takehara, *J. Electrochem. Soc.*, **132**, 2601 (1985).
8. H. S. White, J. Leddy and A. J. Bard, *J. Am. Chem. Soc.*, **104**, 4811 (1982).
9. D. A. Buttry and F.C. Anson, *J. Electroanal. Chem.*, **130**, 333 (1981).
10. N. E. Prieto and C. R. Martin, *J. Electrochem. Soc.*, **131**, 751 (1984).
11. M. N. Szentirmay and C. R. Martin, *Anal. Chem.*, **56**, 1898 (1984).
12. D. A. Buttry and F. C. Anson, *J. Am. Chem. Soc.*, **105**, 685 (1983).
13. I. Rubinstein, *J. Electroanal. Chem.*, **176**, 359 (1984).
14. I. Rubinstein, *J. Electroanal. Chem.*, **188**, 227 (1985).
15. Z. Ogumi, M. Inaba, S. Ohashi, M. Uchida and Z. Takehara, *Electrochim. Acta*, **33**, 365 (1988).
16. J. Marquez and D. Pletcher, *J. Appl. Electrochem.*, **10**, 567 (1980).
17. I. Nishiguchi and T. Hirashima, *Kagaku to Kogyo*, **56**, 298 (1982)
18. M. Inaba, Z. Ogumi and Z. Takehara, *J. Electrochem. Soc.*, **140**, 19 (1993).
19. Z. Ogumi, K. Nishio and S. Yoshizawa, *Denki Kagaku*, **49**, 212 (1981).
20. I. Bergman and J. C. James, *Trans. Faraday Soc.*, **48**, 956 (1952).
21. Z. Chen, T. Mizoe, Z. Ogumi and Z. Takehara, *Bull. Chem. Soc. Jpn.*, **64**, 537 (1991).
22. R. S. Yeo, *Polymer*, **21**, 432 (1980).
23. T. Hashimoto, M. Fujimura and H. Kawai, in "Perfluorinated Ionomer Membranes", ed by A. Eisenberg and H. L. Yeager, ACS Symposium

Series No. 180, American Chemical Society, Washington DC (1982)

Chap. 11.

24. D. M. Bernardi and M. W. Verbrugge, *AIChE J.*, **37**, 1151 (1991).

25. D. M. Bernardi and M. W. Verbrugge, *J. Electrochem. Soc.*, **139**, 2477 (1992).

Chapter 4

Reduction of Nitrobenzene on Solid Polymer Electrolyte Composite Electrodes Using a Hydrocarbon Sulfonate Ion-Exchange Membrane

4.1. Introduction

Solid polymer electrolyte (SPE) composite electrodes have been extensively studied for use in water electrolyzers, brine electrolyzers and fuel cells. The reduction of nitrobenzene with SPE composite electrodes using a perfluorosulfonate ion-exchange membrane, Nafion[®], as SPE material was studied in chapters 1 to 3.¹⁻³⁾ With the composite electrode aniline was obtained selectively with a current efficiency greater than 90%. Owing to the selective aniline production, the SPE method is promising for use in industrial aniline synthesis. However, since perfluorosulfonate membranes are generally expensive, it is desirable to use hydrocarbon sulfonate ion-exchange membranes as the SPE material.

In this chapter, SPE composite electrodes using a hydrocarbon sulfonate ion-exchange membrane, Selemion[®] CMV (Asahi Glass Co.), are prepared, and the reduction of nitrobenzene is studied using the electrodes.

4.2. Experimental

4.2.1. *Cu-Selemion*

Selemion is a co-polymer of styrene and divinylbenzene that contains sulfonate groups as ion-exchange sites, and is reinforced with polyvinyl chloride fibers. A porous copper layer was deposited on one side of the membrane of 3.0 cm in diameter by an electroless plating method.⁴⁾ One face of the membrane was exposed to a reductant solution (0.01 M NaBH₄, 1 M = 1 mol dm⁻³), and the other face to a copper ion solution (0.1 M CuSO₄). A porous copper layer was deposited on the reductant-side surface of the membrane. The copper layer deposited on the Selemion membrane was stable in H₂SO₄ as long as 2 days. The resulting SPE composite electrode is referred to hereafter as Cu-Selemion.

4.2.2. *Nafion-modified Cu-Selemion*

Nafion-modified Cu-Selemion composite electrodes were prepared as follows: 0.3 cm³ of a solution of Nafion dissolved in alcohol (Aldrich, containing 5 wt.% Nafion of EW = 1100) was spread with a microsyringe onto a Selemion membrane with a diameter of 3.0 cm and air-dried to remove the solvent for 10 h. The calculated thickness of the Nafion coating is 8.5 μm. A porous copper layer was deposited on the Nafion layer by the electroless plating method described above.

4.2.3. *Electrolysis and product analysis*

The electrolytic cell was described in chapters 2 and 3.^{1,2)} The cell was composed of two compartments, which were separated by the SPE composite electrode. The SPE composite electrode was used as cathode, and the effective geometric surface area was 3.1 cm². The catholyte was a methanol solution containing 30 vol.% nitrobenzene (6 cm³), and the anolyte was aqueous 0.25 M H₂SO₄ (6 cm³). A platinum wire was inserted in the anolyte and used as the anode. Electrolysis was carried out galvanostatically. The total charge passed during each run was 800 C. After electrolysis, the catholyte was ana-

lyzed by HPLC without pretreatment. Polarization curves were measured using an SPE electrolytic cell fitted with a Luggin capillary placed in the anode compartment.⁵⁾

4.3. Results and Discussion

4.3.1. Effect of current density

The variations of the current efficiency for aniline production and cell voltage with current density obtained with Cu-Selemion are shown in Fig. 4.1. The maximum current efficiency of 80% was obtained at a current density of 16 mA cm⁻². The current efficiency decreased significantly at current densities greater than 32 mA cm⁻². Gas evolution was observed in the cathode compartment at the high current densities, and hence hydrogen evolution is considered to have occurred as a side reaction. Figure 4.1 also shows the variations of the current efficiency for aniline production and cell voltage obtained with Cu,Pt-Nafion in chapter 1.¹⁾ The maximum current efficiency was greater than 95%, and no significant decrease in current efficiency was seen at current densities up to 100 mA cm⁻². The active sites of SPE composite electrodes have been considered to be located inside the ion-exchange membrane,^{1,2,6)} that is, in the region where the membrane phase and electrode material overlap.⁷⁾ Nitrobenzene must diffuse from the catholyte to the active site to receive electrons from the electrode material. Hence, the hydrogen evolution on Cu-Selemion at high current densities means an insufficient mass-transport rate of nitrobenzene from the catholyte to the active sites of the electrode.

Quasi-steady state polarization curves obtained at a slow sweep rate of 1.0 mV s⁻¹ are shown in Fig. 4.2. Curves (a) and (b) were obtained with Cu-Selemion and Cu,Pt-Nafion, respectively, using 20 mM nitrobenzene in methanol as the catholyte. Curves (c) and (d) were obtained with Cu-Selemion and Cu,Pt-Nafion, respectively, using neat methanol (i.e., without added nitrobenzene) as the catholyte. On both SPE composite electrodes, cathodic current for the reduction of nitrobenzene started to flow at -200 mV vs.

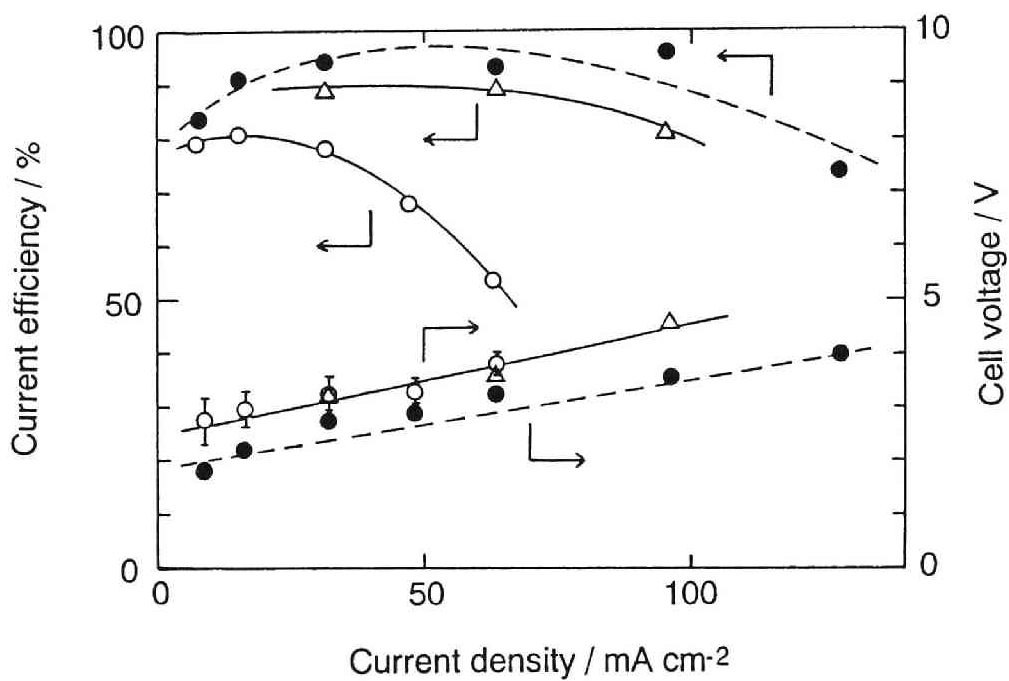


Fig. 4.1. Variations of the current efficiencies for aniline production and cell voltages with current density obtained with (○) Cu-Selemion, (●) Cu,Pt-Nafion,²⁾ and (△) Nafion-modified Cu-Selemion.

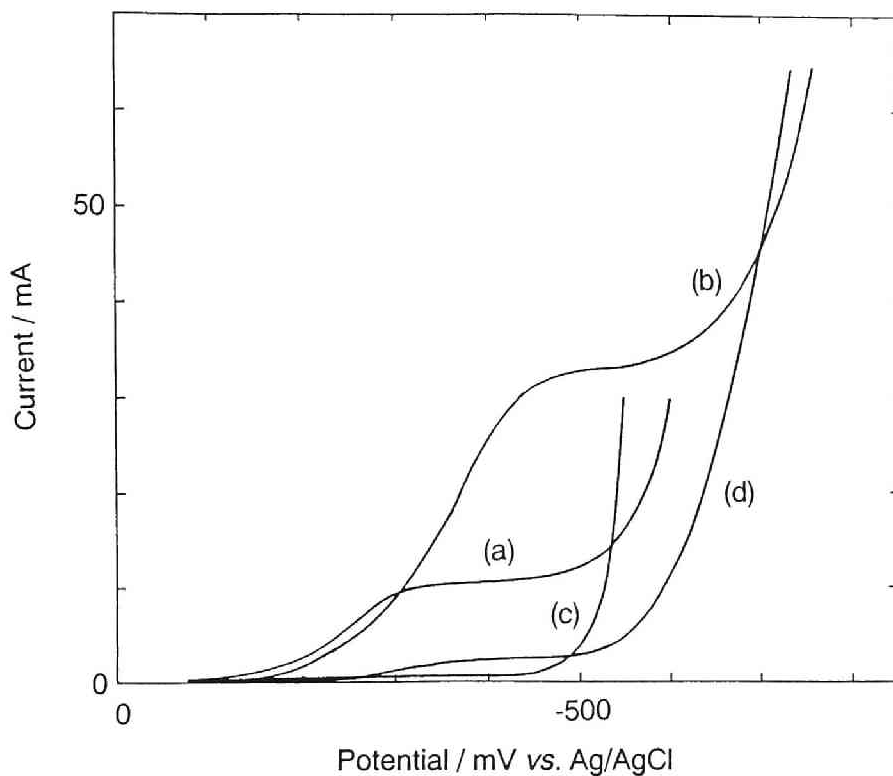


Fig. 4.2. Quasi-steady state polarization curves obtained at 1.0 mV s^{-1} : (a) 20 mM nitrobenzene in methanol and Cu-Selemion, (b) 20 mM nitrobenzene in methanol and Cu,Pt-Nafion, (c) methanol (no added nitrobenzene) and Cu-Selemion, and (d) methanol (no added nitrobenzene) and Cu,Pt-Nafion.

Ag/AgCl. The limiting currents are about 10 and 30 mA for Cu-Selemion and Cu,Pt-Nafion, respectively. These results indicate that the mass-transport rate of nitrobenzene in Selemion is about three times slower than that in Nafion.

Nafion membranes are not cross-linked, and have a flexible structure.⁸⁾ In addition, Nafion membranes are swollen more with many organic solvents than with water.⁹⁾ Hence, the mass transport of nitrobenzene inside Nafion is considered to be fairly easy. On the other hand, Selemion is highly cross-linked, and has a homogeneous structure, in which the ion-exchange sites are distributed uniformly throughout the membrane. It is difficult for organic reactants, such as nitrobenzene, to diffuse through such a rigid structure of Selemion. Therefore, it is reasonable that the mass transport in Selemion is slower than that in Nafion.

With Cu,Pt-Nafion aniline was the sole product, and no other organic by-products were detected by HPLC.¹⁾ On the other hand, with Cu-Selemion an organic by-product was detected by HPLC. The by-product has not been identified yet because of its high reactivity.¹⁰⁾ The molecular ion peak of the mass spectrum was observed at $m/z = 198$, which suggests a dimer production.

The reaction products obtained in the electroreduction of nitrobenzene are known to vary with electrode material, potential, acidity, temperature, etc.^{12,13)} In a highly acidic solution, aniline (6-electron process) and *p*-aminophenol, which is produced via rearrangement of a phenylhydroxylamine intermediate (4-electron process), are obtained, while phenylhydroxylamine and dimerized products, such as azoxybenzene, hydroazobenzene, etc., tend to be generated in a less acidic solution. Perfluorosulfonate membranes provide a higher acidity than hydrocarbon sulfonic acid membranes because of the presence of the fluorocarbon rather than hydrocarbon groups (the fluorine atom is electron-withdrawing),¹³⁾ and the acidity of Nafion in a hydrated membrane is comparable to that of a 10 wt. % H₂SO₄ solution.¹⁴⁾ Hence, the acidity in the vicinity of the active sites of Cu-Selemion is lower than that of Cu,Pt-Nafion. In addition, the ion-exchange sites of Selemion dissociated less in a nitrobenzene/methanol/water mixture under the electrolytic condi-

tions. It is therefore considered that the dimerized by-product was produced due to an insufficient acidity of Selemion. This by-product was generated significantly at current densities less than 32 mA cm^{-2} .

4.3.2. Effect of Nafion-coating

To improve the mass-transport rate of nitrobenzene and the selectivity for aniline production, the surface of Selemion was modified by coating with a thin layer of Nafion. The variations of the current efficiency for aniline production and cell voltage with current density obtained with Nafion-modified Cu-Selemion are shown in Fig. 4.1. The cell voltage was comparable to that without Nafion-coating. The current efficiency was as high as 90% at current densities up to 70 mA cm^{-2} , which was comparable with those obtained with Cu,Pt-Nafion. The current efficiency was greater than 80% even at a high current density of 97 mA cm^{-2} . Aniline was the sole product, and no other organic by-products were detected by HPLC. These facts show that Nafion coating can improve the mass transport rate and the reaction selectivity. The environment in the vicinity of active sites of Nafion-modified Cu-Selemion is similar to that of Cu,Pt-Nafion. Hence, the acidity is high, and the mass transport rate is enhanced. In conclusion, the SPE method using the Nafion-modified Cu-Selemion is promising for use in industrial aniline synthesis.

References

1. Z. Ogumi, M. Inaba, S. Ohashi, M. Uchida, and Z. Takehara, *Electrochim. Acta*, **33**, 365 (1988).
2. M. Inaba, Z. Ogumi, and Z. Takehara, *J. Electrochem. Soc.*, **140**, 19 (1993).
3. M. Inaba, J. T. Hinatsu, Z. Ogumi, and Z. Takehara, *J. Electrochem. Soc.*, **140**, 706 (1993).
4. Z. Ogumi, K. Nishio, and S. Yoshizawa, *Denki Kagaku*, **49**, 212 (1981).

5. Z. Ogumi, K. Inatomi, J. T. Hinatsu, and Z. Takehara, *Electrochim. Acta*, **37**, 1295 (1992).
6. Z. Chen, T. Mizoe, Z. Ogumi, and Z. Takehara, *Bull. Chem. Soc. Jpn.*, **64**, 537 (1991).
7. D. M. Bernardi and M. W. Verbrugge, *AIChE Journal*, **37**, 1151 (1991).
8. "Perfluorinated Ionomer Membranes," ed by A. Eisenberg and H. L. Yeager, ACS Symposium Series No. 180, American Chemical Society, Washington DC (1982).
9. R. S. Yeo, *Polymer*, **21**, 432 (1980).
10. The by-product was tried to be identified by MS, IR and HPLC. The formation of azoxybenzene was supposed to be the by-product because the molecular ion peak of the mass spectrum at $m/z = 198$ coincided with the molecular weight of azoxybenzene. However, the IR spectrum and HPLC chart are not in agreement with those of any products for the reduction of nitrobenzene listed in Refs. 11 and 12 including azoxybenzene.
11. M. R. Rifi and F. H. Covitz, "Introduction to Organic Electrochemistry", Marcel Dekker, New York (1974) Chap. 4.
12. M. Baizer and H. Lund, "Organic Electrochemistry", 2nd Ed., Marcel Dekker, New York (1983) Chap. 8.
13. S. Srinivasan, E. A. Ticianelli, C. R. Derouin, and A. Redondo, *J. Power Sources*, **22**, 359 (1988).
14. K. Kinoshita, "Electrochemical Oxygen Technology," John Wiley & Sons, New York (1992), p. 169.

Chapter 5

Reduction of Nitrobenzene Using a Flow-Through Pt-Nafion Cell

5.1. Introduction

Solid polymer electrolyte (SPE) electrolyzers using composite electrodes made of ion-exchange membranes and porous electrode materials deposited directly on the membranes have been extensively studied for use in water electrolyzers,^{1,2)} brine electrolyzers³⁾ and fuel cells.⁴⁾ Ogumi *et al.*⁵⁻¹⁰⁾ have reported on novel applications of the SPE electrolyzers to electro-organic synthesis. The SPE method eliminates the need for a supporting electrolyte, the addition of which often leads to difficulties in subsequent product separation and purification processes and to unwanted side reactions, and these merits render the method very promising for use in electro-organic synthesis.

The electroreduction of nitrobenzene has been a subject of considerable interest because it is one of valuable and promising reactions as industrial aniline synthesis. However, various kinds of by-products are known to be generated depending on electrolytic conditions, such as electrode material, electrode potential, pH, temperature, etc.^{11,12)} This by-product generation has

hindered the electrolytic method from being used in commercial aniline synthesis. On the other hand, aniline was produced selectively with a current efficiency greater than 90% on an SPE composite electrode in chapter 1;⁸⁾ hence, the SPE method is promising for use in industrial aniline synthesis.

The electroreduction of nitrobenzene using batch-type SPE electrolyzers was studied in chapters 1 to 4.⁸⁻¹⁰⁾ However, continuous operation of large-scale electrolytic systems is preferred for commercial use since it provides with better control of electrolyte temperature and composition, which in turn generally leads to higher product selectivity and better current efficiency. In addition, continuous systems allow more efficient design of the electrical equipment and heat exchangers. Continuous SPE electrolyzers, however, have not been tested for the reduction of nitrobenzene. Furthermore, a large amount of platinum (9.3 mg cm^{-2}) was used as the electrode material in batch-type cells in chapters 1 to 3.⁹⁾ From standpoints of capital cost and the availability of platinum resource, it is necessary to reduce its loading in SPE composite electrodes.

In this chapter, a flow-through cell using an SPE composite electrode with low Pt-loading (0.9 mg cm^{-2}) is fabricated. The reduction of nitrobenzene is preliminary studied using the cell, and the problems to be solved for industrial application are revealed.

5.2. Experimental

5.2.1. SPE composite electrode

A perfluorinated sulfonate ion-exchange membrane, Nafion[®] 415 (E. I. du Pont de Nemours and Co., EW = 1100), was used as the SPE material. The Nafion 415 membrane is reinforced with a polytetrafluoroethylene (PTFE) net. After treated in boiling water in the H^+ -form for more than 1 h, the membrane was immersed in an aqueous solution containing 1.0% platinum tetrammine dichloride, $\text{Pt}(\text{NH}_3)_4\text{Cl}_2$, for 30 min, and $\text{Pt}(\text{NH}_3)_4^{2+}$ was introduced into the membrane as a counter-ion by an ion-exchange reaction. Next, one side of the membrane was brought into contact with a reductant solution con-

taining NaBH_4 (0.5 M) and LiOH (0.1 M) for 30 min, and a platinum layer was deposited on the side of the membrane in a diameter of 3.0 cm. In the same manner, another platinum layer was deposited on the other side of the membrane. The amount of each Pt layer calculated from the ion-exchange capacity of Nafion (0.9 meq. g^{-1}) was 0.9 mg cm^{-2} . One of the platinum layers was modified with copper by an electroplating method in order to enhance its hydrogen overvoltage,⁸⁾ and was used as the cathode. The total charge passed during the Cu deposition was 4.2 C cm^{-2} -membrane. The resulting SPE composite electrode is referred to hereafter as Cu,Pt-Nafion.

5.2.2. *Electrolytic cell and electrolysis*

The flow-through cell used in this study is shown in Fig. 5.1. The cell consisted of two compartments made of PTFE, which were separated by Cu,Pt-Nafion. The inner diameter and the thickness of each compartment were 2.0 and 1.0 cm, respectively. The apparent surface area of each electrode was 3.1 cm^2 . Carbon cloth (Toray Industries, Inc., TO-13K) was stuffed into each compartment to obtain electrical contact with the Pt layer. A titanium plate was pressed onto the carbon cloth in each compartment. The carbon cloth and titanium plates functioned as current feeders. The free volume of each compartment was 1.1 cm^3 after stuffing the carbon cloth. The surface of the titanium plate placed at the end of the anode compartment was covered with RuO_2 by thermal decomposition of a propanol solution containing 6% RuCl_3 . Although this titanium plate could be used as a bipolar plate in a multi-cell configuration, a single-cell configuration was employed in this chapter.

A methanol solution (20 cm^3) containing 50 vol.% nitrobenzene and water (20 cm^3) were circulated at a flow rate of $3.0 \text{ cm}^3 \text{ min}^{-1}$ through the cathode (left-hand side in Fig. 5.1) and anode (right-hand side in Fig. 5.1) compartments, respectively. These solutions did not contain any supporting electrolytes. Electrolysis was carried out galvanostatically using a potentiostat/galvanostat (Hokuto Denko, model HA-301). The current efficiency was measured after 800 C were passed unless otherwise noted. Product mixtures were analyzed with a HPLC (Hitachi 638-30) fitted with a Wakopak[®] column

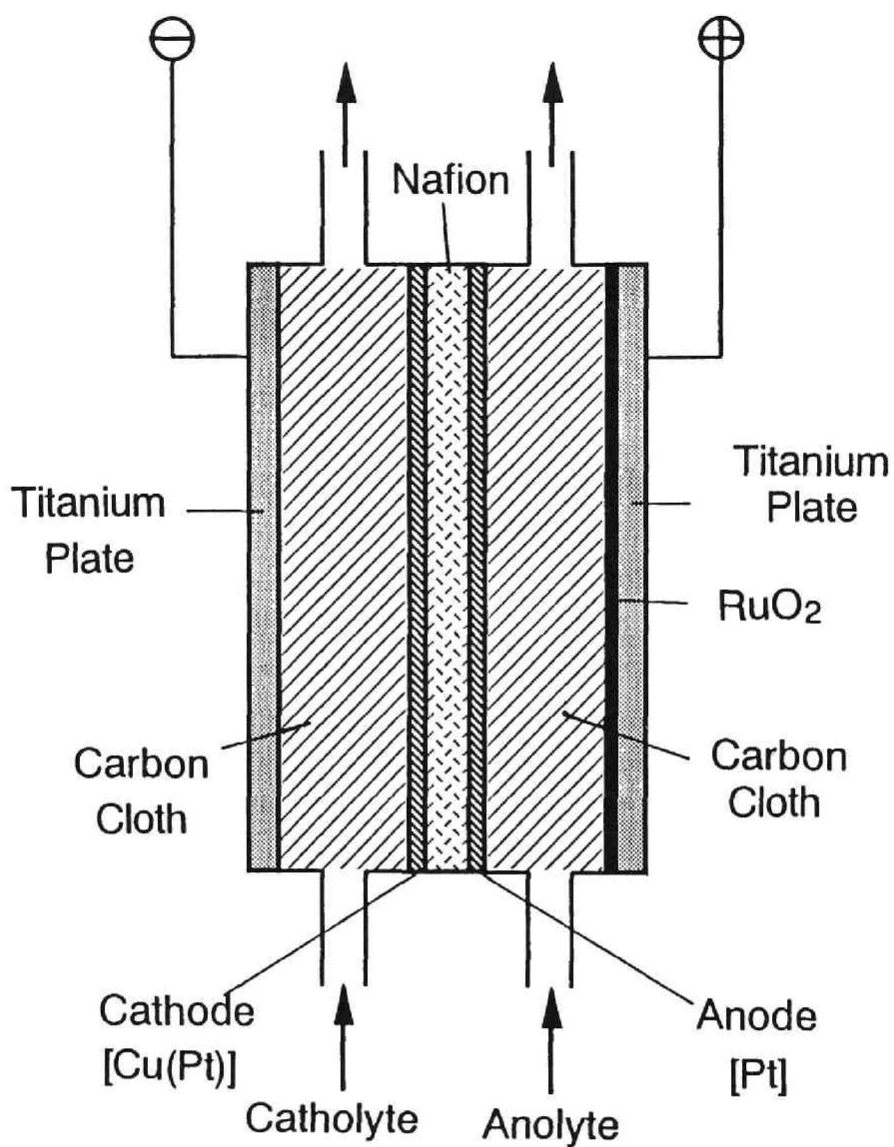


Fig. 5.1. Schematic diagram of flow-through SPE cell.

(Wako Pure Chemical, Lichrosorb RP18-5). After electrolysis, the catholyte was analyzed without pre-treatment.

5.2.3. Chemicals

All chemicals were of reagent grade, and were used without further purification.

5.3. Results and Discussion

5.3.1. Current-cell voltage characteristic

The current-cell voltage curve of the flow-through cell is shown in Fig. 5.2. At current densities less than 10 mA cm^{-2} the cell voltage increased steeply. Ohmic drop was estimated by a current interrupting method, and the cell voltage after corrected for the ohmic drop is also shown in Fig. 5.2. The steep increase in cell voltage at the low current densities is attributed mainly to the polarization of electrochemical reactions, i.e., the reduction of nitrobenzene and oxygen evolution. At current densities higher than 15 mA cm^{-2} , the measured cell voltage increased linearly with increasing current density. The iR -corrected cell voltage increased slightly, and hence ohmic drop is responsible for the linear increase observed at the high current densities. The resistance calculated from the slope in the high current density region was $1.3 \Omega \text{ cm}^2$. It was reported that the resistance of Nafion 117 is ca. $0.3 \Omega \text{ cm}^2$ in 0.3-3.0 M aqueous sulfuric acid at 25°C ,¹³⁾ the value of which is much lower than that obtained in this chapter. Since the Nafion membrane in the present electrolytic conditions is swollen by methanol in the catholyte, its ion-exchange sites are less dissociated than that immersed in aqueous acid solutions. This led to the high membrane resistance. Nevertheless, the resistance is much lower than those of conventional electrolytic cells using organic solvents.

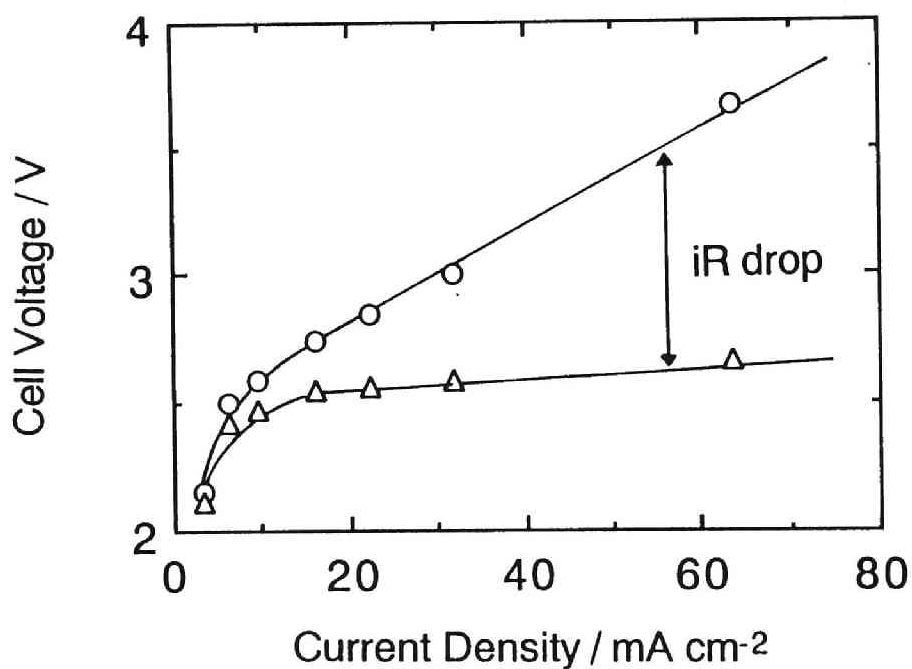


Fig. 5.2. Current-cell voltage curves for the reduction of nitrobenzene using a flow-through SPE cell. ○ : measured cell voltage; △ : after correction for ohmic drop. The catholyte was 20 cm³ of a methanol solution containing 50 vol.% nitrobenzene. The anolyte was 20 cm³ of water. The flow rates of the anolyte and catholyte were 3.0 cm³ min⁻¹, respectively.

5.3.2. Effects of current density on the current efficiency for aniline production

The variation of the current efficiency for aniline production with current density is shown in Fig. 5.3. The current efficiency was ca. 80% at current densities up to 32 mA cm^{-2} , and decreased remarkably with increasing current density at current densities greater than 32 mA cm^{-2} . For comparison, the variation of current efficiency obtained with the batch cell in chapter 1⁸⁾ is also shown in Fig. 5.3. (A methanol solution containing 30 vol.% nitrobenzene was used as the catholyte in chapter 1.) Such a decrease in current efficiency was not observed up to 100 mA cm^{-2} with the batch cell. Above 32 mA cm^{-2} no other organic by-products were detected with HPLC; the decrease in the current efficiency is attributable to an increase in the amount of hydrogen evolution. These results indicate that the mass-transport rate of nitrobenzene was limited above 32 mA cm^{-2} . If the current density at which the current efficiency decreases is assumed to be the mass-transport limiting current density, the limiting current density of the flow-through cell will roughly be estimated to be at least three times lower than that of the batch cell. This low limiting current density is attributed to a small surface area of the electrode material due to low Pt-loading (0.9 mg cm^{-2}).

Recently significant reductions in platinum loading (0.4 to 0.05 mg cm^{-2}) in SPE composite electrodes have been achieved in the field of polymer electrolyte fuel cells (PEFCs).^{14,15)} These reductions have been attained *via* better utilization of Pt catalyst in the gas diffusion electrode structure, e.g., the use of carbon particles with highly dispersed platinum catalyst and impregnation of solution-cast Nafion in the gas-diffusion electrode.¹⁴⁾ These methods may be used for the SPE composite electrodes for electroorganic synthesis to enhance the limiting current density.

Even at current densities less than 32 mA cm^{-2} , the current efficiency obtained with the flow-through cell was slightly lower than those obtained with the batch cell. A small amount of a by-product was found in the product mixtures in this current density region. Although it has not been identified yet because of its high reactivity, it was confirmed with HPLC as the same by-prod-

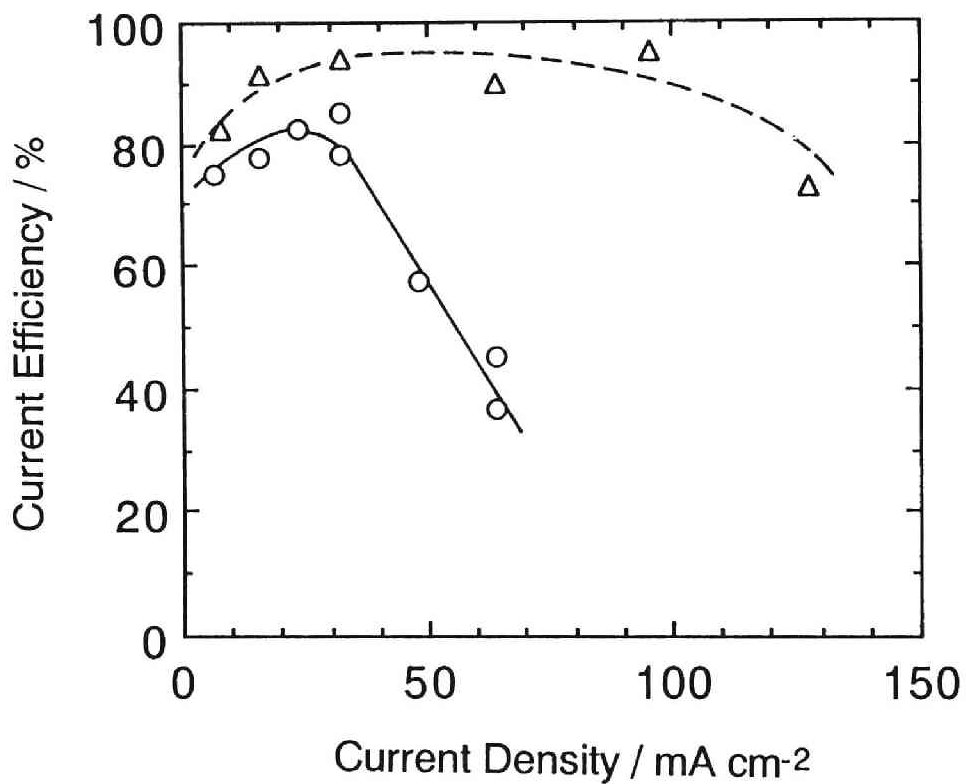


Fig. 5.3. Dependencies of current efficiency for aniline production on current density: (O) 50 vol.% nitrobenzene in methanol with the flow-through cell, and (Δ) 30 vol.% nitrobenzene in methanol with a batch cell.⁸⁾ Current density was 32 mA cm⁻² for each case.

uct as that obtained in the reduction of nitrobenzene using Cu-Selemion in chapter 4, which was made of a hydrocarbon sulfonate ion-exchange membrane, Selemion[®] CMV (Asahi Glass Co.), and copper deposited on the membrane.¹⁰⁾

Products obtained in the reduction of nitrobenzene are known to vary with electrode material, potential, acidity, temperature, etc.^{11,12)} In highly acidic solutions, aniline (6-electron process) and *p*-aminophenol (4-electron process) are obtained, the latter of which is produced *via* rearrangement of a phenylhydroxylamine intermediate. In less acidic solutions phenylhydroxylamine and dimerized products, such as azoxybenzene, hydroazobenzene, etc., tend to be generated. In chapter 4 using Cu-Selemion,¹⁰⁾ the molecular ion peak of the mass spectrum of the by-product was observed at $m/z = 198$, which indicated a dimer production. The formation of the dimerized by-product was attributed to a low acidity of Selemion. On the other hand, such a by-product was not produced, and aniline was selectively obtained with the batch cell in chapter 1 using Cu,Pt-Nafion.⁸⁾ Perfluorosulfonate membranes provide a high acidity comparable with that of an aqueous 10 wt.% H₂SO₄ solution.¹⁶⁾ Hence, it was considered that the high acidity of Nafion suppressed the formation of the dimerized product in chapter 1 using Cu,Pt-Nafion.^{8,17)} A small amount of the dimerized by-product was, however, obtained under the present electrolytic conditions although Nafion was used as the SPE material. This fact implies that the electrode reaction partly occurred at reaction sites being less acidic than that inside Nafion. It is suspected that the carbon cloth in contact with the electrode might participate in the electrode reaction. The acidity at the reaction sites on the carbon cloth is considered to be lower than that on the electrode metal (copper deposited on platinum) which is embedded inside the Nafion membrane. This low acidity led to the dimer production. In order to prove this consideration, preliminary electrolysis was carried out using a bare Nafion membrane (without electrode material) instead of Cu,Pt-Nafion of the cell shown in Fig. 5.1. In this system, a large amount of the dimerized product was formed. (The cell voltage was much higher than that for Cu,Pt-Nafion because of a poor contact of the carbon cloth with Nafion.) This result

proves that the dimerized product was formed on the carbon cloth in contact with Nafion.

This participation of the carbon cloth in the electrode reaction is caused by the leakage of the electrolytic current into the catholyte, which contains no supporting electrolyte. This leakage might be caused by insufficient electrostatic shielding by the deposited electrode and is attributed to the low platinum loading on the Nafion membrane. The enlargement of the reaction area by the methods for PEFCs as mentioned above would lead to suppression of the unwanted side reaction as well as enhancement of the limiting current density.

5.3.3. Effects of nitrobenzene concentration in catholyte on the current efficiency for aniline production

The dependence of the current efficiency for aniline production on the concentration of nitrobenzene in the catholyte is shown in Fig. 5.4. The current density was fixed at 32 mA cm^{-2} . While the current efficiency was almost constant in the range from 30 to 70 vol.%, it decreased at 15 vol.% and at concentrations higher than 70 vol.%. The decrease in the high concentration region was also observed with the batch-type SPE cell in chapter 2,⁹⁾ where the decrease was attributed to the immiscibility of the catholyte and water in the vicinity of the active sites of the electrode. The decrease in current efficiency in the low concentration region was not observed in the case for the batch-type cell. As shown in Fig. 5.2, the limiting current density for the flow-through cell was about 32 mA cm^{-2} even at 50 vol.% nitrobenzene. Hence the low current efficiency obtained at 15 vol.% in Fig. 5.4 is attributed to a low limiting current density due to the small surface area of the electrode.

5.3.4. Performance change with charge passed

The performance of the flow-through cell was examined for long-term operation. The cell voltage increased abruptly after ca. 5000 C were passed. After the electrolysis the surface resistance of the carbon cloth in contact with the anode was measured at 2 cm distance, and was of the order of $\text{k}\Omega$. It was considered that the increase in the surface resistance was caused by the oxida-

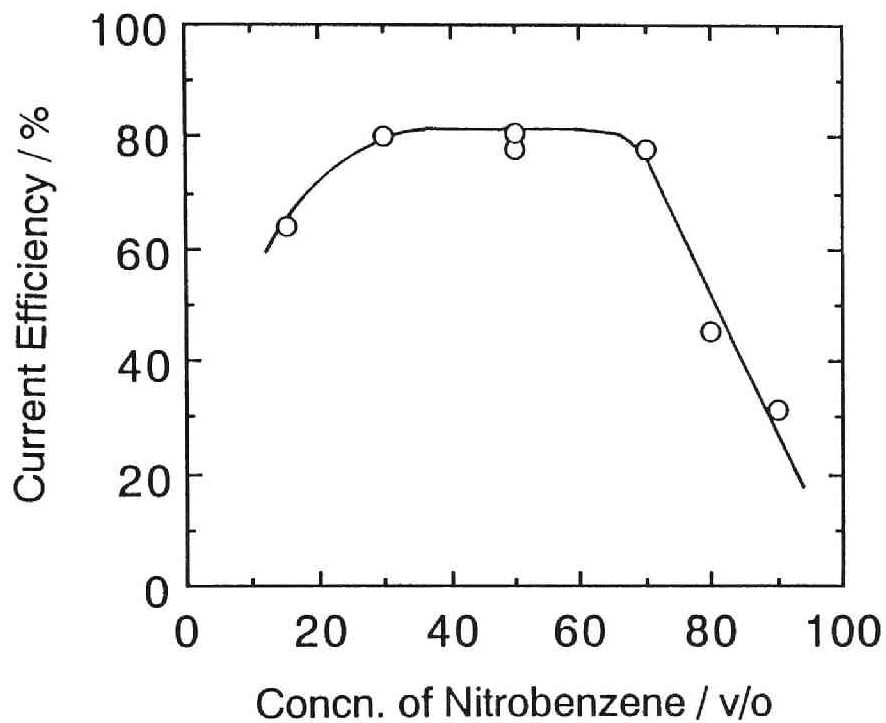


Fig. 5.4. Dependence of current efficiency for aniline production on nitrobenzene concentration in catholyte. Electrolysis was carried out at 32 mA cm^{-2} .

tion of the carbon cloth surface. Thus, a platinum mesh was inserted between the anode and the carbon cloth in order to prevent the carbon cloth from being oxidized during electrolysis, and cell performance was examined for long-period operation. Figures 5.5a and 5.5b show the current efficiency for aniline production and the cell voltage plotted against charge passed (Q). The current densities were 32 and 25 mA cm⁻², and the nitrobenzene concentrations in the catholytes were 50 and 30 vol.% in Figs. 5.5a and 5.5b, respectively. For each case, the current efficiency was high at an initial stage. However, after ca. 2000 C were passed, the current efficiency decreased with increasing Q . The decrease in current efficiency in Fig. 5.5a was more significant than that in Fig. 5.5b. Both cell voltages in Figs. 5.5a and 5.5b were stable, except for a slight increase at an initial stage in Fig. 5.5a.

One of the reasons why the current efficiency decreased was an increase in the amount of hydrogen evolution. At an initial stage of electrolysis (less than ca. 2000 C), gas evolution in the catholyte was sparingly observed. After ca. 2000 C were passed, gas bubbles appeared in the catholyte, and the amount of bubbles increased with increasing Q . The deterioration of the electrode or the membrane does not seem to be responsible for the increase in hydrogen evolution since the cell voltage was stable during the electrolysis.

Although the reasons of this increase in hydrogen evolution are not exactly known, it is inferred that the starvation of the reactant at the reaction sites due to the consumption of nitrobenzene in the catholyte. The current density of 32 mA cm⁻² used in Fig. 5.5a was close to the limiting current density at a nitrobenzene concentration of 50 vol.% (see Fig. 5.2). The decrease in the current efficiency is observed in Fig. 5.5a after a passage of ca. 2000 C. The concentration of nitrobenzene in the catholyte decreases with the consumption by the electrolysis, and the decrease reaches ca. 5% of the initial concentration when 2000 C are passed (see the upper scale of abscissa). The decrease in the nitrobenzene concentration would slow down the mass transport of nitrobenzene and cause a deficiency of nitrobenzene at the active sites of the cathode. The current would therefore be shared with hydrogen evolution.

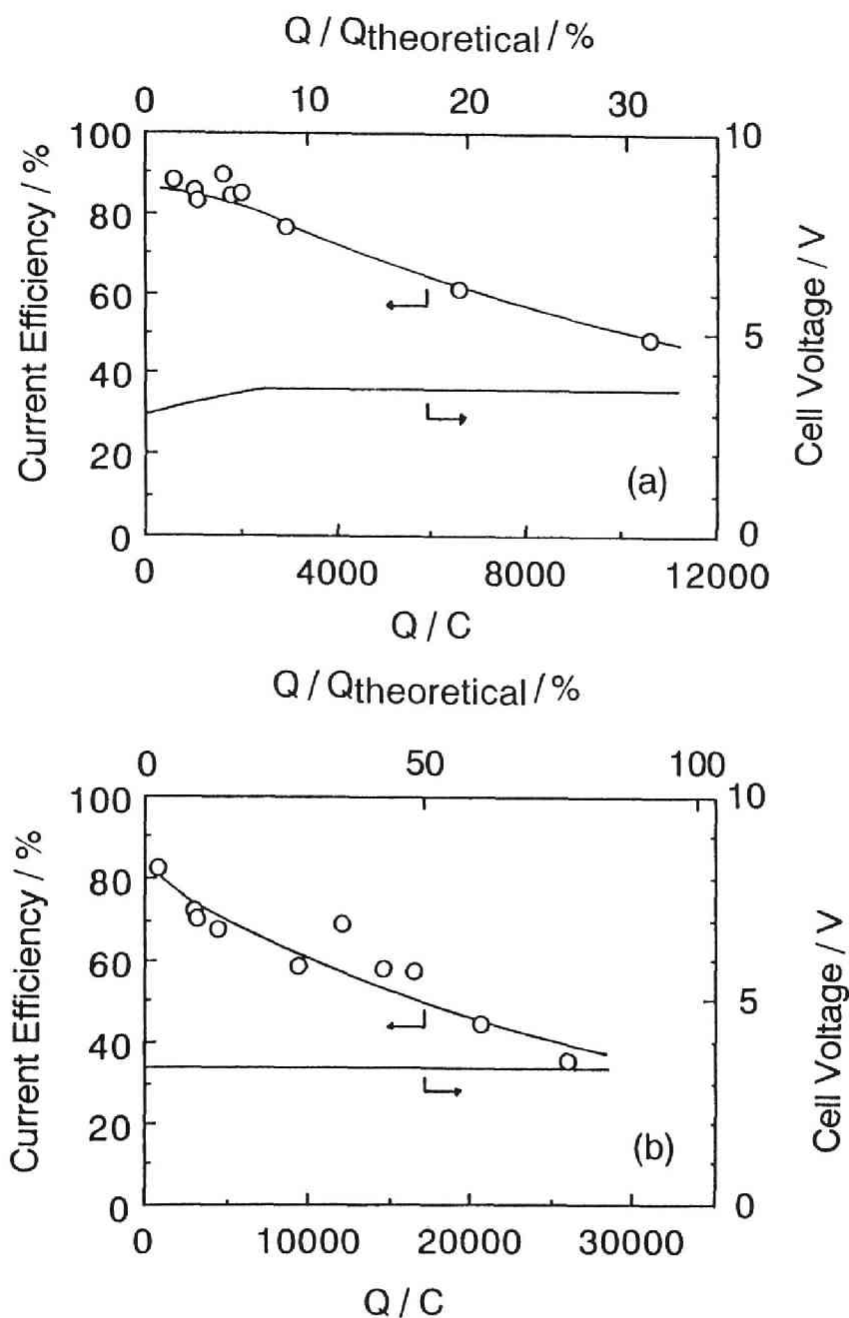


Fig. 5.5. Variation of current efficiency for aniline production and cell voltage during electrolysis. The catholytes contained 50 and 30 vol.% nitrobenzene, and the current densities were 32 and 25 mA cm⁻² for (a) and (b), respectively. A platinum mesh was inserted between the anode and the carbon cloth current feeder.

Another factor which leads to the decrease in current efficiency is the permeation of the product, aniline, through the membrane to the anolyte. The permeation of aniline through a Nafion membrane was reported previously.^{18,19)} Since aniline exists mostly in the form of $C_6H_5NH_3^+$ inside the membranes and Nafion has strong ion-exchange affinity for anilinium cation, aniline can be transported through the Nafion membrane even at a low concentration in the solution. Aniline was, actually, detected in the anolyte. The aniline concentration in the anolyte was measured, and its amount corresponded to a few percents of the current efficiency although the amount is not included in Figs. 5.5a and 5.5b. In addition, aniline is known to be oxidized and to polymerize on anode in acidic solutions.²⁰⁾ Hence a fraction of the permeated aniline is considered to have been lost by polymerization. In fact, a brownish polymerized substance was observed on the surface of the platinum anode after the long-term electrolysis, although the amount was not examined. It is therefore preferable to separate and recover the product from the catholyte during electrolysis to improve the current efficiency. In addition, it is a subject of further investigation to clarify the mass transport of the reactant, product, solvents, *etc.*, through the membrane during electrolysis.

5.3.5. Anode reaction

As mentioned above, the surface of the carbon cloth in contact with the anode was oxidized during long-term electrolysis. This was improved by inserting a platinum mesh between the anode and the carbon cloth. The oxidation of the carbon cloth would also be suppressed by replacing oxygen evolution to an anode reaction having an oxidation potential less positive than that of water. In addition, the use of such a reaction would be effective for a reduction in cell voltage. Thus, the oxidation of iodide ion was examined as an anode reaction. Figure 5.6 shows the current-cell voltage curve obtained using aqueous 3.7 M HI as the anolyte [curve (a)]. For comparison, the current-cell voltage curve which was obtained using water as the anolyte [curve (b)] was also shown in Fig. 5.6. When 3.7 M HI was used, the cell voltage was lower

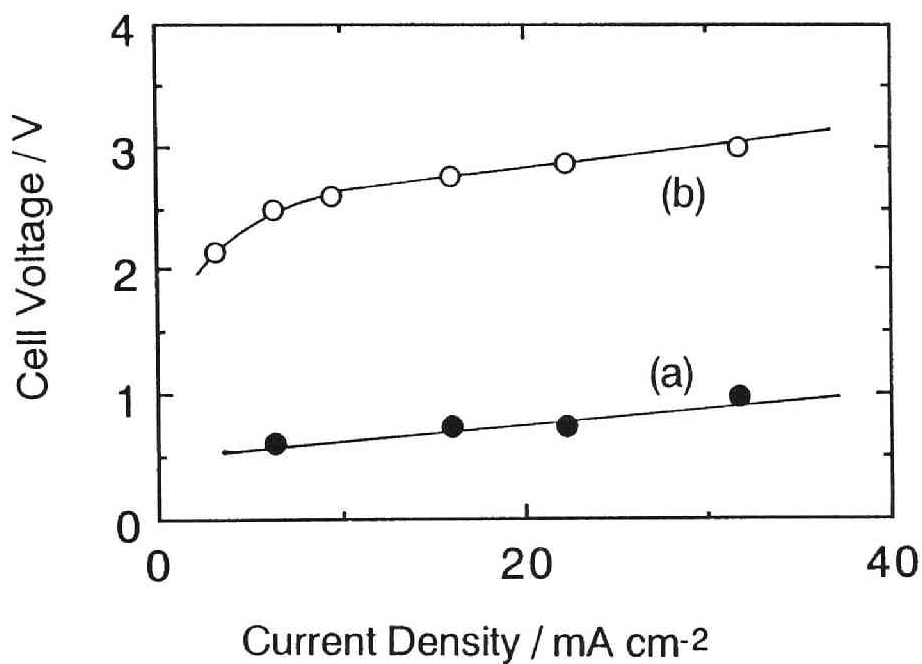


Fig. 5.6. Current-cell voltage curves for the reduction of nitrobenzene using the flow-through cell. (○) water and (●) aqueous 3.7 M HI were used as anolytes. The catholyte contained 50 vol.% nitrobenzene, and the flow rates of the catholyte and anolyte were $3.0 \text{ cm}^3 \text{ min}^{-1}$.

than 1.0 V up to 32 mA cm⁻², and stable for a long period. The following two reactions are known to occur in the oxidation of iodide ion:²¹⁾



The observed low cell voltage is attributed partly to these low oxidation potentials of iodide ion and the small polarization of the electrode reactions. The conductivity of Nafion membranes immersed in an acid solution, such as HBr, increases with increasing the acid concentration up to ca. 4 M.²²⁾ Hence the Nafion membrane in contact with 3.7 M HI had a higher conductivity than that in contact with water. In addition, since the anolyte had a high ionic conductivity, the anode reactions occurred not only on the porous platinum layer embedded inside the Nafion membrane, but also on the surface of the carbon cloth. The increase in membrane conductivity and the enlargement of the area for electrode reactions contributed to the reduction in cell voltage.

Using a 3.7 M HI solution and a 50 vol.% nitrobenzene solution as the anolyte and catholyte, respectively, electrolysis was carried out at 25 mA cm⁻². After 800 C were passed, aniline was obtained at a current efficiency of 80%. However, the current efficiency decreased to 42% after 4023 C were passed. This decrease was more significant than that obtained using oxygen evolution as the anode reaction (see Figs. 5.5a and 5.5b). In Eq. [5.1] iodine is produced on the anode. Iodine is a neutral species, and the solubility of iodine in an aqueous iodide solution (e.g., 35 mM in 0.67 M NaI at 10°C)²³⁾ is much higher than that of oxygen in water (1.3 mM at 20°C).²⁴⁾ After accumulation of iodine formed by Eq. [5.1] in the anolyte, a part of iodine diffused through the membrane to the cathode,²⁵⁾ where iodine was reduced on the cathode or reacted with aniline in the catholyte. This reaction would decrease the current efficiency more significantly than the case where oxygen evolution occurs at the anode. In order to use the iodine oxidation as an anode reaction, the removal of iodine produced in the anolyte must be considered during operation.

As is clearly shown by the fact that SPE composite electrodes are being developed for use in fuel cells,^{1,2)} the structure of the SPE composite electrodes is suitable for gas electrodes. Hydrogen oxidation is one of promising candidates for the anode reaction. The hydrogen oxidation releases only proton, which functions as the charge carrier in the membrane and is consumed at the cathode as one of the reactants in the reduction of nitrobenzene. The oxidation potential of hydrogen, which is close to the reduction potential of nitrobenzene, is useful to reduce the cell voltage of SPE electrolyzers.

5.4. Conclusions

In the present study, a flow-through cell using a solid polymer electrolyte composite electrode with low Pt-loading (0.9 mg cm^{-2}) was fabricated, and the reduction of nitrobenzene was studied. It was revealed that the following problems must be solved for industrial application.

(i) The use of an SPE composite electrode with low metal loading resulted in a low limiting current density and generation of a by-product. The effects of the low metal loading were also observed in long-term electrolysis. These results are attributed to a small surface area of the electrode material. To enhance the limiting current density and product selectivity, it is necessary to improve the electrode metal utilization, e.g., using the methods developed in PEFCs.

(ii) The permeation of the product, aniline, through the Nafion membrane caused a decrease in the current efficiency, in particular, in long-term electrolysis. Hence, it is preferable to separate and recover the product from the catholyte during electrolysis. In addition, extensive investigation is necessary to clarify the mass transport of the reactant, product, solvents, etc. through the membrane.

(iii) The cell voltage was reduced by using iodide oxidation as an anode reaction. However, the product at the anode, iodine, permeated through the Nafion membrane. This resulted in a decrease in the current efficiency, in

particular, in long-term electrolysis. Hence iodine produced on the anode must be removed during electrolysis.

References

1. E. Torikai and H. Takenaka, *Soda to Enso*, 51 (1980).
2. P. W. Lu and S. Srinivasan, *J. Appl. Electrochem.*, **9**, 269 (1979).
3. A. P. Laconti, *Japan Tokkyo Kokai*, 54-112398 (1979).
4. G. A. Eisman, *J. Power Sources*, **29**, 389 (1990).
5. Z. Ogumi, K. Nishio and S. Yoshizawa, *Denki Kagaku*, **49**, 212 (1981).
6. Z. Ogumi, H. Yamashita, K. Nishio, Z. Takehara and S. Yoshizawa, *Denki Kagaku*, **52**, 180 (1984).
7. Z. Ogumi, T. Mizoe, Z. Chen and Z. Takehara, *Bull. Chem. Soc. Jpn.*, **63**, 3365 (1990).
8. Z. Ogumi, M. Inaba, S. Ohashi, M. Uchida and Z. Takehara, *Electrochim. Acta*, **33**, 365 (1988).
9. M. Inaba, Z. Ogumi and Z. Takahara, *J. Electrochem. Soc.*, **140**, 19 (1993).
10. M. Inaba, K. Fukuta, Z. Ogumi and Z. Takehara, *Chem. Lett.*, 1779 (1993).
11. M. R. Rifi and F. H. Covitz, "Introduction to Organic Electrochemistry", Marcel Dekker, New York (1974) Chap. 4.
12. M. Baizer and H. Lund, "Organic Electrochemistry", 2nd Ed., Marcel Dekker, New York (1983) Chap. 8.
13. M. W. Verbrugge and R. F. Hill, *J. Electrochem. Soc.*, **137**, 3770 (1990).
14. E. A. Ticianelli, C. R. Derouin and S. Srinivasan, *J. Electroanal. Chem.*, **251**, 275 (1988).
15. E. J. Taylor, E. B. Anderson and N. R. K. Vilambi, *J. Electrochem. Soc.*, **139**, L45 (1992).

16. K. Kinoshita, "Electrochemical Oxygen Technology", John Wiley & Sons, New York (1992) p. 169.
17. *Para*-aminophenol or *p*-anisidine, which would be produced via rearrangement of phenylhydroxylamine intermediate (4-electron process) under highly acidic conditions, were not produced, and selective aniline production was observed. The reason why these compounds are not produced has not been clarified yet.
18. Z. Ogumi, K. Toyama, Z. Takehara, K. Katakura and S. Inuta, *J. Membrane Sci.*, **65**, 205 (1992).
19. K. Katakura, M. Inaba, K. Toyama, Z. Ogumi and Z. Takehara, *J. Electrochem. Soc.*, **141**, 1827 (1994).
20. A. Kitani, M. Kaya and K. Sasaki, *J. Electrochem. Soc.*, **133**, 1069 (1986).
21. A. J. Bard and L. R. Faulkner, "Electrochemical Methods", John Wiley & Sons, New York (1980) p. 700.
22. R. S. Yeo and J. McBreen, *J. Electrochem. Soc.*, **126**, 1682 (1979).
23. "Kagaku Daijiten Vol. 9", Kyoritsu Shuppan, Tokyo (1962) p447.
24. Chemical Society of Japan, "Kagaku Binran", 4th Ed., Maruzen, Tokyo (1984) p. II-159.
25. F. G. Will, *J. Electrochem. Soc.*, **126**, 36 (1979).

Part II

Utilization of Phase-Transfer
Mediators
Incorporated into Nafion

Chapter 6

Indirect Electrochemical Debromination Using Viologens as Microscopic Phase-Transfer Mediators

6.1. Introduction

Solid polymer electrolyte (SPE) composite electrodes have been extensively studied for use in water electrolyzers¹⁾ brine electrolyzers²⁾ and fuel cells.³⁾ Ogumi *et al.*⁴⁻¹⁰⁾ have previously reported on novel applications of SPE electrolyzers to organic syntheses. The SPE method eliminates the need for a supporting electrolyte, the addition of which often leads to difficulties in subsequent product purification processes and to unwanted side reactions; hence, the method is very promising for use in electro-organic syntheses.

Perfluorosulfonic acid membranes, such as Nafion[®], are generally used as the SPE material due to their chemical stability. Several models of the microstructure of Nafion have been proposed. In the model of Gierke *et al.*, Nafion is microscopically separated into two phases: a hydrophilic ionic cluster domain, and a hydrophobic fluorocarbon backbone domain.^{11,12)} Yeager and Steck¹³⁾ proposed a three-phase model where an "interfacial" region exists between the two domains of Gierke's model. Ogumi *et al.*¹⁴⁾ considered that the interfacial region consists of the amorphous part of the fluorocarbon backbone and the side chains of Nafion.

A major concern of studies on Nafion membranes has been the structure of the ionic cluster, especially with regard to clarifying the mass-transport phenomena of inorganic ions through Nafion.¹⁵⁻¹⁷⁾ Electrodes coated with Nafion also have been a subject of considerable recent interest.¹⁸⁻²⁴⁾ In the latter studies with Nafion-coated electrodes, several workers have observed unusual behavior of organic ions incorporated into Nafion resulting from the multi-phase structure of Nafion, in particular, from interactions of the organic ions with the hydrophobic interfacial region.²²⁻²⁴⁾ In SPE composite electrodes, the electrode materials are covered with Nafion polymer electrolyte; hence, the environment found in SPE composite electrodes is similar to that in the polymer coated electrodes. Since the active sites of SPE composite electrodes are located in the complex environment of the Nafion membrane,⁸⁾ the influence of Nafion's hydrophobic region must be taken into account when organic compounds are treated.

The principal purpose of this chapter is to develop a new SPE method that takes advantage of the multi-phase structure of Nafion. The ionic clusters of Na^+ -form Nafion contain about 1000 molecules of water per unit cluster after the standard pre-treatment in boiling water,²⁵⁾ hence, the ionic cluster region may be regarded as an aqueous phase. On the other hand, the interfacial region consists of the amorphous part of the fluorocarbon backbone and the side chains of Nafion, which are lipophilic and flexible, and thus the interfacial region is expected to behave as an organic phase. Consequently, it is reasonable to expect that if phase-transfer catalysts were to be incorporated into Nafion, they could transfer between the two phases of Nafion, that is, between the hydrophilic ionic cluster region and the hydrophobic interfacial region. *N,N'*-dialkyl-4,4'-bipyridinium salts (viologens, C_nV) were used as phase-transfer catalysts in this chapter. Viologens are known to react through two successive one-electron transfer steps in homogeneous solutions,^{26,27)} as shown in Fig. 6.1. In an organic-aqueous two-phase system, the dication (C_nV^{2+}) resides mainly in the aqueous phase, while the cation radical ($\text{C}_n\text{V}^{+\bullet}$) and the doubly reduced neutral form (C_nV^0) are easily extracted into the organic phase.²⁸⁾ Due to such tendencies, viologens have been used as phase-

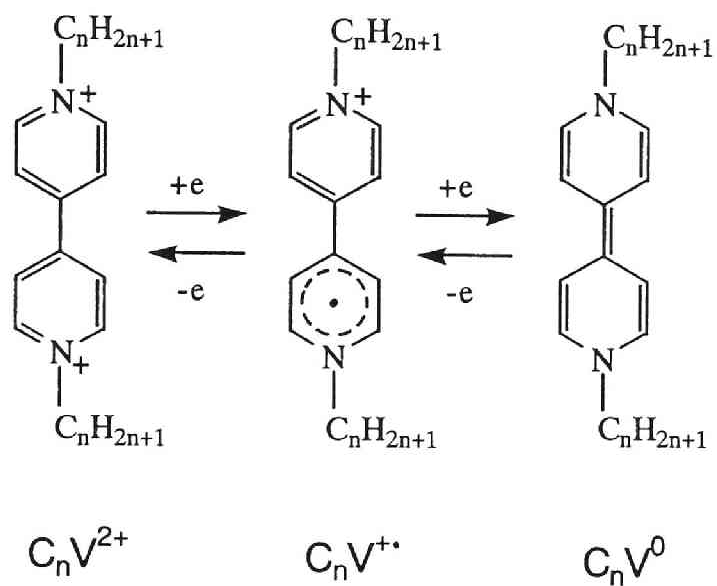


Fig. 6.1. Electrochemical reactions of viologens in homogeneous solutions.

transfer mediators in the chemical reduction of organic compounds, where the viologen compounds function as electron carriers as well as phase-transfer catalysts.²⁹⁻³⁶⁾

In this chapter, indirect electro-debromination of *meso*-1,2-dibromo-1,2-diphenylethane (DBDPE) using viologens as phase-transfer mediators is first examined in an emulsion system consisting dichloromethane and an aqueous solution, and the mechanism for the generation of the active species at the immiscible interface is speculated. Then, the indirect electro-reduction is studied using SPE composite electrodes with incorporated viologens as their counterion, and the reaction mechanism on the SPE composite electrodes is discussed.

6.2. Experimental

6.2.1. Chemicals

N,N'-dialkyl-4,4'-bipyridinium dibromide (C_nVBr_2 , $n = 2,3,5$ and 8) was prepared from 4,4'-bipyridine (1.0 g) and the corresponding alkyl bromide.³⁰⁾ *N,N'*-dimethyl-4,4'-bipyridinium diiodide (C_1VI_2) was prepared from 4,4'-bipyridine (1.0 g) and methyl iodide. The precipitates formed upon heating were filtered, washed several times with acetone, and recrystallized from ethanol solutions.

DBDPE was prepared by bromination of *trans*-stilbene (2.0 g) using pyridinium hydrobromide perbromide.³⁷⁾ The precipitate was filtered and washed with methanol.

Acetonitrile and dichloromethane were of reagent grade and used after distillation. Other chemicals were of reagent grade, and were used without further purification.

6.2.2. Electrochemical measurements with glassy carbon (GC) and Nafion-coated GC electrodes

Electrochemical measurements were carried out using a conventional three-electrode system. The working electrode consisted of a glassy carbon

(GC, 0.071 cm²) mounted in a Teflon[®] tube. The counter electrode was a platinum wire. Potentials were measured as, and referred to as, volts *vs.* Ag/AgCl (3.3 M KCl). Cyclic voltammetry was performed with a potentiostat/galvanostat (Hokuto Denko, model HA-301) and a function generator (Hokuto Denko, model HB-104).

The Nafion-coated GC electrode was prepared as follows: 2 × 10⁻³ cm³ of a solution of Nafion dissolved in alcohol (Aldrich, containing 5 wt.% Nafion of EW = 1100) was spread with a microsyringe onto a GC electrode and air-dried. The thickness of the recast Nafion is roughly estimated to be 7.8 μm by using 1.58 g cm⁻³ as the wet, Na⁺-form density.²¹⁾ The Nafion-coated electrode was then immersed in a 0.01 M viologen solution for 30 min to incorporate viologen in the Nafion coating. The quantity of electroactive viologen in the Nafion coating was determined coulometrically by integrating the current that passed when the electrode potential was stepped from 0 to -0.8 V in aqueous 0.5 M KNO₃.³⁸⁾ This quantity was estimated as the surface concentration (Γ) in units of mol cm⁻².

6.2.3. Debromination of DBDPE by emulsion electrolysis

Emulsion electrolysis was carried out using a cylindrical undivided cell. A copper plate (40 cm²) was used as the cathode, and a platinum wire (1.5 cm²) was used as the anode. The two-phase system consisted of dichloromethane (40 cm³) containing DBDPE (1.5 mmol), and of aqueous phosphate buffer (0.25 M, pH 7, 20 cm³). The two-phase system was stirred vigorously, and viologen (0.2 mmol) was added. Electrolysis was carried out at a constant current of 0.5 mA cm⁻². During runs, CH₂Cl₂-saturated argon was bubbled through the two-phase system to purge oxygen dissolved in the two-phase system. After electrolysis, the organic phase was separated, and was analyzed by HPLC without any preceding separation processes, using a Hitachi 638-30 liquid chromatograph fitted with a Zorbax ODS column (du Pont Co.).

6.2.4. *Cu-modified Pt-SPE composite electrode (Cu,Pt-Nafion)*

Cu-modified Pt-Nafion composite electrodes were prepared as described in chapters 1 to 3.⁸⁾ A perfluorosulfonate cation-exchange membrane, Nafion[®] 415 (E. I. du Pont de Nemours and Co.), was used as the SPE material. The Nafion 415 membrane was treated in boiling water, and then platinum was first deposited on one side of the membrane by an electroless plating method.⁴⁾ The amount of deposited Pt was typically 9.3 mg cm⁻². Copper was then deposited on the Pt layer by an electroplating method to enhance the hydrogen overvoltage.⁸⁾ The total charge passed during Cu deposition was 10 C cm⁻². The resulting Cu-modified Pt-Nafion is referred to hereafter as "Cu,Pt-Nafion".

6.2.5. *Incorporation of Viologens into Cu,Pt-Nafion*

Cu,Pt-Nafion was rinsed with distilled water and immersed in aqueous 0.5 M Na₂SO₄ under argon purging for 3 h to change its counter-ion from Cu²⁺ to Na⁺. Viologen dications were then incorporated into the SPE composite electrode by immersing the electrode in a 0.01 M viologen solution for 12 h under argon purging.

6.2.6. *Debromination of DBDPE by SPE method*

The cell used for SPE electrolysis is shown in Fig. 6.2. The cell was composed of two compartments, which were separated by the SPE composite electrode. The volume of each compartment was 40 cm³. The effective geometric surface area of the SPE composite electrode was 3.1 cm². A platinum wire (1.5 cm²) was used as the counter electrode. The current feeder for the SPE composite electrode consisted of a gold ring, which was pressed onto the outer surface of the deposited Pt layer. Electrode potentials were measured using a Luggin capillary placed in the anode compartment. The measured potentials include the contributions of a fairly large ohmic drop as well as a junction potential. The cathode compartment (left-hand side) was filled with CH₂Cl₂ containing 0.6 mmol DBDPE. No supporting electrolytes were added to the catholyte. The anode compartment (right-hand side) was filled

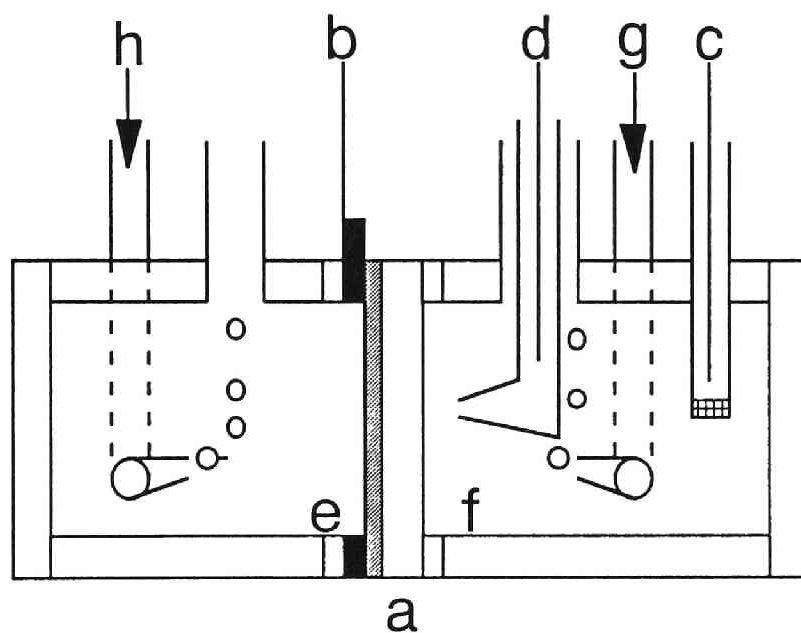


Fig. 6.2. Schematic diagram of the electrolytic cell for the SPE composite electrode. (a) SPE composite electrode; (b) current feeder; (c) platinum wire counter electrode; (d) Ag/AgCl reference electrode; (e) cathode compartment; (f) anode compartment; (g) argon gas inlet; (h) CH_2Cl_2 -saturated argon gas inlet.

with 0.1 M aqueous phosphate buffer (pH 7). Electrolysis was carried out galvanostatically unless otherwise noted. During runs argon and CH₂Cl₂-saturated argon were bubbled through the anode and cathode compartments, respectively. After electrolysis, the catholyte was analyzed by HPLC without any preceding separation processes.

6.3. Results and Discussion

6.3.1. Active species in homogeneous system

Cyclic voltammograms for C₃VBr₂ and DBDPE on a GC electrode in acetonitrile are shown in Fig. 6.3. The cyclic voltammogram for C₃VBr₂ [curve (a) in Fig. 6.3] clearly showed two reversible one-electron reduction waves. Similar results were obtained for C₁VI₂, C₂VBr₂, C₅VBr₂, and C₈VBr₂. The respective half-wave potentials ($E_{1/2} = (E_{pc} + E_{pa}) / 2$)³⁹⁾ are listed in Table 6.1. The first and the second half-wave potentials were almost constant, and independent of the alkyl-chain lengths of viologens. These results are in accordance with the results reported by van Dam and Ponjee.²⁷⁾ Curve (b) in Fig. 6.3 shows a cyclic voltammogram taken in DBDPE solution. The reduction current started to flow at -0.70 V vs. Ag/AgCl. Curve (c) in Fig. 6.3 shows the effect of the addition of DBDPE on the voltammogram for C₃VBr₂. The addition did not affect the reversibility of the first set of redox peaks. On the other hand, the second set of peaks was strongly affected by the addition of DBDPE. A large increase in the cathodic current was observed, and the oxidation wave on the reverse scan was depleted, although the first oxidation wave was not affected. This result suggests a rapid consumption of C₃V⁰ by a chemical reaction between C₃V⁰ and DBDPE.⁴⁰⁾ Similar results were obtained for C₁VI₂, C₂VBr₂, C₅VBr₂, and C₈VBr₂. Consequently, it is concluded that the active species for the reduction of DBDPE in homogeneous solutions is not C_nV⁺⁺, but C_nV⁰.

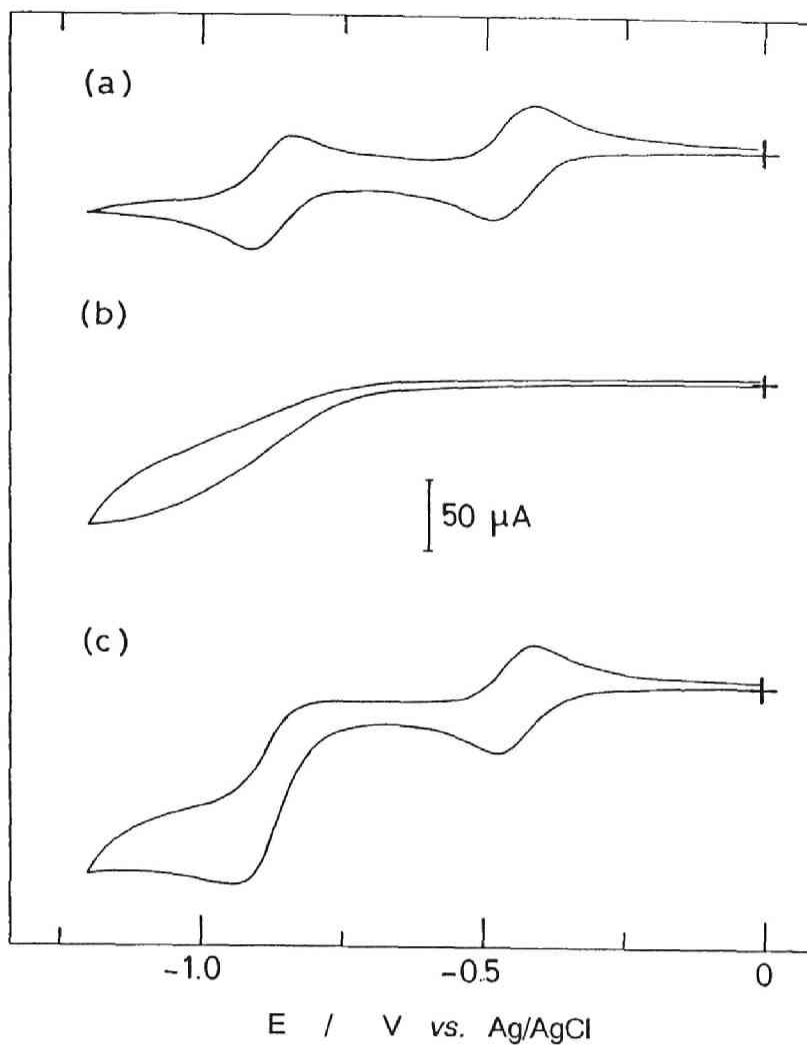


Fig. 6.3. Cyclic voltammograms for (a) $2.1 \text{ mM } \text{C}_3\text{VBr}_2$, (b) 4.0 mM DBDPE and (c) $2.1 \text{ mM } \text{C}_3\text{VBr}_2 + 4.0 \text{ mM DBDPE}$ in $0.2 \text{ M LiClO}_4/\text{acetonitrile}$ on GC (0.071 cm^2). $\nu = 50 \text{ mV sec}^{-1}$.

Table 6.1. Half-wave potentials of various viologens in acetonitrile.

Viologen	$-E_{1/2}$ (V vs. Ag/AgCl)	
	1st step	2nd step
C ₁ VI ₂	0.48	0.89
C ₂ VBr ₂	0.44	0.86
C ₃ VBr ₂	0.45	0.88
C ₅ VBr ₂	0.43	0.86
C ₈ VBr ₂	0.46	0.89

6.3.2. Debromination of DBDPE by emulsion electrolysis

The results for the electrochemical debromination of DBDPE to *trans*-stilbene in the two-phase system consisting of dichloromethane and aqueous phosphate buffer (pH 7) are summarized in Table 6.2. Without any additives (Run 1), the current efficiency for *trans*-stilbene production was 0.9%, that is, the debromination hardly occurred at all. The addition of dodecyltrimethylammonium bromide (DTAB) to the two-phase system (Run 2) accelerated the debromination reaction, and the current efficiency increased to 22.3%. Although DTAB cannot serve as an electron mediator, it improves the wettability of the electrode surface by the organic phase through its adsorption, and gives ionic conductivity to the organic phase. Therefore, DBDPE can be considered to have received electrons directly from the electrode through the "wetting mechanism" proposed by Wendt *et al.*,^{41,42)} resulting in *trans*-stilbene production. A polymer-like substance was observed as a by-product. This by-product may have been produced through the electro-polymerization of *trans*-stilbene at the anode, and the yield (moles *trans*-stilbene produced/moles reactant consumed) was therefore only 78%. Increasing amount of DTAB (Run 3) did not change the current efficiency significantly.

The addition of a catalytic amount (0.2 mmol) of C₈VBr₂ (Run 4 in Table 6.2) enhanced the current efficiency to 37.0%. Polymer-like product was again observed as a by-product. Increasing amount of C₈VBr₂ to 0.4 mmol (Run 5) improved the current efficiency, and increasing charge passed (Run 6) improved the conversion (60.6%).

Several workers have studied chemical debromination of DBDPE catalyzed by viologens in two-phase systems, and two different reaction mechanisms have been proposed.^{29,30)} Endo *et al.*²⁹⁾ have proposed a mechanism in which viologen cation radical extracted from an aqueous phase into an organic phase reacts directly with DBDPE. On the other hand, Maiden *et al.*³⁰⁾ concluded that the doubly reduced neutral form of viologen is generated by the disproportionation of the cation radical in a two-phase system, and that the neutral form reacts with DBDPE.

Table 6.2. Electro-debromination of *meso*-1,2-dibromo-1,2-diphenylethane in two phase system^a.

Run	Catalyst (mmol)	Q (F/mol)	Current efficiency (%)	Yield ^c (%)	
1	none	(0)	2	0.9	-
2	DTAB ^b	(0.2)	2	22.3	78.0
3	DTAB	(0.4)	2	20.7	74.5
4	C ₈ VBr ₂	(0.2)	2	37.0	86.0
5	C ₈ VBr ₂	(0.4)	2	48.3	81.8
6	C ₈ VBr ₂	(0.2)	4	30.3	73.9

^a The two phase system consisted of 40cm³ of CH₂Cl₂ containing 1.0 mmol of *meso*-1,2-dibromo-1,2-diphenylethane, and of 20 cm³ of 0.25 M phosphate buffer solution (pH 7). I = 0.5 mA/cm².

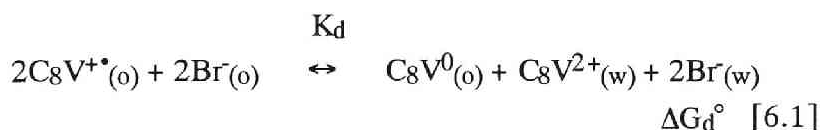
^b Dodecyltrimethylammonium bromide.

^c Yield = (amount of product) / (amount of consumed reactant) × 100 (%).

In the emulsion electrolysis in this chapter, the addition of C_8VBr_2 resulted in a blue color in both the organic and aqueous phases due to $C_8V^{+\bullet}$. Without any stirring, the blue color of $C_8V^{+\bullet}$ prevailed only in the vicinity of the cathode in the aqueous phase. It is therefore inferred that $C_8V^{+\bullet}$ produced on the electrode in the aqueous phase is extracted into the organic phase upon stirring. The electrode potential during Run 4 in Table 6.2 was measured, and was about -0.6 V vs. Ag/AgCl. At this potential, C_8V^0 cannot be produced; only $C_8V^{+\bullet}$ production is possible. Since $C_8V^{+\bullet}$ itself was not active for the debromination (as shown in Fig. 6.3), the active species, C_8V^0 , can reasonably be considered to be produced by the disproportionation of $C_8V^{+\bullet}$, as in the reaction mechanism proposed by Maidan *et al.* The reaction mechanism is outlined in Fig. 6.4. In this mechanism, $C_8V^{+\bullet}$, which is formed on the electrode in the aqueous phase, is extracted into the organic phase, where it disproportionates to C_8V^0 and C_8V^{2+} . Octylviologen dication, C_8V^{2+} , is then extracted back into the aqueous phase, and C_8V^0 reacts with DBDPE in the organic phase.

6.3.3. Estimation of disproportionation constant (K_d) in two-phase system

In order to further substantiate the reaction mechanism proposed above (Fig. 6.4), the disproportionation constant, K_d , of octyl viologen cation radical was estimated for a two-phase system consisting of dichloromethane and water. The disproportionation of octyl viologen cation-radical ($C_8V^{+\bullet}$) in a dichloromethane-water two-phase system is expressed as:



where subscripts (o) and (w) indicate species in the organic phase and in the aqueous phase, respectively, and K_d denotes the disproportionation constant. Bromide ions are included in reaction [6.1] to satisfy the electroneutrality re-

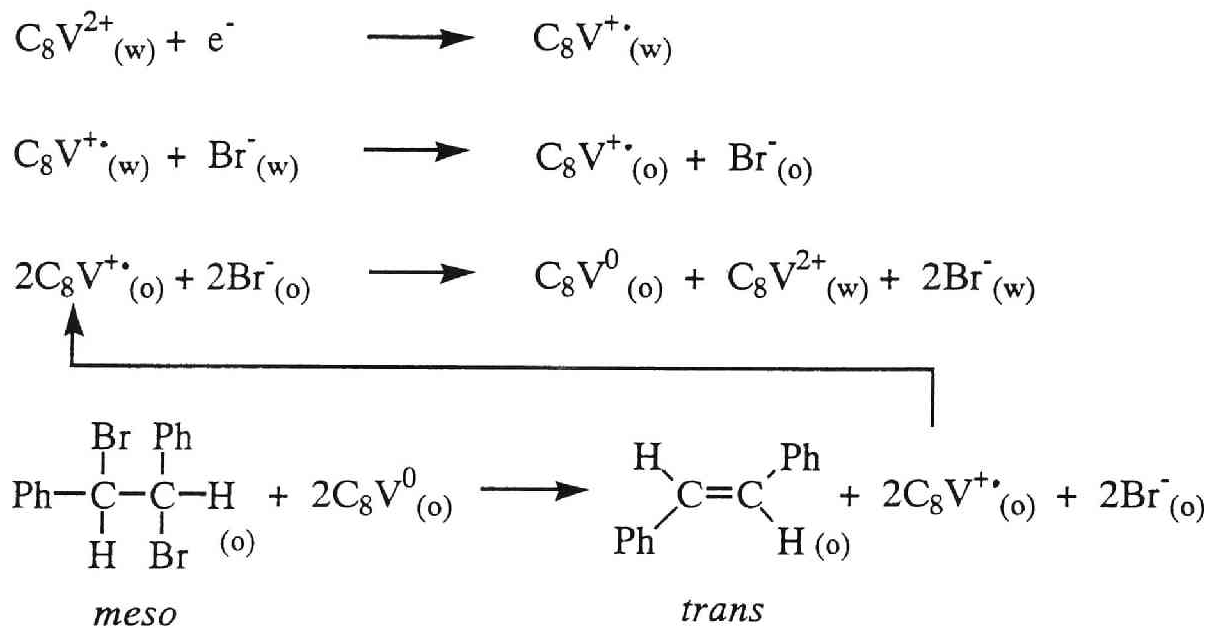
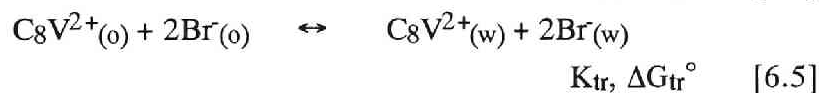
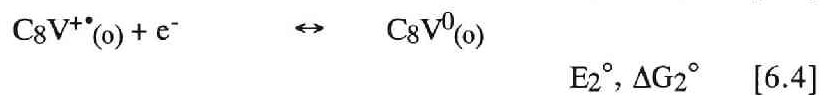
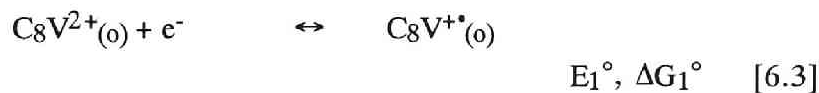


Fig. 6.4. Reactions for debromination of DBDPE by viologens in a two-phase system.

quirement in each phase. The disproportionation constant, K_d , is related to the standard free energy change, ΔG_d° , by the equation

$$\Delta G_d^\circ = -RT \ln(K_d) \quad [6.2]$$

where R is the gas constant and T is the temperature. Reaction [6.1] can be separated into the following three reactions:



where E_1° and E_2° are the standard electrode potentials for $\text{C}_8\text{V}_{(o)}^{2+}/\text{C}_8\text{V}_{(o)}^{+\bullet}$ and $\text{C}_8\text{V}_{(o)}^{+\bullet}/\text{C}_8\text{V}_{(o)}^0$, respectively, and K_{tr} is the extraction constant of C_8VBr_2 from the organic phase to the aqueous phase. ΔG_1° , ΔG_2° and ΔG_{tr}° are the standard free energy changes for reactions [6.3], [6.4] and [6.5], respectively, and are given by

$$\Delta G_1^\circ = -FE_1^\circ \quad [6.6]$$

$$\Delta G_2^\circ = -FE_2^\circ \quad [6.7]$$

$$\Delta G_{tr}^\circ = -RT \ln(K_{tr}) \quad [6.8]$$

where F is the Faraday constant. From equations [6.1] to [6.8], the following relation is obtained:

$$\Delta G_d^\circ = (\Delta G_2^\circ - \Delta G_1^\circ) + \Delta G_{tr}^\circ \quad [6.9]$$

$$= -F(E_2^\circ - E_1^\circ) - RT \ln(K_{tr}) \quad [6.10]$$

The first term in equation [6.10], $E_2^\circ - E_1^\circ$, was estimated from the voltammogram shown in Fig. 6.5, which was taken in water-saturated dichloromethane containing 1.02 mM C_8VBr_2 , 1.33 mM ferrocene (Fc) and 0.1 M tetrabutylammonium perchlorate (TBAP). The anodic and cathodic peaks around 0.55 V, -0.3 V and -0.8 V *vs.* Ag/AgCl are assigned to Fc^+/Fc^0 , $C_8V^{2+}/C_8V^{+\bullet}$ and $C_8V^{+\bullet}/C_8V^0$, respectively. The potential at the midpoint between the anodic and cathodic peaks of each redox couple corresponds to its half-wave potential ($E_{1/2}$).³⁴⁾ Here $E_{1/2}$ was used as the standard electrode potential (E°), assuming the oxidized and reduced halves of each redox couple have equal diffusion coefficients and equal activity coefficients. In Fig. 6.5, $E_2^\circ - E_1^\circ$ is -516 mV, and the first term of equation [6.9], $\Delta G_2^\circ - \Delta G_1^\circ$, is estimated to be 49.8 kJ mol⁻¹. This value corresponds to the standard free energy change for the disproportionation reaction in homogeneous dichloromethane, and the disproportionation constant in the homogeneous system is estimated to be 2.1×10^{-9} . This value shows that the disproportionation reaction sparingly occurs in the homogeneous system.

The value of K_{tr} was determined as follows: A given amount of C_8VBr_2 was dissolved in a two-phase system consisting of dichloromethane and water. The two-phase system was vigorously shaken for 10 min and left standing for 12 h. After the volume of each phase was measured, the concentration of C_8V^{2+} in each phase was determined spectroscopically. The concentration dependence of the partition of C_8V^{2+} was determined, and K_{tr} was estimated by extrapolation to $[C_8V^{2+}] \rightarrow 0$. The temperature of the two-phase system was maintained at $27 \pm 0.5^\circ C$.

The partition of C_8V^{2+} between dichloromethane and water is shown in Fig. 6.6 as a function of the concentration of C_8V^{2+} in water. The logarithm of the ratio of the concentration of C_8V^{2+} in the aqueous phase over its concentration in the organic phase decreased with increasing $[C_8V^{2+(w)}]$ in the concentration range of $\log [C_8V^{2+(w)}] > -2.6$, where a fraction of the viologen in the organic phase is considered to exist in associated forms such as

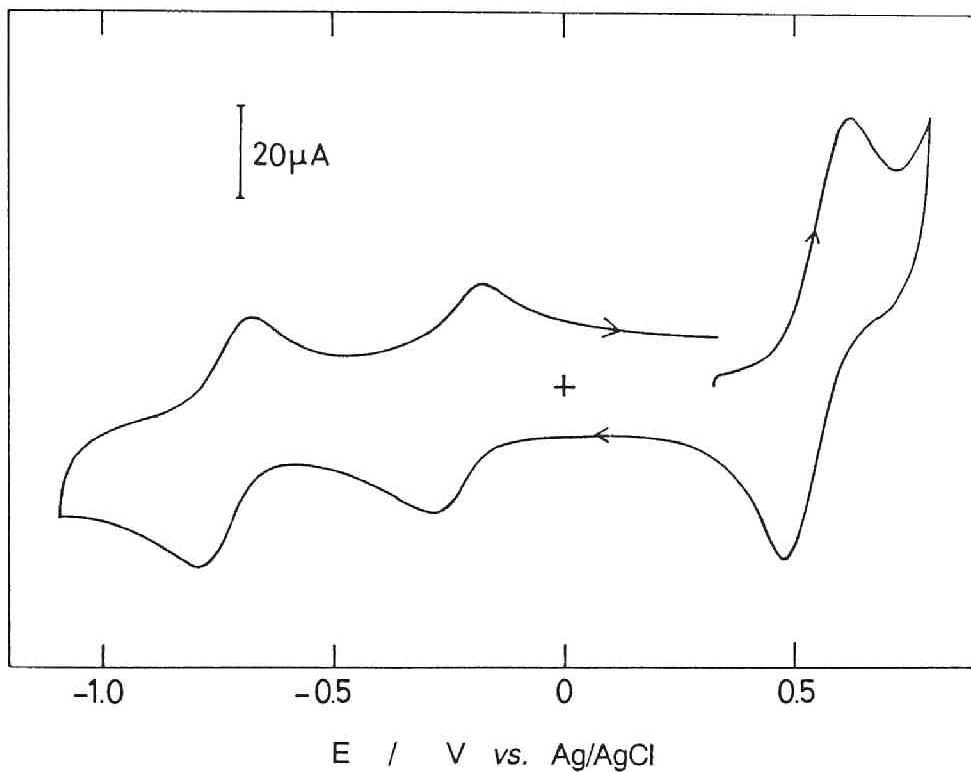


Fig. 6.5. Cyclic voltammogram for 1.33 mM ferrocene and 1.02 mM C_8VBr_2 in 0.1 M TBAP/ CH_2Cl_2 on GC (0.071cm^2). $\nu = 100\text{ mV sec}^{-1}$.

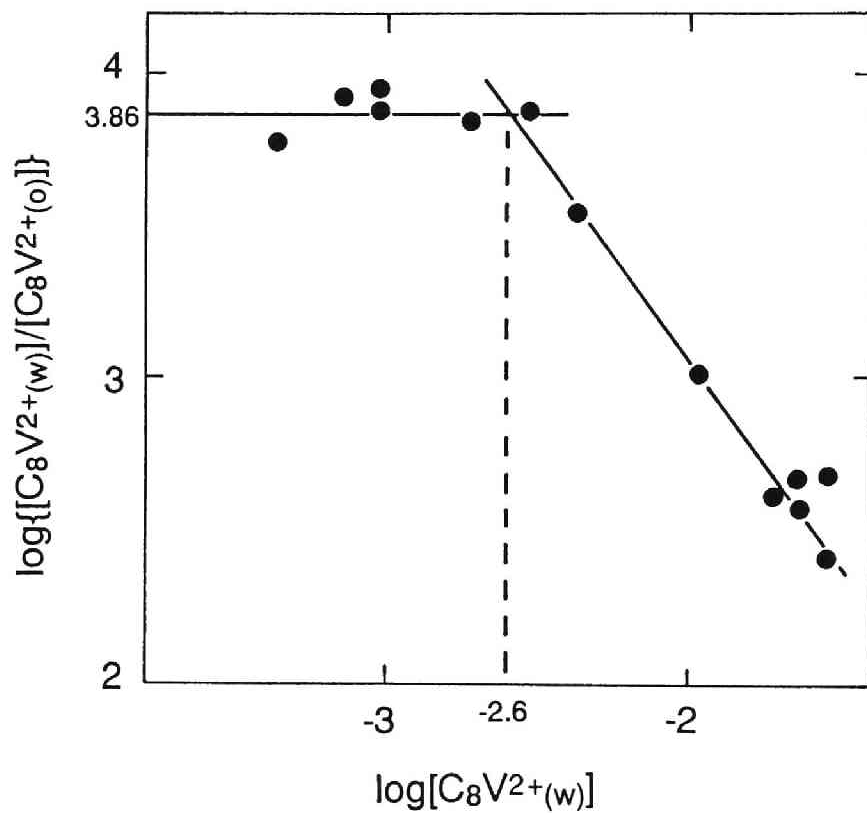


Fig. 6.6. Partition of C_8V^{2+} between water and CH_2Cl_2 .

$C_8VBr^+ + Br^-$ or C_8VBr_2 . However, the ratio remained constant in the concentration range of $\log[C_8V^{2+}_{(w)}] < -2.6$.

The extraction constant, K_{tr} , can be expressed using activities and activity coefficients as:

$$K_{tr} = \frac{\gamma_{C_8V^{2+}_{(w)}} \cdot (\gamma_{Br^-}_{(w)})^2 \cdot [C_8V^{2+}_{(w)}][Br^-_{(w)}]^2}{\gamma_{C_8V^{2+}_{(o)}} \cdot (\gamma_{Br^-}_{(o)})^2 \cdot [C_8V^{2+}_{(o)}][Br^-_{(o)}]^2} \quad [6.11]$$

The electroneutrality requirement in each phase demands that $[Br^-_{(w)}] = 2[C_8V^{2+}_{(w)}]$, and that $[Br^-_{(o)}] = 2[C_8V^{2+}_{(o)}]$. Since the ratio between the concentrations in the aqueous phase and in the organic phase is constant in the range $\log[C_8V^{2+}_{(w)}] < -2.6$, the extrapolation to $c \rightarrow 0$ permits us to assume activity coefficients of unity, and equation [6.12] can be written as

$$K_{tr} = \left\{ \frac{[C_8V^{2+}_{(w)}]}{[C_8V^{2+}_{(o)}]} \right\}^3_{c \rightarrow 0} \quad [6.12]$$

By the extrapolation of the curve in Fig. 6.6 to $c \rightarrow 0$, the value of $\log\left(\frac{[C_8V^{2+}_{(w)}]}{[C_8V^{2+}_{(o)}]}\right)_{c \rightarrow 0}$ is approximately 3.86, which yields $\log(K_{tr}) = 11.58$. Therefore, ΔG_{tr}° is estimated to be $-66.5 \text{ kJ mol}^{-1}$ using equation [6.8].

Substituting the values for $\Delta G_2^\circ - \Delta G_1^\circ$ and ΔG_{tr}° into equation [6.9], ΔG_d° and K_d are estimated to be $-16.7 \text{ kJ mol}^{-1}$ and 809, respectively. These values show that the generation of the doubly reduced form, C_8V^0 , is possible by the disproportionation reaction at the CH_2Cl_2/H_2O interface after the cation radical, $C_8V^{+\bullet}$, is accumulated in the organic phase. This substantiates the applicability to the present system of the reaction mechanism proposed by Maidan *et al.*, in which the active species, C_8V^0 , is generated by the disproportionation of $C_8V^{+\bullet}$.

6.3.4. Debromination of DBDPE on SPE composite electrode with incorporated viologen species

The results for the electrochemical debromination of DBDPE using the SPE composite electrodes with incorporated viologen species are summarized in Table 6.3. Without incorporated viologen (Run 1), very little debromination occurred. However, on the Cu₂Pt-Nafion incorporating C₃V species (Run 2), the current efficiency of the debromination reached 14.0%. During Run 2, the catholyte took on the blue color of C₃V^{•+}. This coloring indicates that a fraction of the C₃V^{•+} produced at the active sites of SPE composite electrode was transported into the catholyte (CH₂Cl₂ solution) because of the lipophilicity of C₃V^{•+}. When electrolysis was interrupted, the blue color of the catholyte persisted for more than 30 min, which suggests that the cation radical dissolved in the catholyte was not reactive with DBDPE, as is the case in the homogeneous system of Fig. 6.3. The transport of C₃V^{•+} to the catholyte decreases the concentration of the C₃V species in the SPE composite electrode. The addition of 7.5 mM of C₃VBr₂ (0.3 mmol) into the anolyte to supply viologen species from the anolyte (Run 3) improved the current efficiency to 45.1%. Also, a higher current efficiency was obtained at a lower current density of 0.17 mA cm⁻² (Run 4). Since no other organic products were detected in the solution, the decrease in the yield (to 75.3%) is attributed to incomplete product recovery, *e. g.*, some of the *trans*-stilbene may have remained in the Nafion membrane, *etc.*

On the other hand, the current efficiency was not improved significantly by incorporating of C₈V species (Runs 5 and 6). These results are contrast to those obtained in the emulsion system, and are discussed in the following sections.

6.3.5. Active species in debromination with SPE composite electrode

Since SPE composite electrodes with incorporated viologen species had high resistance, it was difficult to directly examine the electrochemical behavior. Thus a GC electrode coated with Nafion was employed to examine the electrochemical behavior of viologen species. Cyclic voltammograms of

Table 6.3. Electro-debromination of *meso*-1,2-dibromo-1,2-diphenylethane on Cu,Pt-Nafion incorporating viologen.^a

Run	Counter-ion	Anolyte ^b	I (mA cm ⁻²)	Current efficiency (%)	Yield ^c (%)
1	Na ⁺	none	0.3	2.6	-
2	C ₃ V ²⁺	none	0.3	14.0	100
3	C ₃ V ²⁺	7.5 mM C ₃ VBr ₂	0.3	45.1	87.8
4	C ₃ V ²⁺	7.5 mM C ₃ VBr ₂	0.17	59.7	75.4
5	C ₈ V ²⁺	none	0.3	6.1	69.0
6	C ₈ V ²⁺	7.5 mM C ₈ VBr ₂	0.3	11.8	100

^a The catholyte was 40cm³ of CH₂Cl₂ containing 0.6 mmol of *meso*-1,2-dibromo-1,2-diphenylethane, and the anolyte was 40 cm³ of 0.1 M phosphate buffer solution (pH 7). Q = 2 F mol⁻¹.

^b The concentration of the viologen added to the anolyte.

^c Yield = (amount of product)/(amount of consumed reactant) × 100 (%).

the Nafion-coated GC electrode incorporating C_3V^{2+} are shown in Fig. 6.7. Sodium sulfate was used as supporting electrolyte, and no viologen species were added to the solution.

Curve (a) in Fig. 6.7 was obtained in the potential range between 0V and -0.75 V vs. Ag/AgCl. The reduction-oxidation peaks around -0.6 V correspond to the $C_3V^{2+}/C_3V^{+•}$ couple incorporated in the Nafion film. These peaks were unchanged as long as the potential scans were limited to the potential range between 0 V and -0.75 V. For an electrode coated with a thinner coating film incorporating methyl viologen ($\Gamma_{C_1V^{2+}} = 10$ to 11×10^{-9} mol cm^{-2}), the peaks have been reported to correspond to those expected for an adsorbed species.⁴³⁾ However, in the voltammogram shown in Fig. 6.7a, a diffusion wave is observed because of the relatively thick coating film (7.8 μm) and large amount of C_3V -species ($\Gamma_{C_3V^{2+}} = 1.6 \times 10^{-7}$ mol cm^{-2}) incorporated in Nafion.

When potential was scanned to values more negative than -0.75 V [curve (b) in Fig. 6.7], the cathodic current started to flow at about -1.1 V, but well-defined peaks for $C_3V^{+•}/C_3V^0$ were not obtained. The current increase at -1.1 V is attributed mainly to the observed hydrogen evolution. Well-defined reduction-oxidation peaks were observed around -0.85 V for a $C_3V^{+•}/C_3V^0$ couple on an uncoated GC electrode in aqueous 0.5 M KNO_3 . These facts mean that the peaks in Nafion were shifted negatively by at least 200 mV with respect to those in an aqueous solution. In addition, the oxidation peaks for $C_3V^{2+}/C_3V^{+•}$ was split into two peaks when the potential was scanned to -1.2 V [curve (c) in Fig. 6.7]. Kaifer and Bard⁴⁴⁾ studied the electrochemical behavior and ESR spectra of methyl viologen in solutions containing various kinds of micelles. They observed a significant shift of the $C_1V^{+•}/C_1V^0$ redox peaks in the negative direction in the presence of SDS micelles, and attributed the observed peak shift to the stabilization of the cation radical by hydrophobic interactions with the SDS micelle core. Rubinstein²⁴⁾ has investigated the electrochemical behavior of methyl viologen incorporated into the Nafion (EW = 1100) of a Nafion-coated gold electrode. He also ob-

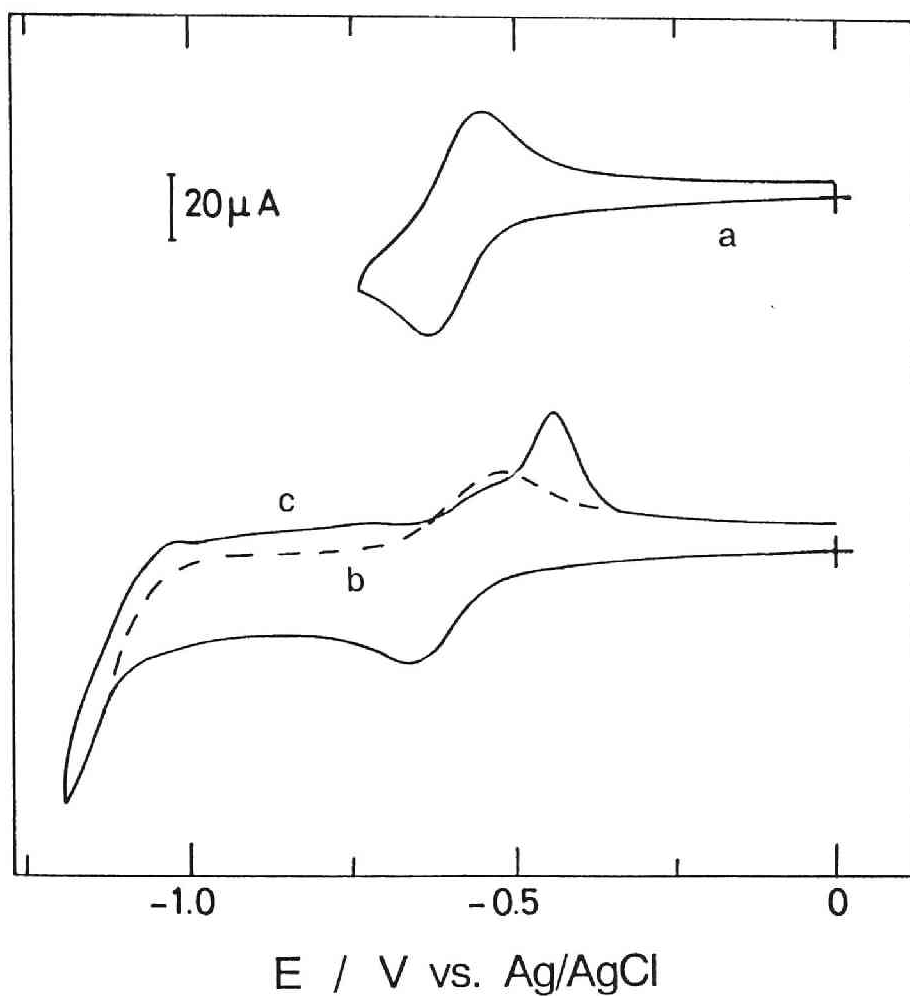


Fig. 6.7. Cyclic voltammograms for a Nafion-coated GC electrode (0.071 cm^2) with incorporated C_3V^{2+} ($\Gamma_{\text{C}_3\text{V}^{2+}} = 1.6 \times 10^{-7} \text{ mol cm}^{-2}$). The electrolyte solution contained only $0.1 \text{ M Na}_2\text{SO}_4$, and no viologen species were added to the solution. $\nu = 50 \text{ mV sec}^{-1}$. Potential was reversed at (a) -0.75 , (b) -1.1 and (c) -1.2 V . The electrode was soaked in a $0.01 \text{ M C}_3\text{V}^{2+}$ solution for 30 min prior to measurements.

served that the reduction peak of the incorporated C_1V^{+*}/C_1V^0 couple was shifted to a considerably more negative potential than that for the same couple in solution, and that the oxidation waves were split into two well-defined peaks for each of C_1V^{+*} and C_1V^0 . They interpreted the shift of the reduction potential in terms of the stabilization of C_1V^{+*} by the hydrophobic interactions with interfacial domain of Nafion, and the peak-splitting in terms of the different moieties of C_1V^{+*} and C_1V^0 residing in the different domains of Nafion, *i. e.*, the ionic cluster region and the interfacial region. Therefore, the similar results obtained in this chapter imply the stabilization of C_3V^{+*} in Nafion, perhaps arising from hydrophobic interactions, and from the phase transfer of C_3V^{+*} from the ionic cluster region to the hydrophobic interfacial region in Nafion.

As shown in Fig. 6.7, C_3V^0 is not produced on the electrode at potentials more positive than -1.0 V. Electrochemical debromination of DBDPE on Cu,Pt-Nafion with incorporated C_3V species was conducted excluding electrochemical formation of C_3V^0 by maintaining carefully the electrode at potentials more positive than -1.0 V. The electrolysis was carried out as follows: From 0 to 7.0 C, the electrolysis was carried out at a constant potential of -0.8V. From 7.0 to 24.0 C, the electrolysis was carried out at a constant current of $32 \mu A cm^{-2}$. From 24.0 to 42.0 C, a constant current of $26 \mu A cm^{-2}$ was applied. Under the constant current conditions, the ohmic drop through the Nafion membrane was measured by a current interrupt method, and the electrode potentials were corrected for the ohmic drop. The *iR*-corrected potentials were more positive than -1.0 V in all cases. The variations in the electrode potential during the electrolysis are shown in Fig. 6.8. The resistance of the Nafion membrane with incorporated C_3V species reached values as high as $4.2 k\Omega cm^{-2}$. It was reported that large organic cations have extremely smaller diffusion coefficients in Nafion than those in solutions because of the hydrophobic interactions with the hydrophobic domains of Nafion.²²⁾ The observed high resistance is attributed to a slow mass-transport rate of C_3V species incorporated in the Nafion membrane.

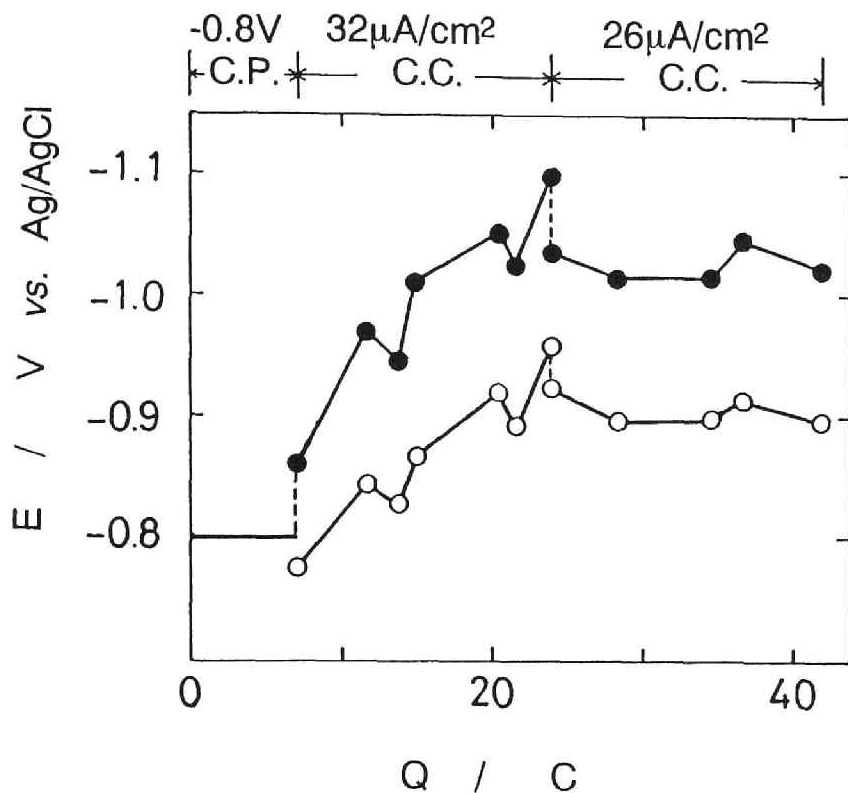


Fig. 6.8. Variation of electrode potential with charge passed (Q);
 ● : measured potential; ○ : after correcting for iR drop. The catholyte was 40 cm^3 of CH_2Cl_2 containing 0.6 mmol of DBDPE. The anolyte was 40 cm^3 of 0.25 M aqueous phosphate buffer (pH 7) containing 7.5 mM C_3VBr_2 .

The current efficiency of *trans*-stilbene production after 0.72 F per mol of the reactant had been passed was 51.1%. C_3V^0 was not produced on the electrode during this electrolysis because the electrode potential was kept more positive than -1.0 V; only $C_3V^{+\bullet}$ was produced. As described above, $C_3V^{+\bullet}$ is not reactive for the debromination. Since DBDPE was nevertheless electro-reduced to *trans*-stilbene, the active species, C_3V^0 , must have been generated by disproportionation of $C_3V^{+\bullet}$ on the SPE composite electrode.

6.3.6. Reaction mechanism on SPE composite electrode

The disproportionation of viologen cation radicals requires an organic-aqueous interface, as indicated in the above section on estimation of the disproportionation constant. In this chapter, a CH_2Cl_2 solution was used as the catholyte, and an aqueous phosphate buffer was used as the anolyte. The interface must be formed between the catholyte and the anolyte. Nafion is known to contain a large amount of water. For example, H^+ -form Nafion (EW = 1200) absorbs about 30 % of its dry weight in water.⁴⁵⁾ Therefore, an organic-aqueous interface is formed between the catholyte (CH_2Cl_2 solution) and the Nafion membrane of the SPE composite at the surface of Nafion. However, this interface is similar to the interface in the unstirred emulsion system, in which the debromination did not proceed at an appreciable rate. As described in the SPE electrolysis section, viologen cation radical dissolved into the catholyte was stable for more than 30 min after the electrolysis was interrupted. This fact demonstrates that cation radicals dissolved in the catholyte cannot participate in the debromination reaction. Therefore, the cation radicals cannot disproportionate at the organic-aqueous interface formed at the Nafion surface in contact with the catholyte.

Let us now focus on effects related to the structure of Nafion. Nafion has a multi-phase structure consisting of a fluorocarbon backbone region and an ionic cluster region.¹¹⁻¹⁴⁾ The ionic clusters are hydrophilic, consisting of the fixed charge sites, counter-ions, co-ions and water, and hence are regarded as an aqueous phase. The viologen dications may mainly reside in this region. On the other hand, the fluorocarbon backbone region is highly

lipophilic, and interacts with non-polar solvents having low solubility parameter values such as dichloromethane⁴⁶⁾ ($\delta = 9.7 \text{ cal}^{1/2} \text{ cm}^{-3/2}$).⁴⁷⁾ Crystallized parts of the fluorocarbon region are known to occupy 12 wt.% of the H⁺-form Nafion (EW = 1100).⁴⁸⁾ It is difficult for viologen species to be dissolved in and to move through such a rigid crystallized region. However, the interfacial region, the presence of which was suggested by Yeager and Steck,¹³⁾ and Ogumi *et al.*,¹⁴⁾ consists of the amorphous part of the fluorocarbon backbone and the side chains of Nafion. It has been proposed that hydrogen and oxygen diffuse through the interfacial region in Nafion membranes.¹⁴⁾ This region is considered to be flexible enough to absorb non-polar solvents and hydrophobic species, such as dichloromethane and viologen cation radical. Although an explicit model has not been shown yet, the interfacial region is expected to function as an organic phase, and is adjacent to the hydrophilic ionic cluster region. This combination forms an organic-aqueous interface. As indicated by the results of the cyclic voltammetry experiments with C₃V-species in a Nafion film, viologen cation radicals have a tendency to be extracted into Nafion, perhaps because of hydrophobic interactions with the interfacial region in Nafion and resulting transfer from the ionic cluster region to the interfacial region. This interface is microscopic, and has a large interfacial area. The cation radicals can make effective use of this interface to disproportionate and release neutral forms of viologen which then reside in the hydrophobic interfacial region. The disproportionation of C_nV^{+•} and the debromination of DBDPE at the interface in the SPE composite electrode are shown schematically in Fig. 6.9. First, viologen dications in the ionic cluster region are reduced to cation radicals on the electrode material. Next, the cation radicals are extracted into the hydrophobic interfacial region, and the extracted cation radicals disproportionate to form a doubly reduced form and a dication. Then, the doubly reduced form reacts in the interfacial region with DBDPE (the latter is transported into the Nafion through the porous electrode layer). The doubly reduced form is oxidized to the cation radical, and the active species (the doubly reduced form) is regenerated by disproportionation.

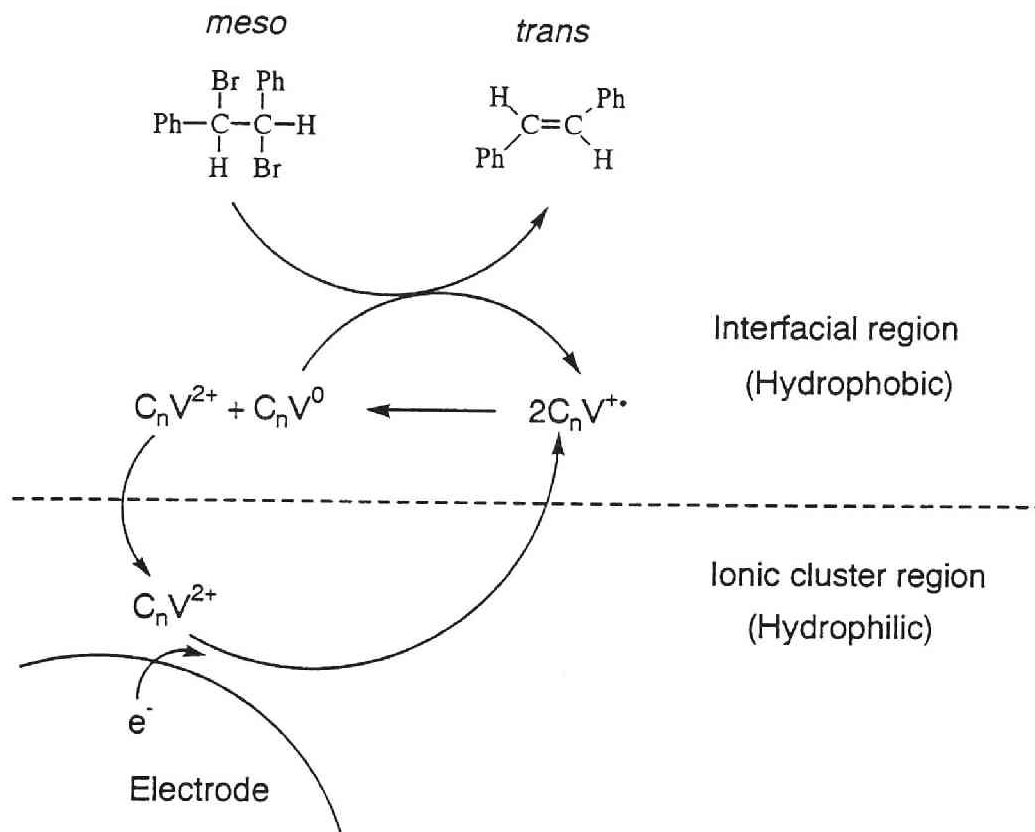


Fig. 6.9. Reaction mechanism for the electro-debromination in the SPE composite electrode.

6.3.7. *Effects of the alkyl-chain length of viologen compounds*

While octyl viologen did not show high activity for the debromination of DBDPE on the SPE composite electrode, it was active in the emulsion system. This fact implies that alkyl-chain length of viologen compounds significantly affects their activity for debromination. The effect of the chain length was examined, and the variations of the current efficiency with chain length (n) for the emulsion system and the SPE composite electrode were compared. The results are shown in Fig. 6.10. Electrolyses were carried out at constant currents of 0.5 and 0.3 mA cm⁻² for the emulsion system and for the SPE composite electrode, respectively.

In the emulsion system, the current efficiency was low when viologen compounds with $n \leq 5$ were used as catalysts. Octyl viologen facilitated the debromination, and the current efficiency was improved. The long alkyl-chain increases the hydrophobicity of C₈VBr₂, and facilitates the phase transfer and the disproportionation of the cation radical. In chemical debromination of DBDPE using Na₂S₂O₄ as a reductant, viologen compounds with $n \geq 3$ was reported to be effective as catalysts.²⁹⁾ In the chemical debromination, a large amount of viologen cation radical is produced in the two-phase system by instantaneous reduction of viologen dication, while in the emulsion electrolysis viologen cation radical is produced and accumulates in proportion to the electricity that passes. When viologens with short side chains are used in the emulsion electrolysis, the disproportionation does not proceed appreciably until the concentration of the cation radical increases, probably because the lipophilicity of viologens with short alkyl chains is low. Hence the cation radicals are considered to be re-oxidized at the anode before they disproportionate.

On the SPE composite electrode, the current efficiency was high even when viologen species with $n \leq 5$, which were rather ineffective in the emulsion system, were incorporated. The current efficiency was highest when C₃V-species was incorporated into the Nafion membrane. The hydrophobicity of viologen cation radical increases with increasing alkyl chain length.²⁸⁾ The more hydrophobic a cation radical is, the more easily it can be extracted

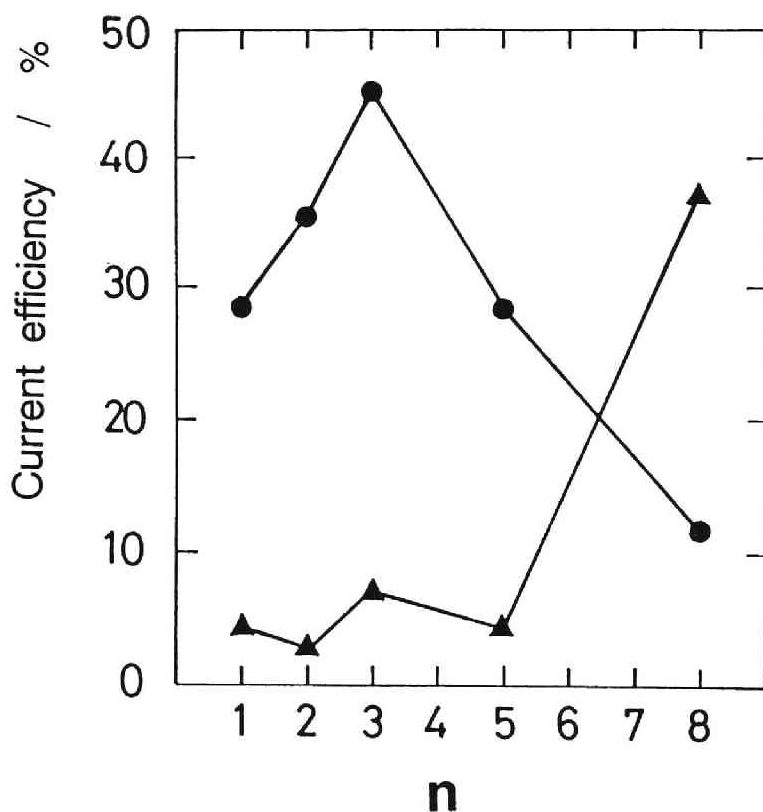


Fig. 6.10. Effect of alkyl-chain length (n) of viologens on current efficiency; ● : on the SPE composite electrode;▲ : in the emulsion system. The emulsion system consisted of 40cm^3 of CH_2Cl_2 containing 1.0 mmol of DBDPE and of 20 cm^3 of 0.25 M phosphate buffer (pH 7) containing 0.2 mmol viologen. In the SPE method, the catholyte was 40 cm^3 CH_2Cl_2 containing 0.6 mmol of DBDPE and the anolyte was 40 cm^3 of 0.1 M phosphate buffer (pH 7) containing 7.5 mM viologen.

into the hydrophobic region of Nafion. The concentration of viologen is much higher in the Nafion membrane than that in the emulsion system, because the viologens are fixed inside the Nafion membrane. The local accumulation of cation radicals inside the Nafion allows the disproportionation to occur relatively easily, even when viologens with short alkyl-chains are incorporated.

Let us now focus on the behavior of C_8VBr_2 . While C_8VBr_2 was the most effective mediator of the viologens tested in the emulsion system (see Fig. 6.10), it was less effective for the debromination when incorporated in Cu,Pt-Nafion. As described above, hydrophobic cations have low diffusivities in Nafion because of their strong interaction with the hydrophobic parts of Nafion.²²⁾ Thus, C_8V^{2+} may interact strongly with Nafion, resulting in retardation of its mass transport to the active sites. This retardation allows hydrogen evolution to occur more easily as a side reaction. In addition, some C_8V^{2+} might already reside in the hydrophobic interfacial region even before disproportionation. It is also reported that water uptake is greatly reduced by the incorporation of hydrophobic cations.⁴⁵⁾ These two factors, the affinity of the interfacial region for C_8V^{2+} and the suppression of water uptake, should suppress the disproportionation reaction.

6.4. Conclusions

The major findings of this chapter can be summarized as follows:

(i) Electro-debromination of DBDPE was carried out in an emulsion system consisting of dichloromethane and an aqueous solution. Viologen compounds, especially octyl viologen dibromide, were found to be effective as catalysts. It was inferred that the doubly reduced neutral form of viologen, which acts as the active species, is generated by the disproportionation of cation radical, according to the mechanism proposed by Maidan *et al.*

(ii) The standard free energy of the disproportionation and the disproportionation constant of octyl viologen cation radicals to a doubly reduced neutral form and a dication in the dichloromethane-water two-phase system

were estimated to be $-16.7 \text{ kJ mol}^{-1}$ and 809, respectively. These values indicate that the disproportionation is possible, and support the reaction mechanism proposed by Maidan *et al.*

(iii) DBDPE was electro-debrominated to *trans*-stilbene on SPE composite electrodes with incorporated viologen species. Viologen species with shorter alkyl-chains ($n \leq 5$) were more effective when incorporated in the SPE composite electrodes than when used in the emulsion system. The current efficiency was highest when propyl viologen was incorporated. The active species in the SPE composite electrodes was considered to be generated by disproportionation of the cation radical. The details of the reaction mechanism were explained by assuming microscopic phase-transfer disproportionation between the ionic cluster region and the hydrophobic interfacial region of the Nafion: In the proposed reaction mechanism, viologen dications in the hydrophilic ionic cluster region are reduced to cation radicals on the electrode. The cation radicals are extracted into the hydrophobic interfacial region, and a doubly reduced neutral form, which functions as the active species, is then generated by disproportionation of the cation radicals.

References

1. P. W. T. Lu and S. Srinivasan, *J. Appl. Electrochem.*, **9**, 269 (1979).
2. A. P. Laconti, *Japan Tokkyo Kokai*, 54-112398 (1979).
3. G. A. Eisman, *J. Power Sources*, **29**, 389 (1990).
4. Z. Ogumi, K. Nishio and S. Yoshizawa, *Denki Kagaku*, **49**, 212 (1981).
5. Z. Ogumi, H. Yamashita, K. Nishio, Z. Takehara and S. Yoshizawa, *Electrochim. Acta*, **28**, 1687 (1983).
6. Z. Ogumi, S. Ohashi and Z. Takehara, *Nippon Kagaku Kaishi*, 1788 (1984).

7. Z. Ogumi, T. Mizoe, N. Yoshida and Z. Takehara, *Bull. Chem. Soc., Jpn.*, **60**, 4233 (1987).
8. Z. Ogumi, M. Inaba, S. Ohashi, M. Uchida, and Z. Takehara, *Electrochim. Acta*, **22**, 365 (1988).
9. M. Inaba, J. T. Hinatsu, Z. Ogumi and Z. Takehara, *J. Electrochem. Soc.*, **140**, 706 (1993).
10. M. Inaba, K. Fukuta, Z. Ogumi and Z. Takehara, *Chem. Lett.*, 1799 (1993).
11. T. D. Gierke and W. Y. Hsu, in "Perfluorinated Ionomer Membranes", ed. by A. Eisenberg and H. L. Yeager, ACS Symposium Series No.180, Washington DC (1982) Chap. 13.
12. T. D. Gierke, G. E. Mann and F. C. Wilson, *J. Polym. Sci. Polym. Phys.*, **19**, 1687 (1981).
13. H. L. Yeager and A. Steck, *J. Electrochem. Soc.*, **128**, 1880 (1981).
14. Z. Ogumi, T. Kuroe and Z. Takehara, *J. Electrochem. Soc.*, **132**, 2601 (1985).
15. M. V. Verbrugge and R. F. Hill, *J. Electrochem. Soc.*, **137**, 3770 (1990).
16. R. S. Yeo, *J. Electrochem. Soc.*, **130**, 533 (1983).
17. W. Y. Hsu and T. D. Gierke, *Macromolecules*, **15**, 101 (1982).
18. H. S. White, J. Leddy and A. J. Bard, *J. Am. Chem. Soc.*, **104**, 4811 (1982).
19. D. A. Buttry and F. C. Anson, *J. Electroanal. Chem.*, **130**, 333 (1981).
20. N. E. Prieto and C. R. Martin, *J. Electrochem. Soc.*, **131**, 751 (1984).
21. M. N. Szentirmay and C. R. Martin, *Anal. Chem.*, **56**, 1898 (1984).
22. C. R. Martin and K. A. Dollard, *J. Electroanal. Chem.*, **159**, 127 (1983).
23. I. Rubinstein, *J. Electroanal. Chem.*, **176**, 359 (1984).
24. I. Rubinstein, *J. Electroanal. Chem.*, **188**, 227 (1985).

25. R. A. Komoroski and K. A. Mauritz, in "Perfluorinated Ionomer Membranes", ed. by A. Eisenberg and H. L. Yeager, ACS Symposium Series No. 180, Washington DC (1982) Chap. 7.
26. T. Osa and T. Kuwana, *J. Electroanal. Chem.*, **22**, 389 (1969).
27. H. T. van Dam and J. J. Ponjee, *J. Electrochem. Soc.*, **121**, 1555 (1974).
28. I. Tabushi, *Pure & Appl. Chem.*, **54**, 1733 (1982).
29. T. Endo, Y. Saotome and M. Okawara, *J. Am. Chem. Soc.*, **106**, 1124 (1984).
30. R. Maidan, Z. Gohen, J. Y. Becker and I. Willner, *J. Am. Chem. Soc.*, **106**, 6217 (1984).
31. T. Endo, Y. Saotome and M. Okawara, *Tetrahedron Lett.*, **26**, 4525 (1985).
32. H. Tomioka, K. Ueda, H. Ohi, and Y. Izawa, Y., *Chem. Lett.*, 1359 (1986).
33. T. Endo, K. Ageishi and M. Okawara, *J. Org. Chem.*, **51**, 4309 (1986).
34. K. K. Park, C. W. Lee, S. -Y. Oh and J. W. Park, *J. Chem. Soc., Perkin Trans. 1*, 2356 (1990).
35. K. K. Park, C. W. Lee and S. Y. Choi, *J. Chem. Soc., Perkin Trans. 1*, 601 (1992).
36. K. K. Park, C. H. Oh and W. K. Joung, *Tetrahedron Lett.*, **46**, 7445 (1993).
37. L. F. Fieser and K. L. Williamson, in "Organic Experiments", 3rd Edn., D. C. Heath and Co. (1975) pp. 273-274.
38. N. Oyama and F. C. Anson, *J. Electrochem. Soc.*, **127**, 640 (1980).
39. A. Fujishima, M. Aizawa and T. Inoue, in "Denki Kagaku Sokuteihou", Gihoudo-Shuppan, Tokyo (1984) p. 158.
40. A. J. Bard and L. R. Faulkner, in "Electrochemical Methods", John Wiley & Sons, New York (1980) p. 435.

41. R. Dworak and H. Wendt, *Ber. Bunsen-Ges. Phys. Chemie*, **82**, 728 (1977).
42. H. Feess and H. Wendt, *J. Chem. Tech. Biotechnol.*, **30**, 297 (1980).
43. N. Oyama, T. Ohsaka, M. Kaneko, K. Sato and A. Yamada, *J. Am. Chem. Soc.*, **105**, 6003 (1983).
44. A. E. Kaifer and A. J. Bard, *J. Phys. Chem.*, **89**, 4876 (1985).
45. E. I. du Pont de Nemours & Co. (Inc.), E-05569, 2/76 (catalog).
46. A. F. M. Barton, *Chem. Rev.*, **75**, 731 (1975).
47. R. S. Yeo, *Polymer*, **21**, 432 (1980).
48. T. Hashimoto, M. Fujimura and H. Kawai, in "Perfluorinated Ionomer Membranes", ed by A. Eisenberg and H. L. Yeager, ACS Symposium Series No. 180, Washington DC (1982) Chap. 11.

Chapter 7

Structure of Perfluorinated Ionomer Membranes Incorporating Organic Cations

7.1. Introduction

"Nafion" perfluorinated ionomer membranes are well known to be microscopically separated into two phases: an ionic cluster domain, which contains most of the sulfonate groups, cations and absorbed water, and a hydrophobic fluorocarbon backbone domain, which surrounds the ionic clusters.^{1,2)} Electrodes coated with Nafion have been a subject of considerable recent interest.³⁻⁹⁾ Several workers in this field have observed unusual behavior of organic cations incorporated into Nafion.⁶⁻⁹⁾ For example, Nafion has strong affinity for large organic cations,⁶⁾ the organic cations incorporated in Nafion have extremely small diffusion coefficients,⁷⁾ etc. These unusual properties have been generally interpreted using the cluster-network model of Nafion, and attributed to the interactions between organic cations and Nafion. However, the presence of the ionic clusters has been confirmed only for the Nafion membranes incorporating inorganic cations, and few studies have been reported on the structure of Nafion incorporating organic cations.

In this chapter, the structure of Nafion incorporating large organic cations, tetraethylammonium (TEA^+) and 1,1'-dialkyl-4,4'-bipyridinium cations (viologen), is studied using small-angle X-ray scattering (SAXS).

7.2. Experimental

A perfluorinated sulfonate membrane, Nafion[®] 117 (E. I. du Pont de Nemours and Co., EW = 1100), was used in this chapter. Nafion samples (2 cm \times 2 cm \times 170 μm) were immersed in aqueous 1 M H_2SO_4 containing 3% H_2O_2 for 7 days to exchange the counter-ion from Na^+ to H^+ and to remove organic impurities, and were then treated in boiling water for 1 h. The samples were converted to various ionic forms by immersion in solutions containing the corresponding salts for 5 or 50 days at room temperature. Some of the samples were again boiled in the salt solutions for 1 h. These treatment conditions are summarized in Table 7.1.

SAXS measurements were performed using a 6-m SAXS system at the High Intensity X-ray Laboratory (HIXLAB) of Kyoto University. The sample was cut into a piece (ca. 5 \times 5 mm^2), and was mounted in a cell for liquid samples equipped with a mica windows (20 μm thick) to prevent from drying. The X-ray is $\text{CuK}\alpha$ ($\lambda = 1.54056 \text{ \AA}$) from a fine-focus X-ray generator (Rigaku Co., RU-1000C3) operated at 40 kV and 50 mA. Isotropic two-dimensional intensity of X-ray scattering collected by a two dimensional position-sensitive proportional counter was corrected for the intensity of background and for the non-uniformity of detector sensitivity, and then circularly averaged to give the one-dimensional data.

The content of absorbed water in the membrane was determined as follows: The sample was quickly blotted between two sheets of filter paper and weighed. After it was dried under vacuum at 100 $^\circ\text{C}$ for 72 h, the content of absorbed water was determined by subtracting the weight of the dry polymer from the total weight. The density of dry polymer was calculated from the weight and size of the sample after dried.

Table 7.1. Treatment conditions of Nafion 117 membranes and the results of SAXS and water absorption measurements.

Salt Solution	Immersion time (day)	Boiling time (h)	Bragg spacing (nm)	Water content (%-dry polymer)	Polymer density (g cm ⁻³)	Cluster size (nm)
1 M H ₂ SO ₄	7	1 ^a	5.3	31	1.9	4.9
1 M KOH	5	-	5.3	19	1.9	4.5
1 M KOH	5	1	5.1	18	2.0	4.3
100 mM TEAClO ₄ ^b	5	-	5.2	21	1.7	4.4
10 mM C ₃ VBr ₂ ^c	5	-	5.3	18	1.8	4.4
50 mM C ₃ VBr ₂	5	-	5.1	19	1.8	4.3
30 mM C ₃ VBr ₂	50	-	4.9	18	1.8	4.1
10 mM C ₈ VBr ₂ ^d	5	-	6.1	19	1.8	5.1
50 mM C ₈ VBr ₂	5	-	5.8	18	1.7	4.7
50 mM C ₈ VBr ₂	50	-	3.5 + 4.9 ^e	8	1.6	2.6 + 3.3 ^e
50 mM C ₈ VBr ₂	5	1	3.3	7	1.6	2.2

^a The membrane was boiled in water. ^b Tetraethylammonium perchlorate. ^c 1,1'-dipropyl-4,4'-bipyridinium dibromide. ^d 1,1'-dioctyl-4,4'-bipyridinium dibromide. ^e Two maxima were observed on the Iq² vs. q plot.

1,1'-dipropyl-4,4'-bipyridinium dibromide (C_3VBr_2) and 1,1'-dioctyl-4,4'-bipyridinium dibromide (C_8VBr_2) were prepared from 4,4'-bipyridine and the corresponding alkyl bromides, and recrystallized from ethanol solutions. Other chemicals were of reagent grade, and were used without further purification.

7.3. Results and Discussion

Although details of the configuration of the ionic clusters cannot be obtained from SAXS results alone, the cluster-network model proposed by Gierke *et al.*¹⁾ to calculate the inter-cluster distance and cluster size. In the cluster-network model, the counter-ion, ion-exchange sites and absorbed water are distributed in simple spherical domains, and the spherical clusters are connected by short narrow channels. In this model, the Bragg spacing (d), which is calculated from a SAXS maximum using scattering angle ($2q$) and the Bragg equation ($\lambda = 2d \sin\theta$), is assigned to the average distance between clusters. The average size of the clusters is estimated using the amount of absorbed water assuming that the clusters would be distributed on a simple cubic lattice with an average lattice constant, i.e., the Bragg spacing.

Figures 7.1 to 7.3 show the Iq^2 vs. q plots for inorganic ion-, C_3V^{2+} - and C_8V^{2+} -form membranes, respectively. Here, I and q are scattering intensity and scattering vector, $q = (4\pi/\lambda)\sin\theta$, respectively. In Fig. 7.1, strong scattering maxima were observed at ca. $q = 0.12$ for swollen H^+ - and Na^+ -form membranes, while as-received dry Na^+ -form membrane did not exhibit a maximum. Hence, these maxima are attributed to the formation of the ionic clusters by swelling treatments, which is in agreement with the results reported by Gierke *et al.*¹⁾

C_3V^{2+} - and C_8V^{2+} -form membranes also exhibited scattering maxima. This fact clearly shows the presence of the ionic clusters in these forms. For C_3V^{2+} -form membranes (Fig. 7.2), the Bragg spacing decreased with an increase in C_3V^{2+} concentration in the salt solution and with immersion time, although the decrease is not so significant. For C_8V^{2+} -form membranes (Fig.

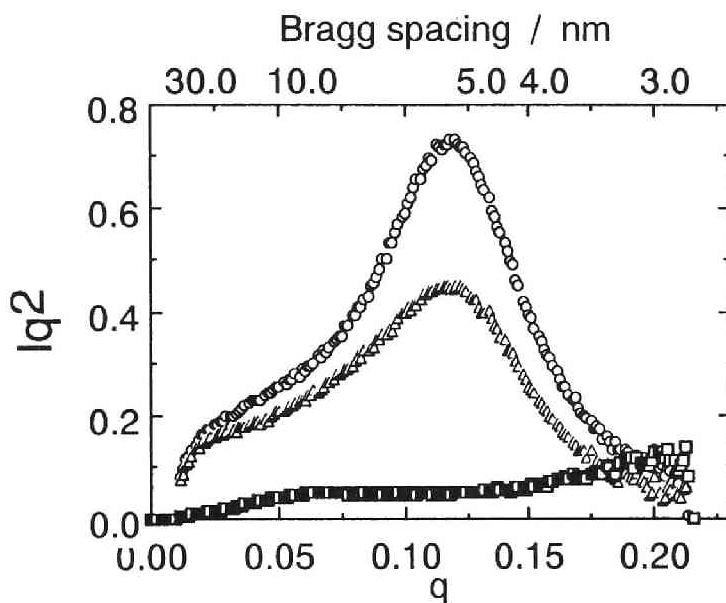


Fig. 7.1. Iq^2 vs. q plot of SAXS intensity for inorganic ion-form Nafion 117. (\circ) H⁺-form, (\triangle) K⁺-form, and (\square) as-received dry Na⁺-form. $q = (4\pi/\lambda)\sin\theta$, where $\lambda =$ wavelength in \AA and $2\theta =$ scattering angle.

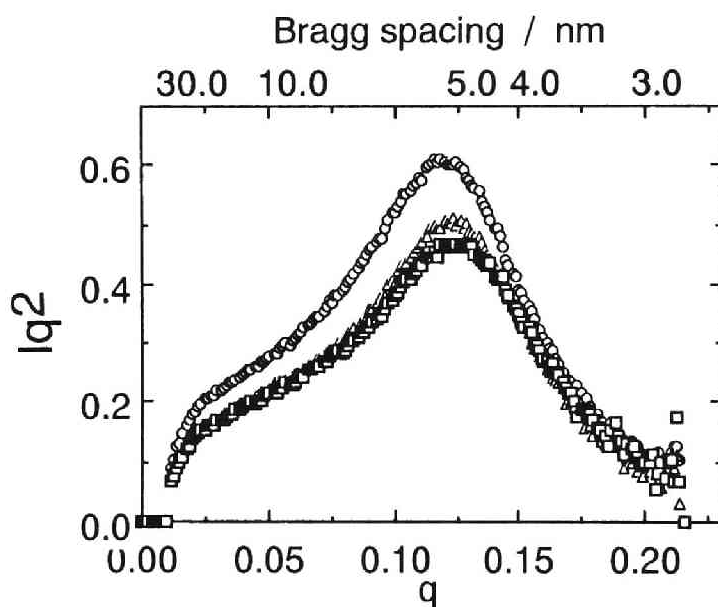


Fig. 7.2. Iq^2 vs. q plot of SAXS intensity for C_3V^{2+} -form Nafion 117. The counter-ion was exchanged to C_3V^{2+} immersing the H^+ -form membranes in (○) 10 mM and (△) 50 mM C_3VBr_2 solutions for 5 days, and (□) in 30 mM solution for 50 days.

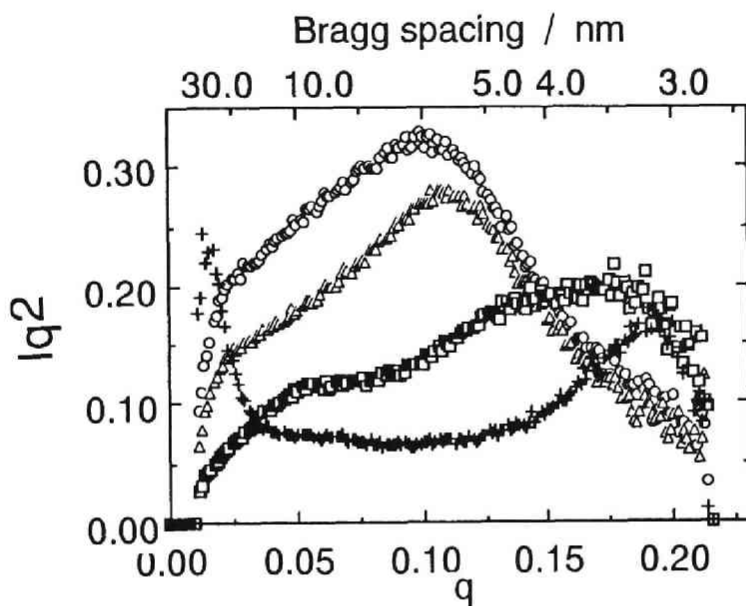


Fig. 7.3. Iq^2 vs. q plot of SAXS intensity for C_8V^{2+} -form Nafion 117. The counter-ion was exchanged to C_8V^{2+} immersing the H^+ -form membranes in (O) 10 mM and (Δ) 50 mM C_3VBr_2 solutions for 5 days, (\square) in 50 mM solution for 50 days, and ($+$) in 50 mM solution for 5 days followed by boiling for 1 h.

7.3), the Bragg spacing decreased slightly with an increase in C_8V^{2+} concentration in the salt solution. On the other hand, it decreased significantly with immersion time, and after immersion for 50 days in a 50 mM salt solution a broad peak consisting of two maxima were observed, which shows that the inter-cluster distance was not uniform. The Bragg spacing further decreased after boiling for 1 h, and another sharp maximum was observed at $q = 0.017$ ($d = \text{ca. } 37 \text{ nm}$) in addition to the maximum assigned to the ionic clusters. This membrane was opaque, and hence this sharp maximum is attributable to the partial crystallization of the backbone domain.¹⁾

The results for SAXS and water absorption measurements are summarized in Table 7.1 together with the treatment conditions. For the membranes incorporating inorganic cations, H^+ and Na^+ , the cluster size was in the range from 4 to 5 nm, which is in agreement with the results reported by Gierke *et al.*¹⁾ When the counter-ion was exchanged to TEA^+ , the amount of adsorbed water and the cluster size were still as large as those of Na^+ -form (ca. 4 nm in diameter). The cluster size of the C_3V^{2+} -form membranes tended to decrease slightly with an increase in the concentration of C_3V^{2+} in the salt solution and with immersion time for C_3V^{2+} -form.

For C_8V^{2+} -form membranes after 5-day immersion, the Bragg spacing, i.e., the inter-cluster distance expanded to a value larger than that of H^+ -form. The water content and cluster size were of the order of those of Na^+ -form. After the membrane was immersed in the salt solution for 50 days or boiled for 1 h, the Bragg spacing and water content again decreased, resulting in a significant decrease in cluster size. The highly hydrophobic C_8V^{2+} cation would interact strongly with the fluorocarbon backbone domain of Nafion. Yeager and Steck¹⁰⁾ have reported that a hydrophobic Cs^+ ion diffuses through the hydrophobic interfacial region located between the ionic cluster and fluorocarbon domains of Nafion. It is therefore considered that C_8V^{2+} cation resides in the hydrophobic domain of Nafion, which includes the interfacial region and even the fluorocarbon domain, as well as in the ionic clusters. This will cause structural changes of the fluorocarbon domain. Al-

though the exact reason for the drastic change in the structure of the ionic cluster observed for C_8V^{2+} -form has not been clarified, it may be attributed to strong interactions between the highly hydrophobic C_8V^{2+} cation and the fluorocarbon backbone domain.

The above results clearly show the presence of the ionic clusters even when organic cations are incorporated in Nafion membranes. However, if strongly hydrophobic cations such as C_8V^{2+} are incorporated, the structure of the clusters will change significantly with immersion time or by boiling treatment. The model must be used carefully when highly hydrophobic cations are incorporated.

References

1. T. D. Gierke and W. Y. Hsu, "Perfluorinated Ionomer Membranes," ed by A. Eisenberg and H. L. Yeager, ACS Symposium Series No. 180, Washington DC (1982) Chaps. 10 and 13.
2. T. D. Gierke, G. E. Mann, and F. C. Wilson, *J. Polym. Sci., Polym. Phys.*, **19**, 1687 (1981).
3. H. S. White, J. Leddy, and A. J. Bard, *J. Am. Chem. Soc.*, **104**, 4811 (1982).
4. D. A. Buttry and F. C. Anson, *J. Electroanal. Chem.*, **130**, 333 (1981).
5. N. E. Prieto and C. R. Martin, *J. Electrochem. Soc.*, **131**, 751 (1984).
6. M. N. Szentirmay and C. R. Martin, *Anal. Chem.*, **56**, 1898 (1984).
7. C. R. Martin and K. A. Dollard, *J. Electroanal. Chem.*, **159**, 127 (1983).
8. I. Rubinstein, *J. Electroanal. Chem.*, **188**, 227 (1985).
9. R-J. Lin, T. Onikubo, K. Nagai, and M. Kaneko, *J. Electroanal. Chem.*, **348**, 189 (1993).
10. H. L. Yeager and A. Steck, *J. Electrochem. Soc.*, **128**, 1880 (1981).

Chapter 8

Raman Spectroscopic Analysis of Electrochemical Behavior of Propylviologen in Nafion

8.1. Introduction

A perfluorosulfonate cation-exchange membrane, Nafion[®], is chemically and thermally stable, and applied to a variety of processes such as proton-exchange membrane fuel cells,¹⁾ water electrolyzers,²⁾ brine electrolyzers,³⁾ sensors,⁴⁾ batteries,⁵⁾ and electrolyzers for electro-organic synthesis.⁶⁻⁸⁾ One of the most outstanding properties of Nafion is its multi-phase structure. Gierke *et al.*^{9, 10)} presented a cluster-network model that Nafion is microscopically separated into two phases: an ionic cluster domain, which contains most of the sulfonate groups, counter-ions and absorbed water, and a hydrophobic backbone domain, which surrounds the ionic clusters. Yeager and Steck¹¹⁾ later proposed a three phase model in which an "interfacial region" exists between the two domains of Gierke's model. Ogumi *et al.*¹²⁾ considered that the interfacial region consists of the amorphous part of the fluorocarbon backbone and the side chains of Nafion. Various properties such as solvent uptake,¹³⁾ ion-exchange selectivity,¹⁴⁾ permeation of inor-

ganic cations,^{9, 11)} gases,^{12, 15)} and organic molecules,^{16, 17)} etc., have been explained in terms of the multi-phase structure of Nafion.

Electrodes coated with Nafion have received much attention owing to their properties that various electrochemically and optically active cations can be incorporated into the Nafion film.¹⁸⁻²⁰⁾ Some workers have recently reported that the multi-phase structure causes interesting electrochemical behavior of organic cations incorporated into the Nafion film.²¹⁻²⁴⁾ Rubinstein²¹⁾ reported that the potential shifts and splitting of the redox peaks of ferrocene/ferricinium incorporated in the Nafion film. He interpreted this unusual behavior in terms of the different interactions of the two redox forms with different domains of Nafion. This was later supported by Harth *et al.*²²⁾ Similar behavior was reported for $[\text{Ru}(\text{bpy})(\text{trpy})(\text{OH}_2)]^{2+}$ (bpy : 2,2'-bipyridine; trpy: 2,2',2''-terpyridine) incorporated into a Nafion-coated electrode by Vining and Meyer²³⁾ and for thionine and methylene blue by John and Ramaraj.²⁴⁾ However, these studies have been carried out using cyclic voltammetry and no direct evidence that shows the residence sites in Nafion has been reported.

In this chapter, the unusual electrochemical and Raman spectroscopic behavior of 1,1'-dipropyl-4,4'-bipyridinium dication (propylviologen, C_3V^{2+}) incorporated into a Nafion film is reported. Viologens are reduced through two successive one-electron transfer steps.²⁵⁾ Whereas the dication is rather hydrophilic, the reduced species, i.e., the cation radical and the doubly reduced form, are strongly hydrophobic.²⁶⁾ Hence, different interactions of these three forms with different domains of Nafion are expected. The structure of Nafion can be regarded as a kind of an assembly of reversed anionic micelles. Thus, the electrochemical and Raman spectroscopic behavior of C_3V^{2+} in solutions containing micelles is examined. The results are compared with those for C_3V^{2+} incorporated into Nafion, and the residence sites of propylviologen in Nafion are discussed.

8.2. Experimental

8.2.1. Nafion-coated silver electrode

The working electrode was a silver rod (5 mm in diameter), and was mounted in a Teflon sheath. The electrode surface (0.196 cm^2) was polished with an emery paper (#2000) and washed with water. A solution ($4 \times 10^{-3} \text{ cm}^3$) of Nafion dissolved in alcohol (Aldrich, containing 5% Nafion of EW = 1100) was spread with a microsyringe onto the Ag electrode and air-dried. The thickness of the recast Nafion is roughly estimated as $5.7 \mu\text{m}$ by using 1.58 g/cm^3 of the wet, Na^+ -form density.¹⁴⁾ The Nafion-coated electrode was immersed in a 0.01 M propylviologen dibromide (C_3VBr_2) solution for 2 h to incorporate viologen into the Nafion coating. The quantity of electroactive viologen in the Nafion coating was determined coulometrically by integrating the current that passed when the electrode potential was stepped from -0.2 to -0.7 V, and was $1.6 \times 10^{-7} \text{ eq. cm}^{-2}$.

8.2.2. Electrochemical and Raman measurements

Figure 8.1 shows the electrochemical cell for *in situ* Raman measurements. The cell was made of Pyrex glass. The laser-incident portion of the cell was made of optically flat Pyrex glass. The gap between the working electrode and the optically flat glass was minimized (typically 1 mm). The counter electrode was a platinum wire. The electrolyte solution was 0.5 M KNO_3 , and contained no viologen species. Potentials were measured as, and referred to as, volts vs. Ag/AgCl (3.3 M KCl). Electrochemical measurements were carried out using a potentiostat (EG & G, PAR 273A). Prior to each measurement the solution was purged with argon for 30 min to exclude dissolved oxygen.

Raman spectra were excited using a 514.5 nm line (50 mW) of an argon ion laser (NEC, GLG3260). The electrode surface was irradiated with the laser beam through the optically flat glass. The scattered light was collected in a backscattering geometry. Each Raman spectrum was measured at 5 min after the electrode was stepped to a desired potential. The spectra were

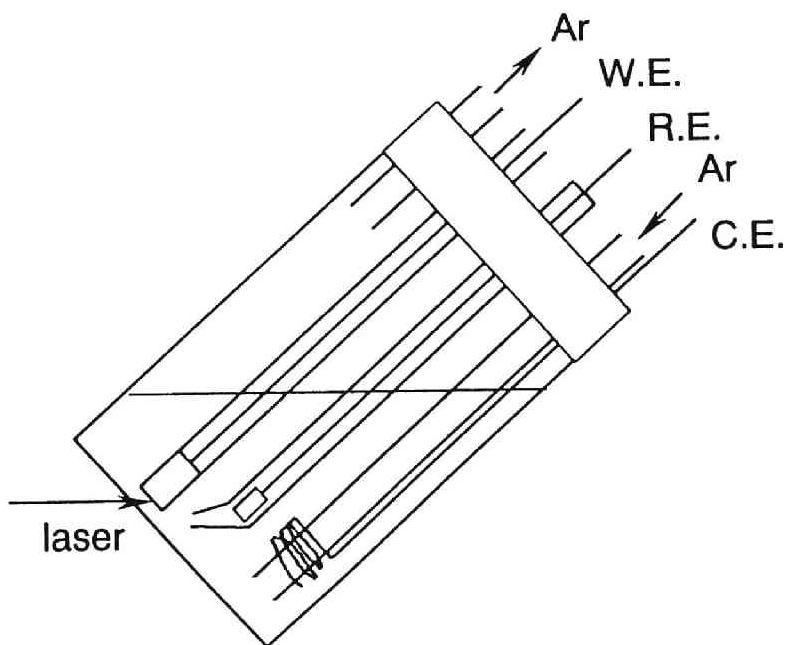


Fig. 8.1. Electrochemical cell used for *in situ* Raman measurements.

recorded using a spectrometer (Jobin-Yvon, T64000) equipped with a multi-channel CCD detector. For each measurement the integration time was 300 s. All experiments were carried out at ambient temperature.

8.2.3. Raman spectra in micellar solutions

The electrochemical properties and Raman spectra of propylviologen in the presence of various types of micelles were measured using the cell shown in Fig. 8.1 and a silver electrode (0.196 cm²) without Nafion coating. The electrolyte solution contained 1 mM C₃VBr₂ and 50 mM surfactants. Cetyltrimethylammonium bromide (CTAB), *t*-octylphenoxypolyethoxyethanol (Triton X-100) and sodium dodecyl sulfate (SDS) were used as the surfactants. The electrochemical and Raman measurements were carried out in a similar manner to that described above.

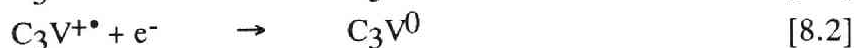
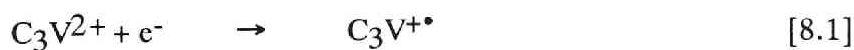
8.2.4. Chemicals

Propylviologen was synthesized from 4,4'-bipyridine and 1-bromopropane, and recrystallized from an ethanol solution.²⁷⁾ CTAB and SDS was obtained from Wako Pure Chemical, and Triton X-100 from Sigma Chemical. These surfactants were used as received. Other chemicals were of reagent grade, and were used without further purification.

8.3. Results

8.3.1. Cyclic voltammogram of C₃V²⁺ incorporated in Nafion

Cyclic voltammograms of C₃V²⁺ dissolved in an aqueous solution and incorporated in the Nafion film are shown in Fig. 8.2. Curve (a) shows the voltammogram of 1 mM C₃V²⁺ on Ag in 0.5 M KNO₃. Two redox couples observed in the voltammogram are attributed to the well-known two-step reduction of viologen:²⁵⁾



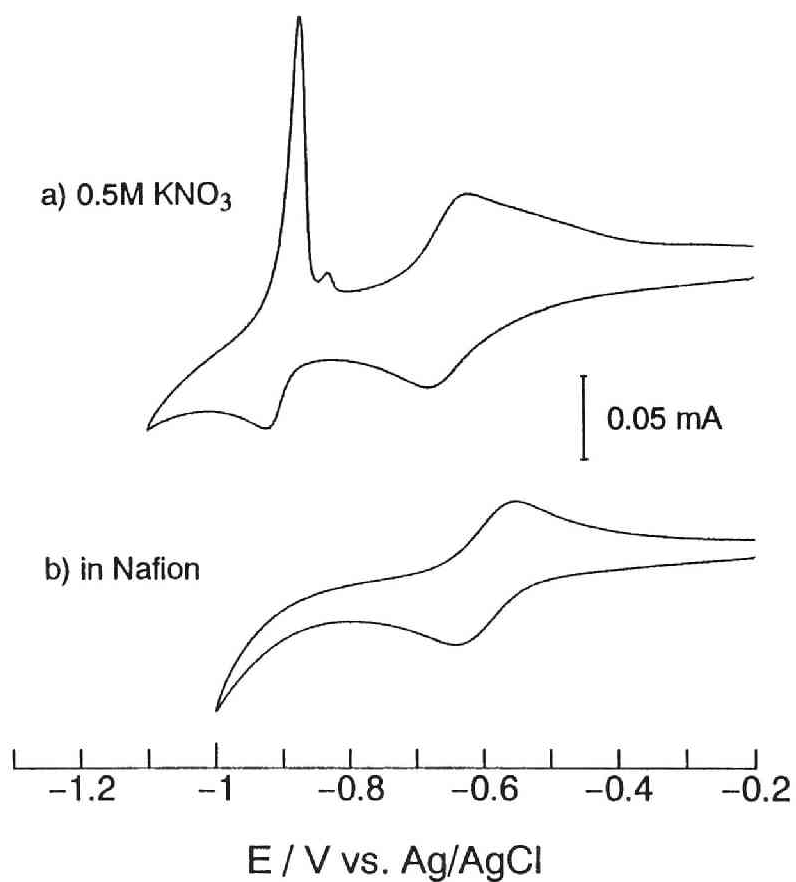


Fig. 8.2. Cyclic voltammograms of (a) 1 mM C_3VBr_2 on Ag (0.196 cm^2) and (b) C_3V^{2+} incorporated in Nafion-coated Ag electrode (0.196 cm^2 , $\Gamma_{\text{C}_3\text{V}} = 1.6 \times 10^{-7} \text{ eq. cm}^{-2}$) in aqueous 0.5 M KNO_3 . The sweep rate was 50 mV s^{-1} .

The respective peak potentials and half-wave potentials are shown in Table 8.1. The shape of the re-oxidation wave for the second step corresponded to that expected for an adsorbed species, which indicates that the doubly reduced form (C_3V^0) was precipitated on the electrode. Curve (b) shows the voltammogram of C_3V^{2+} incorporated in the Nafion film. The redox peaks for the first step were observed at around -0.6 V, and the half-wave potential ($E_{1/2}$) was shifted slightly to a positive potential with respect to that for solution species (see Table 8.1). Cathodic current, which is attributed to hydrogen evolution, started to flow from about -0.9 V, and redox peaks corresponding to the second step were not observed in the potential range to -1.0 V. Hence the redox peaks for the second step is considered to have been shifted to potentials more negative than -1.0 V.

8.3.2. *In situ Raman spectra of C_3V -species incorporated into Nafion*

Figure 8.3 shows the Raman spectra of propylviologen on Ag in 0.5 M KNO_3 at various potentials. At -0.2 V Raman bands of C_3V^{2+} were observed at 1169, 1293 and 1636 cm^{-1} ,²⁸⁻³²⁾ although their intensities were rather low. A line at 1047 cm^{-1} is assigned to the symmetric stretching mode of nitrate anion. At -0.75 V typical bands assigned to $C_3V^{+\bullet}$ appeared with strong intensity at 822, 1026, 1194, 1244, 1337, 1355, 1510, 1528 and 1656 cm^{-1} .²⁸⁻³²⁾ The strong intensities are attributed to the resonance effect of $C_3V^{+\bullet}$.³⁰⁾ At -0.95 V new bands appeared at 993, 1286, 1412, 1539 and 1657 cm^{-1} , which are assigned to C_3V^0 .²⁸⁻³¹⁾ It should be noted that the 1657 cm^{-1} band overlapped with the 1656 cm^{-1} band of $C_3V^{+\bullet}$. These bands were also strong because C_3V^0 precipitated and accumulated on the electrode as shown by the cyclic voltammogram [curve (a) in Fig. 8.2]. (Comparing the absorption coefficient of the doubly reduced viologen at 514.5 nm with that of the cation radical,²⁷⁾ the resonance effect of C_3V^0 is considered to be weaker than that of $C_3V^{+\bullet}$. As will be described later C_3V^0 dissolved in solution shows bands with much lower intensities.) Pure C_3V^0 bands were not obtained at -0.95 V because the spectra involved scattering

Table 8.1. Electrochemical data for propylviologen incorporated in Nafion and in micellar solutions.

Electrode	Medium	First reduction			Second reduction		
		$-E_{pc}$	$-E_{pa}$	$-E_{1/2}^{a)}$	$-E_{pc}$	$-E_{pa}$	$-E_{1/2}^{a)}$
Ag ^{b)}	0.5 M KNO ₃	0.69	0.63	0.66	0.93	0.88	0.91
Nafion/Ag ^{c)}	0.5 M KNO ₃	0.63	0.57	0.60	-	-	^{d)}
Ag ^{b)}	0.5 M KNO ₃ + 50 mM Triton X-100	0.68	0.63	0.65	0.92	0.86	0.89
Ag ^{b)}	25 mM Na ₂ SO ₄ + 50 mM CTAB	-	0.58	^{e)}	0.89	0.81	0.85
Ag ^{b)}	25 mM Na ₂ SO ₄ + 50 mM SDS	0.67	0.60	0.64	1.13	1.04	1.08

a) $E_{1/2} = 1/2(E_{pc} + E_{pa})$. b) 1 mM C₃VBr₂ was added to the solution. c) C₃V²⁺ was incorporated in Nafion film ($\Gamma_{C3V} = 1.6 \times 10^{-7}$ eq. cm⁻²). d) The redox peaks for the second reduction were not observed in the potential range to -1.0 V. e) The reduction peak was not observed clearly.

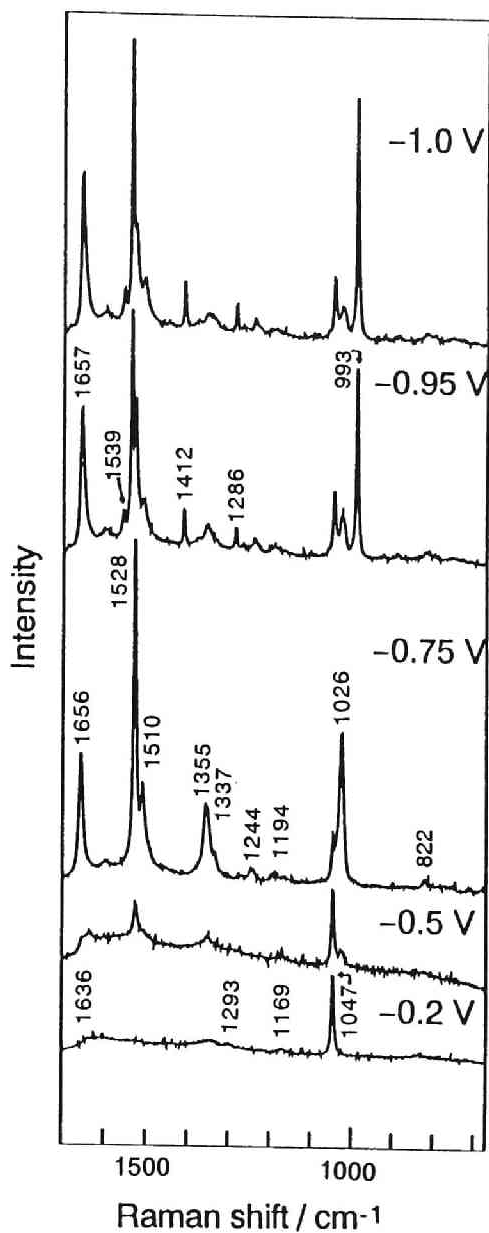


Fig. 8.3. Raman spectra of 1 mM C₃VBr₂ on Ag in aqueous 0.5 M KNO₃ at various potentials. A band at 1047 cm⁻¹ is assigned to the symmetric stretching mode of NO₃⁻.

from the species in the solution phase, i.e., $C_3V^{+\bullet}$, in the vicinity of the electrode as well as that from C_3V^0 precipitated on the electrode.

Figure 8.4 shows the Raman spectra of propyl viologen incorporated in the Nafion film at various potentials. Raman bands of $C_3V^{+\bullet}$ appeared at -0.75 V. However, Raman bands indicative of C_3V^0 formation were not observed at -0.95V. (The spectrum at -0.95 V is not shown.) This result is in agreement with the observed electrochemical behavior [curve (b) in Fig. 8.2]. At -1.0 V a Raman band at 993 cm^{-1} indicative of C_3V^0 formation appeared; that is, the potential for C_3V^0 formation was shifted negatively by 50 mV with respect to that for solution species. However, the intensity of the 993 cm^{-1} band was extremely low, and remained almost unchanged when a more negative potential (-1.1 V) was imposed. These results show that the formation of the doubly reduced viologen was thermodynamically less favorable in Nafion than in the aqueous solution.

8.3.3. Behavior of C_3V -species in the presence of various micelles

Cyclic voltammograms of 1 mM C_3V^{2+} on Ag in the three micellar solutions are shown in Fig. 8.5. Curve (a) in Fig. 8.5 shows the voltammogram in the presence of 50 mM Triton X-100. The $E_{1/2}$ values for the first and second redox reactions were almost unchanged from those in the micelle-free solution (see Table 8.1). The peak currents for the first redox peaks are nearly equal to those obtained in the micelle-free solution. The re-oxidation peak of C_3V^0 showed a diffusion wave, which indicates that C_3V^0 was not precipitated on the electrode.

Curve (b) in Fig. 8.5 shows the voltammogram in the presence of 50 mM CTAB. The first redox peaks are complicated, and this unusual behavior has not been clarified yet. The second step showed a clear diffusion wave, and the $E_{1/2}$ value was slightly shifted to a positive potential with respect to those obtained in the micelle-free solution (see Table 8.1).

The electrochemical behavior of C_3V^{2+} in a solution containing 50 mM SDS is shown in curve (c) in Fig. 8.5. While the $E_{1/2}$ value for the first redox step was slightly shifted to a positive potential, that for the second step

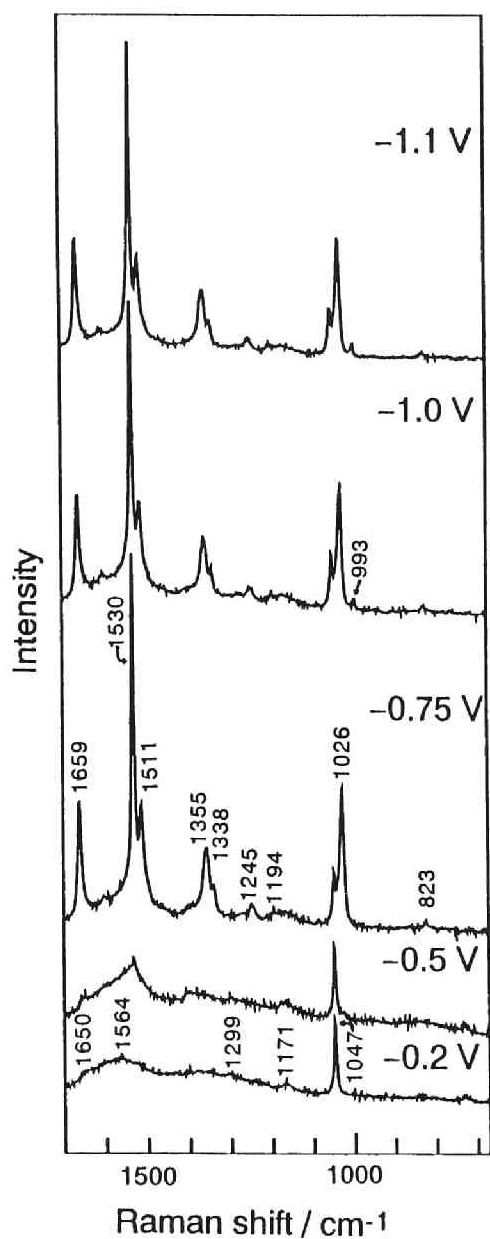


Fig. 8.4. Raman spectra of C_3V^{2+} incorporated in Nafion-coated Ag electrode (0.196 cm^2 , $\Gamma_{C_3V} = 1.6 \times 10^{-7}\text{ eq. cm}^{-2}$) in aqueous 0.5 M KNO_3 at various potentials. A band at 1047 cm^{-1} is assigned to the symmetric stretching mode of NO_3^- .

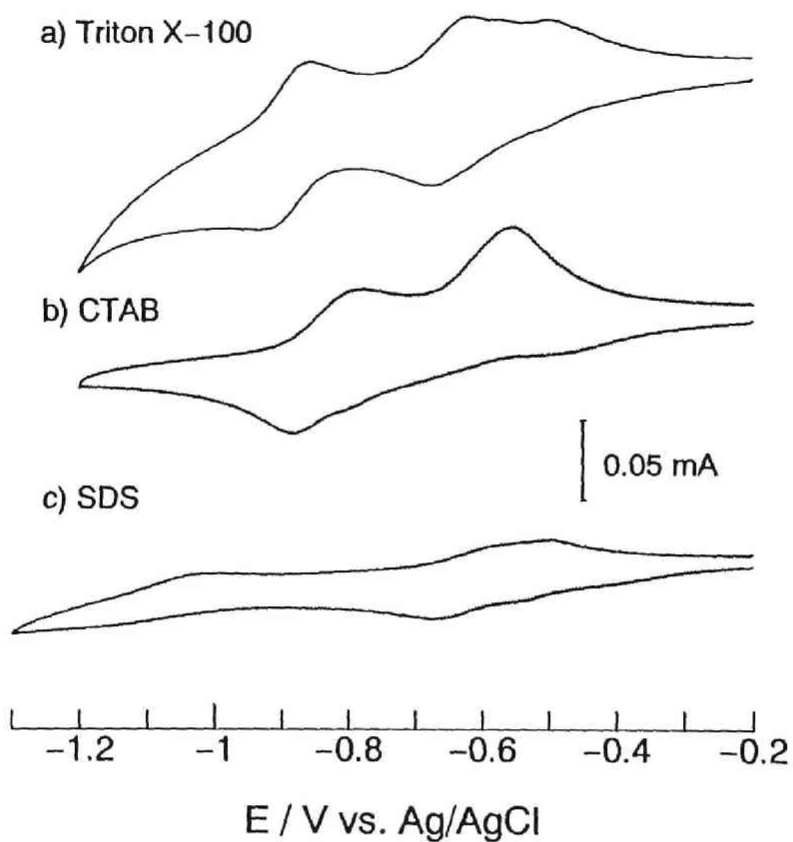


Fig. 8.5. Cyclic voltammograms of 1 mM C_3VBr_2 on Ag (0.196 cm^2) in (a) 0.5 M KNO_3 + 50 mM Triton X-100, (b) 25 mM Na_2SO_4 + 50 mM CTAB, and (c) 25 mM Na_2SO_4 + 50 mM SDS. The sweep rate was 50 mV s^{-1} .

to a negative potential by about 200 mV with respect to those in the micelle-free solution. These facts show that the presence of SDS micelles makes the first step thermodynamically easier and the second step more difficult; that is, $C_3V^{+\bullet}$ is stabilized. Furthermore, all the peak currents were remarkably suppressed compared with those in the micelle-free solution and the other micellar solutions. The suppression in the peak currents for the second step was more remarkable than that for the first step.

The Raman spectra obtained in the solution containing Triton X-100 micelles are shown in Fig. 8.6. Whereas the bands of C_3V^0 appeared at -0.95 V, their intensities were lower than those obtained in the micelle-free solution (see Fig. 8.3). As was shown in the curve (a) in Fig. 8.5, C_3V^0 was not precipitated on the electrode, but diffused into the solution phase. Hence, the scattering intensities were lower than those for the precipitated species.

Similar spectra were obtained in the solution containing CTAB micelles (Fig. 8.7). Although the voltammogram [curve (b) in Fig. 8.5] did not show a well-defined peak for the first reduction, Raman bands of $C_3V^{+\bullet}$ and C_3V^0 appeared at -0.75 and -0.95 V, respectively.

The Raman spectra in the SDS micellar solution is shown in Fig. 8.8. The 993 cm^{-1} band indicative of C_3V^0 formation was not observed at -0.95 V, but appeared at a more negative potential of -1.1 V. This potential shift is in agreement with the result by cyclic voltammetry [curve (b) in Fig. 8.2]. The intensity of the 993 cm^{-1} band was much lower than that in the Triton X-100 or CTAB micellar solution, and was hardly enhanced at a more negative potential of -1.2 V. These results obtained in the SDS micellar solution, i.e., the potential shift for C_3V^0 formation to a negative potential and the low intensity of the C_3V^0 band, were very similar to the behavior for C_3V^{2+} incorporated in the Nafion film.

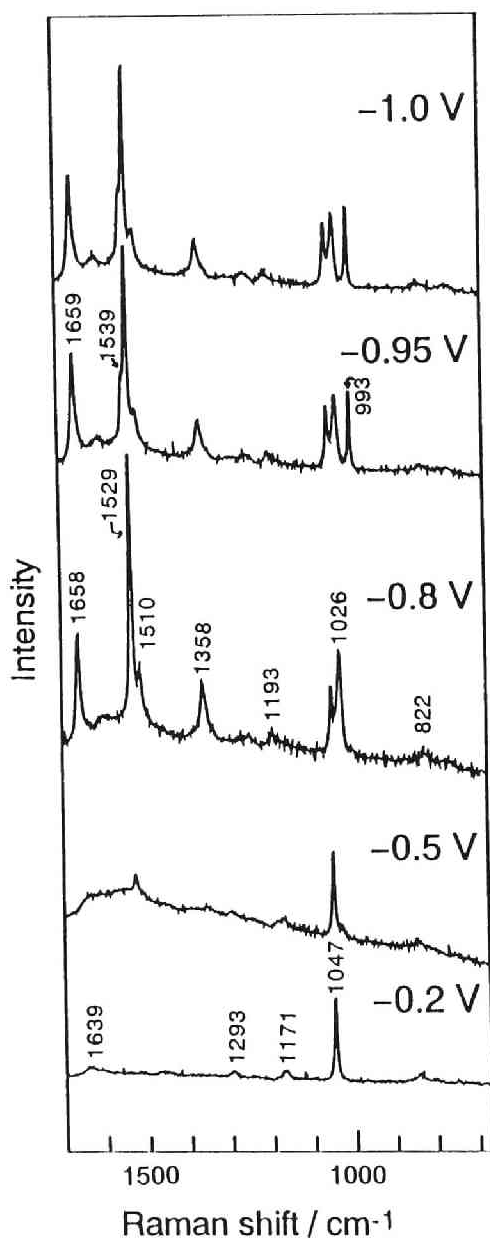


Fig. 8.6. Raman spectra of $1 \text{ mM } \text{C}_3\text{VBr}_2$ on Ag (0.196 cm^2) in $0.5 \text{ M } \text{KNO}_3 + 50 \text{ mM } \text{Triton X-100}$ at various potentials. A band at 1047 cm^{-1} is assigned to the symmetric stretching modes of NO_3^- .

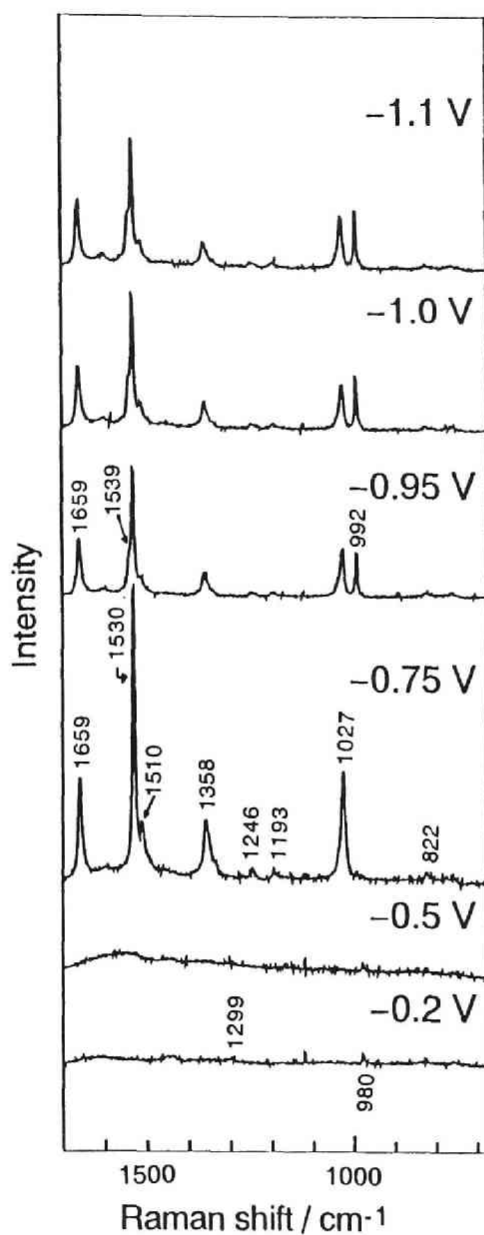


Fig. 8.7. Raman spectra of 1 mM C_3VBr_2 on Ag (0.196 cm^2) in 25 mM Na_2SO_4 + 50 mM CTAB at various potentials. A band at 980 cm^{-1} is assigned to the symmetric stretching modes of SO_4^{2-} .

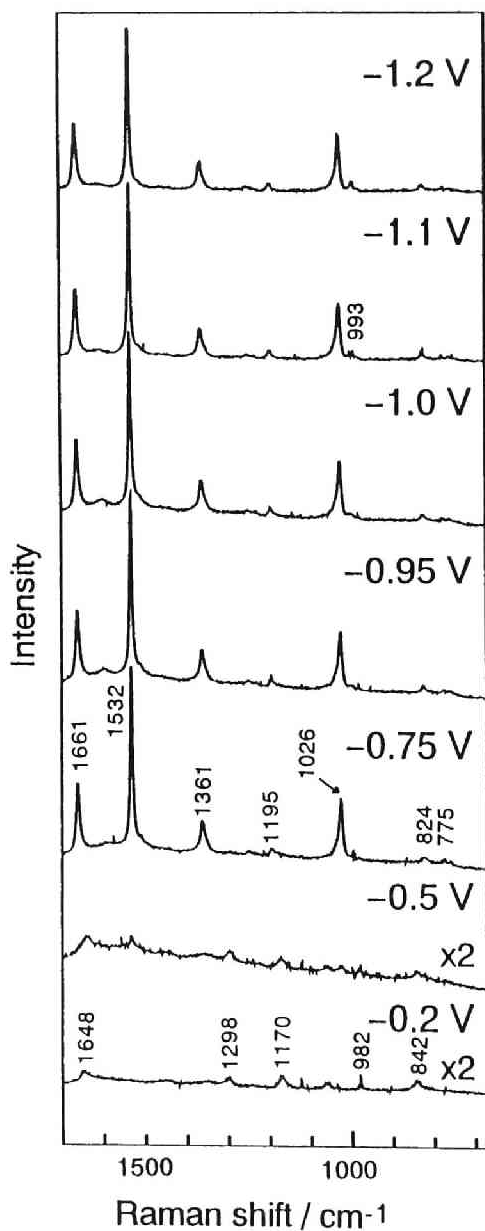


Fig. 8.8. Raman spectra of 1 mM C_3VBr_2 on Ag (0.196 cm^2) in 25 mM Na_2SO_4 + 50 mM SDS at various potentials. A bands at 980 cm^{-1} is assigned to the symmetric stretching modes of SO_4^{2-} .

8.4. Discussion

8.4.1. Association of viologen species with micelles

In a surfactant solution the concentration of micelles, $[M]$, is related to a total concentration of surfactant, C_{surf} , and the critical micelle concentration, CMC, by

$$[M] = (C_{\text{surf}} - \text{CMC})/\bar{n}, \quad [8.3]$$

where \bar{n} denotes the aggregation number.³³⁾ The micelle concentration in the SDS micellar solution is calculated to be 0.7 mM for a surfactant concentration of 50 mM, using the critical micelle concentration (CMC) of 8.1 mM³³⁾ and aggregation number of 60.³³⁾ Similar micelle concentrations are calculated for CTAB and Triton X-100 micelles using their CMCs and aggregation numbers.^{33, 34)} Therefore, the concentration of the micelles is almost the same as that of C_3V^{2+} (1 mM) for each micellar solution in this chapter.

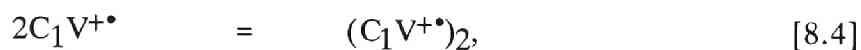
In the nonionic Triton X-100 micellar solution, the peak currents for the first redox reaction are nearly equal to those in the micelle-free solution, which shows that the diffusion coefficient of the C_3V^{2+} was not changed in the presence of Triton X-100 micelles. Hence, C_3V^{2+} was not associated with Triton X-100 micelles. The re-oxidation peak for the second step showed a diffusion wave, which indicates that C_3V^0 was associated with Triton X-100 micelles. The weaker intensities of the Raman bands of C_3V^0 than those in the micelle-free solution confirms this consideration. The present results did not clarify whether $C_3V^{+\bullet}$ was associated with the SDS micelles or not. Hoshino *et al.*³⁵⁾ studied the diffusion coefficients of the three forms of methylviologen using cyclic voltammetry in the presence of Triton X-100 micelles, and reported that the cation radical is associated with Triton X-100 micelles. The cation radical of propylviologen is more hydrophobic than methylviologen cation radical.³⁶⁾ Hence, it is reasonable to assume that $C_3V^{+\bullet}$ was associated with Triton X-100 micelles.

In the cationic CTAB micellar solution, a complicated wave-form for

the first redox reaction in the cyclic voltammogram was observed [curve (b) in Fig. 8.5], and the information about the residence sites of C_3V^{2+} and $C_3V^{+\bullet}$ was not obtained. The second reduction step, however, showed a clear diffusion wave, which indicates that the C_3V^0 was associated with CTAB micelles.

SDS micelles significantly affected the electrochemical and Raman spectroscopic properties of propylviologen. In the cyclic voltammogram, the peak currents for the first step were suppressed compared with those in the micelle-free solution. This means a decrease in the diffusion coefficient of the electroactive species, i.e., C_3V^{2+} , which can be attributed to the association of C_3V^{2+} with the SDS micelles. The clear diffusion wave of the second step indicates that both $C_3V^{+\bullet}$ and C_3V^0 were also associated with the SDS micelles. In addition, the $E_{1/2}$ value for the first step was slightly shifted to a positive potential with respect to that in the micelle-free solution, and for the second step to a negative potential by about 200 mV. The latter potential shift was also confirmed by the Raman measurements. These peak shifts clearly indicate that the cation radical is more stabilized than the dication in the presence of SDS micelles. The observed greater stabilization of the cation radical compared with the dication suggested that some factors other than electrostatic interactions are important.

Kaifer and Bard³⁶⁾ studied the electrochemical properties of methylviologen in Triton X-100, CTAB, and SDS micellar solutions, and observed a shift in $E_{1/2}$ for the second step to a negative potential in the SDS micellar solution as was also observed in the present study. In addition, they observed by UV/Vis absorption spectroscopy that the concentration of the cation radical dimer in the SDS micellar solution is greatly decreased. The cation radical dimer is produced by the following equilibrium:



The presence of the other surfactants did not affect the dimerization equilibrium. The dimerization of alkylviologen cation radical was less favored in

nonaqueous solvents than in aqueous media. From these results they suggested that the water-free micelle core was the residence site of $C_1V^{+\bullet}$, and that its hydrophobic interactions with the SDS micelle core played an important role in the stabilization of the cation radical.

In Figs. 8.6 to 8.8, it should be noted that the relative intensity of a band at 1510 cm^{-1} of $C_3V^{+\bullet}$ in the presence of the SDS micelles is much lower than those in the presence of Triton X-100 or CTAB micelles. This band has been assigned to the $C_3V^{+\bullet}$ cation radical dimer. The low intensity of the 1510 cm^{-1} band indicates that the dimer production was suppressed in the presence of SDS micelles as is the case of $C_1V^{+\bullet}$ in the presence of SDS micelles by Kaifer and Bard;³⁶⁾ that is, $C_3V^{+\bullet}$ in the SDS micellar solution resided in water-free core of the SDS micelle. Thus, stabilization of $C_3V^{+\bullet}$ was caused by its hydrophobic interactions with the SDS micelle core. This reasoning was supported by both the small peak currents for the second step observed in the cyclic voltammogram and the low intensity of the C_3V^0 band at 993 cm^{-1} in the Raman spectrum in the presence of SDS micelles. The weaker stabilization of C_3V^{2+} compared with $C_3V^{+\bullet}$ is reasoned by weaker hydrophobic interactions of C_3V^{2+} ; that is, C_3V^{2+} might interact only with the micelle head groups. The doubly reduced form is more hydrophobic than the cation radical. Hence, C_3V^0 is also considered to have resided in the SDS micelle core although no direct evidence was obtained from the results in this chapter.

8.4.2. Residence sites in Nafion

Nafion has a multi-phase structure that the hydrophilic ionic cluster domain is microscopically separated from the hydrophobic backbone domain.^{9, 10)} Between the two region, the flexible, hydrophobic interfacial region exists.^{11, 12)} In chapter 7, the cluster-network structure of Nafion 117 membranes incorporating large organic cations including C_3V^{2+} was studied by small angle X-ray scattering (SAXS).³⁷⁾ From the observed SAXS maximum it was concluded that Nafion membranes incorporating C_3V^{2+} as the counterion have ionic clusters with an average diameter of c.a. 4 nm, which is

nearly the same size as that of the Nafion membrane incorporating Na^+ as the counterion. On the basis of the microstructure, Nafion can be regarded as a kind of an assembly of reversed anionic micelles that have sulfonate as head groups. Comparing the microstructure of Nafion with that of SDS micelles, the ionic cluster domain corresponds to the aqueous phase in the micellar solution, and the hydrophobic interfacial region to the micelle core.

The electrochemical behavior and Raman spectra of propylviologen incorporated into the Nafion film were very similar to those in the SDS micellar solution. For example, the potential for C_3V^0 formation was shifted to a negative potential, and only a small amount of C_3V^0 was produced. This similarity indicates that the three forms of propylviologen resided in similar environments to those in the SDS micellar solution as described above. The active sites for the charge-transfer reactions of metal/Nafion composite electrodes are located in the hydrophilic ionic clusters.^{6,38)} The clear redox peaks for the first step in the voltammogram shows that C_3V^{2+} resided in the ionic clusters although C_3V^{2+} might have interacted with sulfonate groups. Furthermore, the observed similarity in the electrochemical and Raman spectral properties as mentioned above suggests that $\text{C}_3\text{V}^{+\bullet}$ interacts strongly with either of the two hydrophobic regions, that is, the interfacial region and backbone domain. It was reported that crystallized parts of the backbone domain occupy 12 wt.% of the H^+ -form Nafion (EW = 1100).³⁹⁾ It is difficult for viologen species to be dissolved in such a rigid crystallized region. The interfacial region, on the other hand, consists of the amorphous parts of the fluorocarbon backbone and the side chains of Nafion.¹²⁾ This region is considered to be flexible enough to permit the penetration of $\text{C}_3\text{V}^{+\bullet}$. Therefore, it is concluded that the cation radical resided in the interfacial region of Nafion. The observed stabilization of $\text{C}_3\text{V}^{+\bullet}$ in the Nafion film is attributed to its hydrophobic interactions with the interfacial region of Nafion.

Nevertheless, an intensive dimer band was observed at 1511 cm^{-1} in the Raman spectra of $\text{C}_3\text{V}^{+\bullet}$ incorporated in Nafion (see Fig. 8.4 at -0.75 V). This fact is not in conflict with our model, where $\text{C}_3\text{V}^{+\bullet}$ resides in the

hydrophobic interfacial region, because the dimer production is dependent not only on the polarity of solvents but also on the concentration of the cation radical.³⁰⁾ The concentration of C_3V^{2+} in the Nafion film is calculated to be about 0.28 M from the surface concentration (1.7×10^{-7} eq. cm^{-2}) and the film thickness (5.7 μm). This value is much higher than those in the micellar solutions (1 mM) although the peak currents in the voltammogram [curve (b) in Fig. 8.2] were low due to a slow mass-transport rate inside Nafion. Hence, the high $C_3V^{+\bullet}$ concentration in the Nafion film is responsible for the observed dimer production.

8.5. Conclusion

Propylviologen incorporated into the Nafion film showed unusual electrochemical and Raman behavior. For example, the $E_{1/2}$ value for the second redox step was shifted to a negative potentials, and only a small amount of C_3V^0 was produced. The structure of Nafion can be regarded as an assembly of reversed anionic micelles. On the basis of this assumption, the electrochemical and Raman spectroscopic properties were compared with those in solutions containing CTAB, Triton X-100 and SDS micelles, and were shown to be very similar to those in the SDS micellar solution. In addition, the Raman spectra of $C_3V^{+\bullet}$ showed that the presence of SDS micelles suppressed the dimer formation. This fact suggests that $C_3V^{+\bullet}$ resides in the hydrophobic micelle core, and that hydrophobic interactions play an important role in the observed stabilization of $C_3V^{+\bullet}$. The observed similarity in the electrochemical and Raman characteristics of propylviologen incorporated in Nafion and dissolved in the SDS micellar solution reveals that hydrophobic interactions are also important for the stabilization of $C_3V^{+\bullet}$ in Nafion. It is therefore inferred that $C_3V^{+\bullet}$ resides in the hydrophobic interfacial region while C_3V^{2+} in the hydrophilic ionic cluster domain in Nafion. In other words, in the Nafion film C_3V^{2+} is reduced to form $C_3V^{+\bullet}$ in the hydrophilic ionic clusters, and then $C_3V^{+\bullet}$ phase-transferred from the hydrophilic ionic cluster domain to the hydrophobic interfacial region because of

its increased hydrophobic nature.

References

1. E. A. Ticianelli, C. R. Derouin and S. Srinivasan, *J. Electroanal. Chem.*, **251**, 275 (1988).
2. R. S. Yeo, J. McBreen, G Kissel, F. Klesa and S. Srinivasan, *J. Appl. Electrochem.*, **10**, 741 (1980).
3. D. Bergner, *J. Appl. Electrochem.*, **12**, 631 (1982).
4. K. Katakura, Z. Ogumi, A. Noma and Z. Takehara, *Chem. Lett.*, 1291 (1990).
5. F. G. Will, *J. Electrochem. Soc.*, **126**, 36 (1979).
6. Z. Ogumi, M. Inaba, S. Ohashi, M. Uchida and Z. Takehara, *Electrochim. Acta*, **33**, 365 (1988).
7. M. Inaba, Z. Ogumi and Z. Takehara, *J. Electrochem. Soc.*, **140**, 19 (1993).
8. M. Inaba, K. Fukuta, Z. Ogumi and Z. Takehara, *Chem. Lett.*, 1779 (1993).
9. T. D. Gierke and W. Y. Hsu, in "Perfluorinated Ionomer Membranes", ed by A. Eisenberg and H. L. Yeager, ACS Symposium Series No. 180, Washington DC (1982) Chap. 13.
10. T. D. Gierke, G. E. Mann and F. C. Wilson, *J. Polym. Sci., Polym. Phys.*, **19**, 1687 (1981).
11. H. L. Yeager and A. Steck, *J. Electrochem. Soc.*, **128**, 1880 (1981).
12. Z. Ogumi, T. Kuroe and Z. Takehara, *J. Electrochem. Soc.*, **132**, 2601 (1985).
13. R. S. Yeo, *Polymer*, **21**, 432 (1980).
14. M. N. Szentirmay and C. R. Martin, *Anal. Chem.*, **56**, 1898 (1984).
15. Z. Ogumi, Z. Takehara and S. Yoshizawa, *J. Electrochem. Soc.*, **131**, 769 (1984).
16. Z. Ogumi, K. Toyama, Z. Takehara, K. Katakura and S. Inuta, *J.*

- Membrane Sci.*, **65**, 205 (1992).
17. K. Katakura, M. Inaba, K. Toyama, Z. Ogumi and Z. Takehara, *J. Electrochem. Soc.*, **141**, 1827 (1994).
 18. H. S. White, J. Leddy and A. J. Bard, *J. Am. Chem. Soc.*, **104**, 4811 (1982).
 19. D. A. Buttry and F. C. Anson, *J. Electroanal. Chem.*, **130**, 333 (1981).
 20. N. E. Prieto and C. R. Martin, *J. Electrochem. Soc.*, **131**, 751 (1984).
 21. I. Rubinstein, *J. Electroanal. Chem.*, **88**, 227 (1985).
 22. R. H. Harth, U. Mor, D. Ozer, and A. Bettelheim, *J. Electrochem. Soc.*, **136**, 3863 (1989).
 23. W. J. Vining and T. J. Meyer, *J. Electroanal. Chem.*, **237**, 191 (1987).
 24. S. S. John and R. Ramaraj, *J. Chem. Soc., Faraday Trans.*, **90**, 1241 (1994).
 25. H. T. Van Dam and J. J. Ponjee, *J. Electrochem. Soc.*, **121**, 1555 (1974).
 26. I. Tabushi, *Pure & Appl. Chem.*, **54**, 1733 (1982).
 27. R. Maidan, Z. Gohen, J. Y. Becker and I. Willner, *J. Am. Chem. Soc.*, **106**, 6217 (1984).
 28. S. Ghoshal, T. Lu, Q. Feng and T. M. Cotton, *Spectrochim. Acta*, **44A**, 651 (1988).
 29. Q. Feng, W. Yue and T. M. Cotton, *J. Phys. Chem.*, **94**, 2082 (1990).
 30. T. Lu and T. M. Cotton, *J. Phys. Chem.*, **91**, 5978 (1987).
 31. T. Lu, T. M. Cotton, J. K. Hurst and D. H. P. Thompson, *J. Phys. Chem.*, **92**, 6978 (1988).
 32. R. E. Hester and S. Suzuki, *J. Phys. Chem.*, **86**, 4626 (1982).
 33. J. H. Fendler, "Membrane Mimetic Chemistry", John Wiley & Sons, New York (1982) Chap. 1.
 34. J. H. Fendler and E. J. Fendler, "Catalysis in Micellar and Macromolecular Systems", Academic Press, New York (1975) Chap. 2.
 35. K. Hoshino, H. Sasaki, K. Suga and T. Saji, *Bull. Chem. Soc., Jpn.*,

- 60, 1521 (1987).
36. A. E. Kaifer and A. J. Bard, *J. Phys. Chem.*, **89**, 4876 (1985).
 37. M. Inaba, Y. Osa, T. Yao and Z. Ogumi, *Chem. Lett.*, 1669 (1994).
 38. Z. Chen, T. Mizoe, Z. Ogumi and Z. Takehara, *Bull. Chem. Soc., Jpn.*, **64**, 537 (1991).
 39. T. Hashimoto, M. Fujimura and H. Kawai, in "Perfluorinated Ionomer Membranes", ed by A. Eisenberg and H. L. Yeager, ACS Symposium Series No. 180, Washington DC (1982) Chap. 11.

Chapter 9

Bromination of the Methyl Group of Toluene on a Pt-Nafion Composite Electrode

9.1. Introduction

Electrochemical halogenation of aromatic compounds is a simple, safe and non-polluting method and has been widely studied by many workers.¹⁻⁵⁾ Conventional electrolytic methods require a large amount of supporting electrolyte to give a high conductivity to the electrolyte solution, and a highly polar solvent such as anhydrous acetic acid to dissolve the supporting electrolyte. The application of solid polymer electrolyte (SPE) electrolyzers to organic syntheses has been reported by Ogumi *et al.*⁶⁻⁹⁾ and in chapters 1 to 6. The SPE method eliminates the need for a supporting electrolyte, the addition of which often leads to difficulties in subsequent product purification processes and to unwanted side reactions. This advantage that the SPE method needs no supporting electrolyte may further give the flexibility in solvent choice; that is, non-polar solvents or neat reactants may be used in the SPE method as well as polar solvents.

In this chapter, the anodic bromination of toluene is studied on a Pt-Nafion composite electrode using neat toluene as the anolyte without adding a

supporting electrolyte. The reaction mechanism for bromination and the mass transport of the reactant in the SPE composite electrode are discussed.

2. Experimental

A perfluorosulfonate cation-exchange membrane, Nafion[®] 415 (E. I. du Pont de Nemours and Co.) was used as the SPE material. After treating the Nafion 415 membrane in boiling water, platinum was deposited on one side of the membrane by an electroless plating method reported by Ogumi *et al.*⁶⁾ The amount of deposited Pt was typically 9.3 mg cm^{-2} .

The SPE composite electrode, with an effective geometric surface area of 3.1 cm^2 , was placed in a cell fitted with a silica glass optical window faced to the Pt surface of the electrode (Fig. 9.1). The volume of each compartment was 6 cm^3 . A platinum wire was used as the counter electrode. A commercially available fluorescent light (Matsushita Electric and Industrial Co., FL15W, 15 W) was placed at 10 cm apart from the optical window. The anode compartment was filled with neat toluene, and the cathode compartment with aqueous HBr of various concentrations. No supporting electrolyte was added to the anolyte. Electrolysis was carried out galvanostatically using a potentiostat/galvanostat (Hokuto Denko, HA301). The total charge passed during each run was 800 C unless otherwise noted. During runs the surface of the Pt layer of Pt-Nafion was irradiated with the fluorescent light through the optical window and the anolyte. When electrolysis was carried out in the dark, the cell was placed in a light-shielded box. Electrode potentials were measured using a Luggin capillary placed in the cathode compartment.⁹⁾ Potentials were measured as, and referred to as, volts vs. Ag/AgCl (3.3 M KCl, $\text{M} = \text{mol dm}^{-3}$).

Product mixtures were analyzed by gas chromatography (Perkin Elmer, Model 990). After electrolysis, the catholyte was analyzed without pre-treatment. All chemicals were of reagent grade, and were used without further purification.

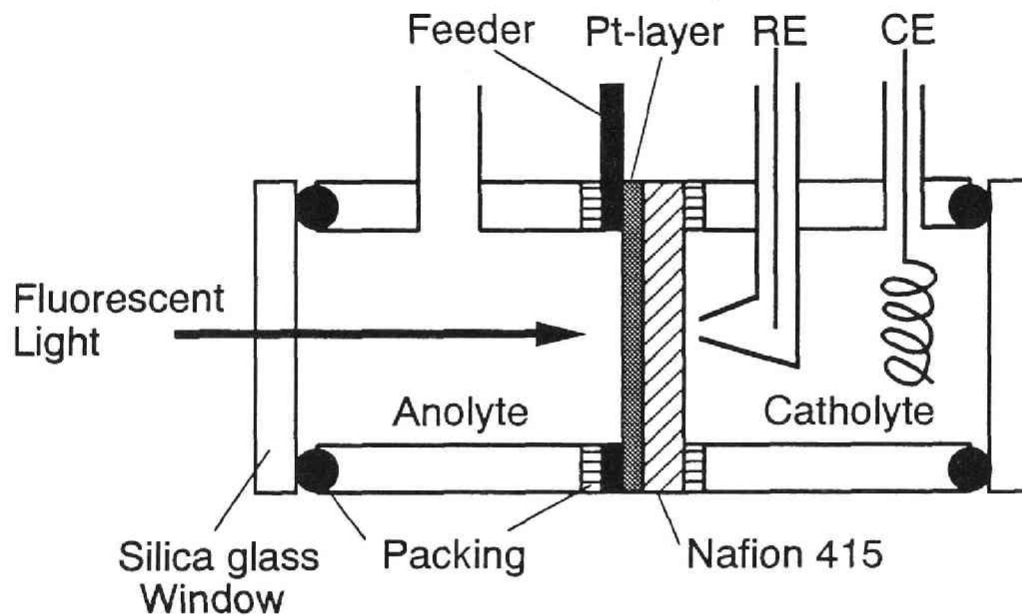


Fig. 9.1. Schematic diagram of electrolytic cell. WE = porous platinum cathode deposited on Nafion 415 solid polymer electrolyte; SPE = Nafion 415; CE = platinum wire anode; feeder = gold ring current feeder.

9.3. Results and Discussion

9.3.1. Effects of irradiation of light and reaction mechanism on SPE composite electrode

Table 9.1 shows the effects of the irradiation with fluorescent light. In the dark brominated products were sparingly produced. Under irradiation with fluorescent light benzyl bromide was obtained with a high current efficiency of 70.5%. Bromotoluene and benzaldehyde were obtained only with trace amounts; hence, the bromination of the methyl group of toluene proceeded preferentially. It was reported that aromatic bromination mainly proceeds in the anodic bromination of toluene using acetonitrile or anhydrous acetic acid as a solvent in conventional electrolysis methods.¹⁻⁵⁾ On the other hand, it is well known that the bromination of the methyl group proceeds predominantly in chemical bromination under irradiation with light.^{2,10)} It is therefore considered that toluene reacted photochemically with bromine molecules, which were produced electrochemically, in the SPE method.

The structure of Nafion, which was used as the SPE material, generally is accepted to be microscopically separated into two phases: a hydrophilic ionic cluster domain and a hydrophobic polytetrafluoroethylene-like backbone domain.^{11,12)} Non-polar organic compounds such as toluene are known to interact only with the hydrophobic domain of Nafion, and cannot penetrate into the hydrophilic ionic clusters.¹³⁾ The active sites of the SPE composite electrode are located in the hydrophilic ionic clusters.⁸⁻¹⁰⁾ Since toluene has a very low solubility in water, i.e., to the ionic clusters, it cannot undertake charge-transfer reactions directly with the electrode because of its very low solubility in water. Hence electro-bromination was sparingly proceeded without irradiation.

On the other hand, Br(1-) species resides in the hydrophilic ionic clusters; hence, a charge-transfer reaction

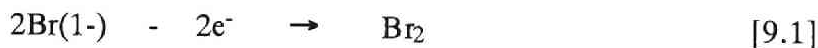
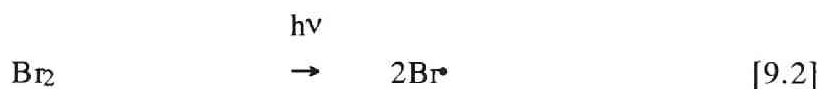


Table 9.1. The effects of irradiation with fluorescent light on the anodic bromination of toluene^a).

	Current efficiency / %		
	Benzyl bromide	Bromo- toluene	Benz- aldehyde
In the dark	4.1	0.8	trace
Fluorescent light	70.5	trace	trace

a) The anolyte and catholyte were neat toluene and 5.0 M aqueous HBr, respectively. Electrolysis was carried out at a constant current density of 5.0 mA cm⁻².

proceeds at the active sites of the electrode, where Br(1-) denotes either Br⁻ anion or neutral HBr and will be discussed later. The dissociation energy for reaction [9.1] is 190 kJ mol⁻¹ (1.97 eV), which corresponds to a wavelength of 629 nm.¹⁴⁾ Since the solubility of Br₂ to organic solvents is relatively high, the Br₂ molecules produced on the electrode can penetrate into the hydrophobic region in Nafion or into the toluene phase in the vicinity of the active sites of the electrode. That is, the Br₂/Br(1-) redox couple serves as a kind of phase-transfer catalysts in the present system. Under irradiation, Br radical is formed photochemically in the hydrophobic region of Nafion or in the toluene phase in the vicinity of the electrode, and reacts with toluene by the following chain reaction:¹⁰⁾



9.3.2. Effects of current density

Figure 9.2 shows the variations of the current efficiency for benzyl bromide production with current density under irradiation with fluorescent light. The amounts of other organic by-products such as bromotoluene and benzaldehyde were negligible. The current efficiency for benzyl bromide production decreased significantly with increasing current density at each HBr concentration. The decrease in the current efficiency is mainly attributable to an increase in the amount of oxygen evolution, which will be discussed in the following section. Figure 9.3 shows the variations of the current efficiency with the amount of charge passed. Benzyl bromide was not produced in proportion to the amount of charge passed. After 500 C were passed, the current efficiency drastically increased. It is considered that accumulation of Br₂ at the active sites is necessary to continue the chain reaction [9.2] to [9.4].

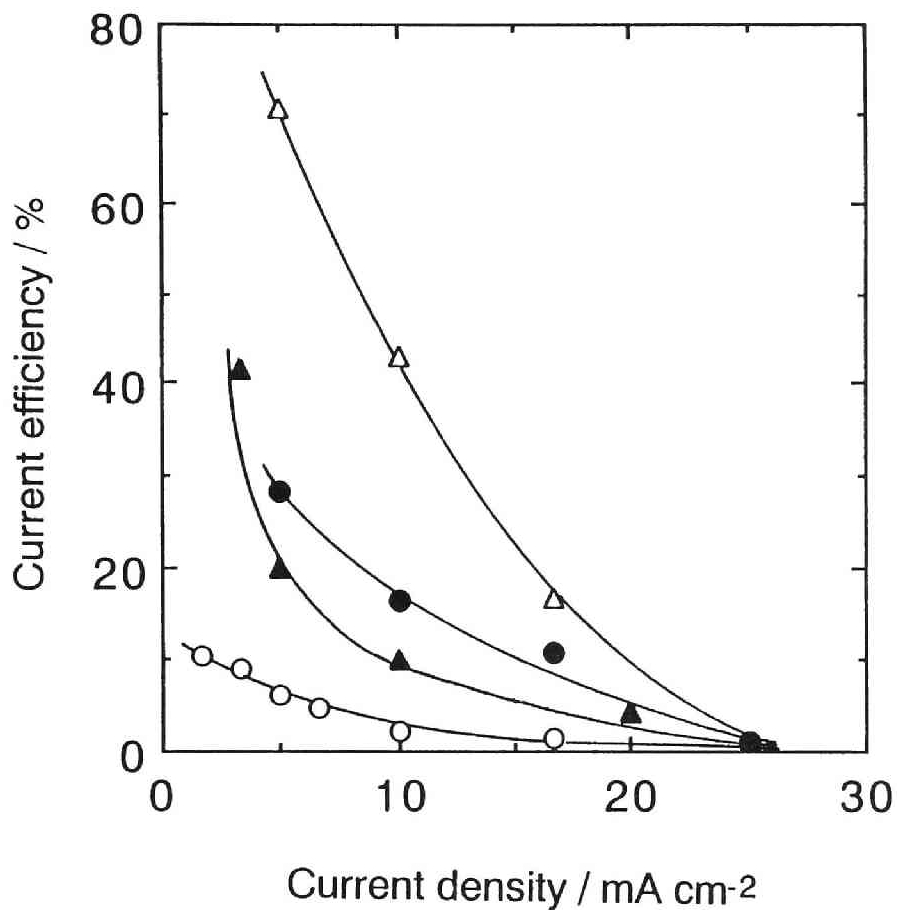


Fig. 9.2. Variations of current efficiency for benzyl bromide production with current density under irradiation with fluorescent light. The concentrations of HBr in the catholytes were (O) 1 M, (●) 3 M, (Δ) 5 M and (▲) 8.5 M.

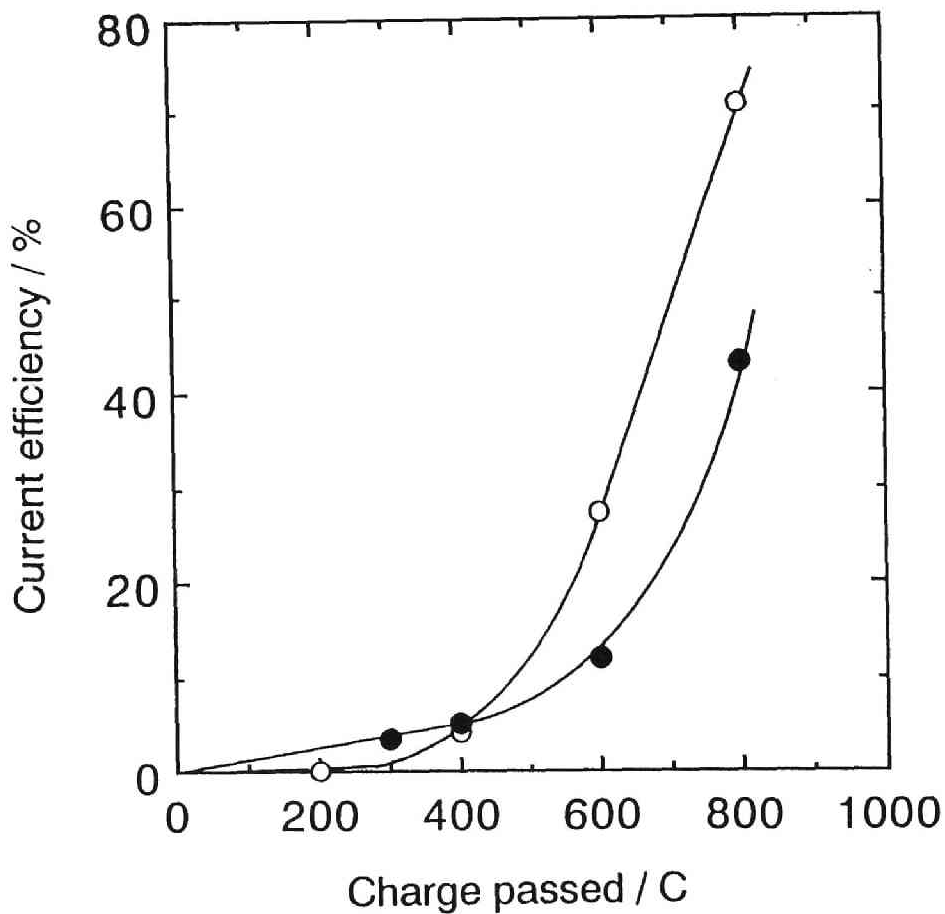


Fig. 9.3. Variations of current efficiency for benzyl bromide production with the amount of charge passed under irradiation with fluorescent light. The concentration of HBr in the catholyte was 5 M. (O) $I = 5 \text{ mA cm}^{-2}$; (●) $I = 10 \text{ mA cm}^{-2}$.

9.3.3. *Effects of HBr concentration in the catholyte*

It is noted in Fig. 9.2 that the current efficiency is dependent on the HBr concentration in the catholyte as well as on current density. The current efficiency dependence on the HBr concentration in the catholyte at a current density of 5 mA cm^{-2} is shown in Fig. 9.4. The optimum current efficiency was obtained at 5 M. The linear sweep voltammogram for each HBr concentration at 0.2 mV/s showed the limiting current density at potentials higher than about $0.8 \text{ V vs. Ag/AgCl}$. The limiting current density, which is plotted in Fig. 9.4, showed a dependency very similar to that of current efficiency on the HBr concentration. The driving force of $\text{Br}(1-)$ diffusion in the Nafion membrane is a concentration gradient of $\text{Br}(1-)$ across the membrane because $\text{Br}(1-)$ is supplied from the catholyte to the electrode material through the membrane. Since Nafion is a cation-exchange membrane, Br^- is excluded from the membrane due to the Donnan equilibrium. Hence the mass transport of $\text{Br}(1-)$ species was limited at low HBr concentration below 3 M, which led to oxygen evolution as a side reaction. However, when the concentration of HBr in the catholyte increases, bromide ion, permitted by the Donnan equilibrium, or neutral HBr can penetrate into the membrane. The limiting current density for the oxidation of $\text{Br}(1-)$ therefore increased with HBr concentration, resulting in an increase in current efficiency for benzyl bromide production.

Nevertheless, both current efficiency and limiting current density in Fig. 9.4 decreased with increasing HBr concentration above 5 M. It was reported that the hydrophilic ionic clusters, which is the diffusion path for $\text{Br}(1-)$ species, shrink when Nafion membranes are in contact with concentrated electrolyte solutions.¹⁵⁾ Similar dependency on HCl concentration was reported on the conductivity of Nafion 120 immersed in aqueous HCl solutions¹⁶⁾. Therefore the diffusion of $\text{Br}(1-)$ in the membrane was again limited at HBr concentrations higher than 5 M.

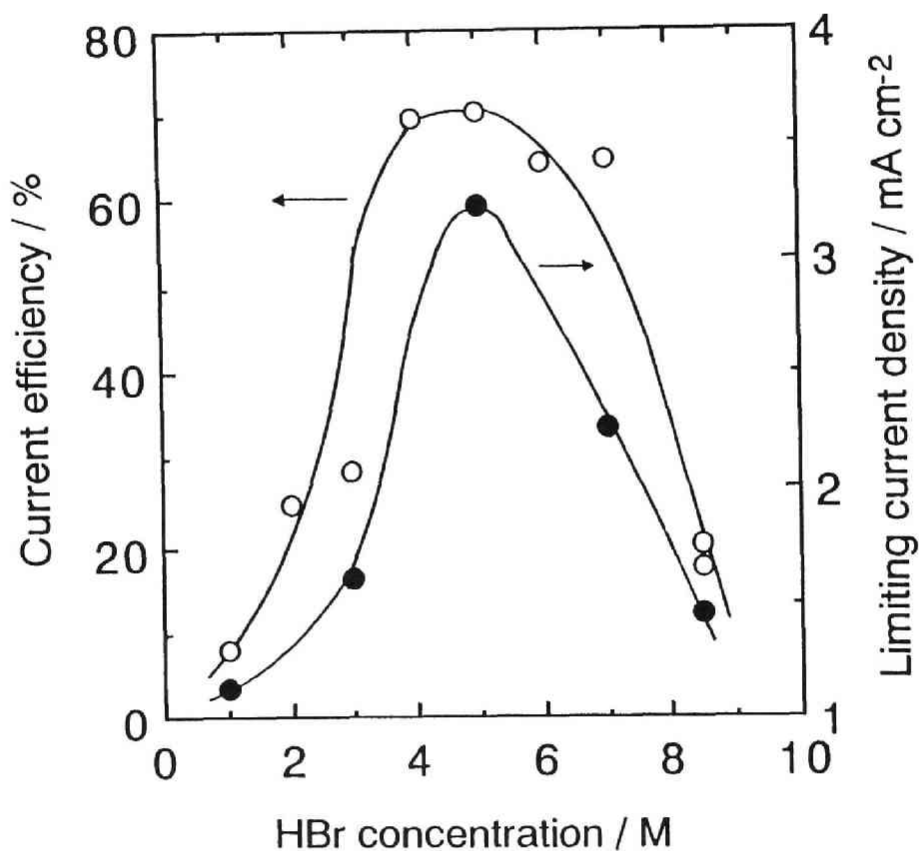


Fig. 9.4. Dependencies of (O) current efficiency for benzyl bromide production under irradiation with fluorescent light ($I = 5 \text{ mA cm}^{-2}$) and (●) the limiting current density on HBr concentration in the catholyte.

References

1. M. Mastrangostino, G. Casalbore and S. Valcher, *J. Electroanal. Chem.*, **56**, 117 (1974).
2. G. Casalbore, M. Mastrangostino and S. Valcher, *J. Electroanal. Chem.*, **61**, 33 (1975).
3. J. Gourcy and J. Simonet, *Electrochim. Acta*, **24**, 1039 (1979).
4. Y. Matsuda, A. Terashima and K. Nakagawa, *Denki Kagaku*, **51**, 790 (1983).
5. T. Matsue, M. Fujihira and T. Osa, *J. Electrochem. Soc.*, **126**, 500 (1979).
6. Z. Ogumi, K. Nishio and S. Yoshizawa, *Denki Kagaku*, **49**, 212 (1981).
7. Z. Ogumi, M. Inaba, S. Ohashi, M. Uchida and Z. Takehara, *Electrochim. Acta.*, **22**, 365 (1988).
8. Z. Chen, T. Mizoe, Z. Ogumi and Z. Takehara, *Bull. Chem. Soc. Jpn.*, **64**, 537 (1991).
9. M. Inaba, Z. Ogumi and Z. Takehara, *J. Electrochem. Soc.*, **140**, 19 (1993).
10. T. W. G. Solomon, "Organic Chemistry", 4th ed., John Wiley & Sons, New York (1988) pp. 414-422.
11. T. D. Gierke and W. Y. Hsu, in "Perfluorinated Ionomer Membranes, ed by A. Eisenberg and H. L. Yeager, ACS Symposium Series No. 180, Washington DC (1982) Chap. 13.
12. Z. Ogumi, T. Kuroe and Z. Takehara, *J. Electrochem. Soc.*, **132**, 2601 (1985).
13. R. S. Yeo, *Polymer*, **21**, 432 (1980).
14. J. E. Huheey, E. A. Keiter and R. L. Keiter, "Inorganic Chemistry", 4th ed., Harper Collins, New York (1993) p. A-29.
15. M. Fujiwara, T. Hashimoto and H. Kawai, *Macromolecules*, **15**, 136 (1982).
16. R. S. Yeo and J. McBeen, *J. Electrochem. Soc.*, **126**, 1682 (1979).

Publication List

The content of each chapter has been or will be published as follows:

Chapter 1

Application of the Solid Polymer Electrolyte Method to Organic Electrochemistry-VII. The Reduction of Nitrobenzene on a Modified Pt-Nafion

Zempachi OGUMI, Minoru INABA, Shin-ichi OHASHI, Masaaki UCHIDA, and Zen-ichiro TAKEHARA, *Electrochim. Acta*, **33**, 365 (1988).

Chapter 2

Application of the Solid Polymer Electrolyte Method to Organic Electrochemistry-XIV. Effects of Solvents on the Electroreduction of Nitrobenzene on Cu,Pt-Nafion

Minoru INABA, Zempachi OGUMI, and Zen-ichiro TAKEHARA, *J. Electrochem. Soc.*, **140**, 19 (1993).

Chapter 3

Application of the Solid Polymer Electrolyte Method to Organic Electrochemistry-XV. Influence of the Multiphase Structure of Nafion on Electroreduction of Substituted Aromatic Nitro Compounds on Cu,Pt-Nafion

Minoru INABA, James T. HINATSU, Zempachi OGUMI, and Zen-ichiro TAKEHARA, *J. Electrochem. Soc.*, **140**, 706 (1993).

Reaction Selectivity in SPE Electroorganic Synthesis -Effects of Nafion on Reduction of Aromatic Nitro Compounds

Zen-ichiro TAKEHARA, Zempachi OGUMI, and Minoru INABA, in "Recent Advances in Electroorganic Synthesis", Proceedings of the 1st International Symposium on Electroorganic Synthesis, ed by S. Torii, Kodansha Ltd, Tokyo (1987) pp. 409-412.

Chapter 4

Reduction of Nitrobenzene on Solid Polymer Electrolyte Composite Electrodes Using a Hydrocarbon Sulfonate Ion-Exchange Membrane
Minoru INABA, Kenji FUKUTA, Zempachi OGUMI, and Zen-ichiro TAKEHARA, *Chem. Lett.*, 1779 (1993).

Chapter 5

Application of the Solid Polymer Electrolyte Method to Organic Electrochemistry-XVIII. Reduction of Nitrobenzene Using a Flow-Through Pt-Nafion[®] Cell
Minoru INABA, Shinichi KINOSHITA, Zempachi OGUMI, and Zen-ichiro TAKEHARA, *Denki Kagaku*, in press.

Chapter 6

Application of the Solid Polymer Electrolyte Method to Organic Electrochemistry-XVII. Indirect Electrochemical Debromination Using Viologens as Microscopic Phase-Transfer Mediators.
Minoru INABA, Zempachi OGUMI, and Zen-ichiro TAKEHARA, *J. Electrochem. Soc.*, **141**, 2579 (1994).

Chapter 7

Structure of Perfluorinated Ionomer Membranes Incorporating Organic Cations
Minoru INABA, Yumi OSA, Takeshi YAO, and Zempachi OGUMI, *Chem. Lett.*, 1669 (1994).

Chapter 8

Raman Spectroscopic Analysis of Electrochemical Behavior of Propylviologen in Nafion

Minoru INABA, Yumi OSA, and Zempachi OGUMI, *J. Electroanal. Chem.*, accepted for publication.

In Situ Raman Study on the Behavior of Propylviologen Incorporated into Nafion-Coated Ag Electrode

Minoru INABA, Yumi OSA, and Zempachi OGUMI, in "Novel Trends in Electroorganic Synthesis", Proceedings of the 2nd International Symposium on Electroorganic Synthesis, ed by S. Torii, Kodansha Ltd, Tokyo, submitted for publication.

Chapter 9

Bromination of the Methyl Group of Toluene on a Pt-Nafion[®] Composite Electrode

Minoru INABA, Shinichi KINOSHITA, Zempachi OGUMI, and Zen-ichiro TAKEHARA, *Denki Kagaku*, in press.

